Study on Suspect and Non-Target Screening of Per- and Polyfluoroalkyl Substances (PFASs) by Ion Mobility Mass Spectrometry

SATORU YUKIOKA

Doctoral Dissertation

Course in Global Environmental Studies

Graduate School of Global Environmental Studies

Kyoto University

Kyoto, Japan - 2020

Acknowledgments

First of all, I would like to thank my main supervisors Professor Shigeo FUJII and Associate professor Shuhei TANAKA. Fujii-sensei, thank you for your guidance and supports during master and doctoral programs at Kyoto University. I could continue research works every day to hear your word “Omoshiroi!!” in the lab seminar. That word encouraged me. Shuhei-sensei, thank you for all your guidance, support, and discussions throughout five years. Your enthusiasm for research is exceptional and attractive to me. I’m looking forward to working with you in the future. I would like to thank Assistant professor Hidenori HARADA, your advice was accurate and I could see my research objectively. And I could get the scholarship next year. Thank you for my assistant supervisor Dr. Yuji SUZUKI (PWRI), I discussed the details of the research with you and you taught me how to write my manuscripts. I still need your supports.

Thank you for Dr. Akio HAYASHI (Agilent Technologies), your advice was accurate every time for developing the methods using ion mobility mass spectrometry. I would like to thank Associate professor Anna Kärrman (Örebro University), thank you for all your guidance, support, I enjoyed my first overseas challenge in Sweden. Thank you for your support from the Okinawa prefectural enterprise bureau.

Thank you for Fujii lab members, PFCs group and microplastics group and my friends in Sweden. I really enjoyed research works with all of you, beyond words. All experience here is my property.

Thank you for Professor Jun NAKAJIMA, I want to be a researcher who sincerely enjoyed researches, like you.

My dear family, thank you for your kind supports for long periods. I feel so lucky to be part of my family. I love you all.

I am very happy to enjoy research works!! Continue with **Non Stop!!**

January 8, 2020 It has been raining since this morning. ***Satoru YUKIOKA***

Table of Contents

Appendix

A profile analysis with suspect screening of PFASs in firefighting foam impacted waters in Okinawa, Japan (Paper I)

A new data-independent between linking precursor and fragment ions of PFASs by drift time using ion mobility mass spectrometry (Paper II)

A method to search for PFASs by linking fragmentation flags with their precursor ions by drift time using ion mobility spectrometry (Paper III)

Abstract

Per- and polyfluoroalkyl substances (PFASs) are a group of persistent contaminants that have been detected in the environments. To understand PFASs contamination in firefighting foam impacted environmental waters, this study examined the profile analysis with suspect screening of PFASs in firefighting foam impacted waters in Okinawa, Japan; and developed the data-independent method linking precursor and fragment ions by drift time using ion mobility mass spectrometry. The main objective of this study was to examine suspect and non-target screening for PFASs by ion mobility mass spectrometry.

Previous studies have performed suspect and non-target screening by high-resolution mass spectrometry (HRMS) to determine the composition of contaminant PFASs and to discover unknown PFASs. This study performed a profile analysis with suspect screening against two lists in the NORMAN Suspect List Exchange in firefighting foam impacted environmental and drinking water (n = 18) collected in Okinawa, Japan, in April 2019. Samples were analyzed by liquid chromatography (LC) quadrupole time-of-flight (QTOF) MS in electron spray ionization mode. Suspect screening returned 116 candidate PFASs with their molecular weights, functional groups, and perfluoroalkyl chain lengths. Long-chain PFAAs and some of their precursors were specifically found around the firefighting training area. Short-chain PFAAs were assumed to form from their precursors in groundwater. Drinking water treatment processes can form perfluoroalkyl sulfonic acids (PFSAs) from their perfluoroalkyl sulfonamide precursors. In contrast, biological activated carbon filtration formed perfluoroalkyl carboxylic acids (PFCAs). Thus, PFASs in firefighting foam impacted waters were profiled.

Previous studies have performed target MS/MS mode by LC-QTOF-MS to improve the identification confidence level for discovering unknown PFASs. All ions MS/MS mode has been used for rapid identification of environmental samples to get comprehensive information. However, it is difficult to link precursor and the fragment ions because of co-eluting ions at specific retention times. This study used

drift time acquired by ion mobility MS to link precursor and fragment ions of PFASs in firefighting foam impacted groundwater (n =8). The method was evaluated in consideration of the intensity of co-eluting ions relative to that of targeted ions to see how many co-eluting ions could be excluded. The 99 compound groups were obtained by suspect screening using NORMAN exchange lists. Without drift time, 5%–19% of PFASs (4–9 PFASs) were linked. With drift time, 37%–49% of PFASs (15–43 PFASs) were linked. Success or failure in linking may depend not on samples but on whether the substances have co-eluting ions at the same retention or drift time. As the method can acquire a lot of MS/MS information in one analysis, it is not essential to reanalyze samples, whose chemical composition might have changed during storage, even when the original database, screening list, or statistical filtering / data cleaning approach are changed. Thus, the method compensates for the disadvantages of all-ion MS/MS and can acquire comprehensive data. It will be particularly effective for studies that must analyze a large number of environmental samples.

To discover unknown PFASs, previous researchers have applied HRMS using fragmentation flagging approach with common fragment ion at the same retention time as the flags. The study attempted to utilize drift time acquired by ion mobility spectrometry for making linkages between the relevant ions. For validating the process, standard solution spiked with PFASs were analyzed by LC/IM-QTOF. Fluorinated fragment ions (fragmentation flags) were categorized into three classes: ***Class 1*** (120 types of $[C_xF_y]^-$), ***Class 2*** (123 types of $[C_xF_yO]^-$), ***Class 3*** (131 types of $[C_xF_yO_3S]^-$) and all overlapping fragmentation flags detected at an identical retention time were bundled together as a "flag set". Injecting standard mixed solution of 20 types of PFASs resulted in picking up 20 flag sets by fragmentation flagging. All the fragmentation flags were detected within a designated range of drift time, and their precursor ion was confirmed as a PFAS spiked in the standard solution even when co-eluting compounds were found at almost same retention time. This method was applied to a household fire extinguisher liquid, resulting in finding out nine precursor ions. Therefore, the new linking method achieved rapid searching for the prospective precursor ions using LC/IM-QTOF.

List of Papers

The Ph.D. thesis consists of a summary and three articles listed below;

Paper I

Yukioka, S.; Tanaka, S.; Suzuki, Y.; Fujii, S.; Echigo, S.; Kärrman, A. (-) "A profile analysis with suspect screening of PFASs in firefighting foam impacted waters in Okinawa, Japan" *Proceeding*

Paper II

Yukioka, S.; Tanaka, S.; Suzuki, Y.; Fujii, S.; Echigo, S. (-) "A new data-independent method linking precursor and fragment ions of PFASs by drift time using ion mobility mass spectrometry" *Proceeding*

Paper III

Yukioka, S.; Tanaka, S.; Suzuki, Y.; Fujii, S.; Echigo, S. (2020) "A new method to search for per- and polyfluoroalkyl substances (PFASs) by linking fragmentation flags with their molecular ions by drift time using ion mobility spectrometry" **Chemosphere**, 239, 124644

Abbreviations

General

ACN	Acetonitrile
AFFF	Aqueous film-forming foams
CAS	Chemical abstract service
CE	Collision Energy
CIC	Combustion ion chromatography
CSS	Collision cross section
Da	Dalton
DWTP	Drinking water treatment plant
EIC	Extracted ion chromatogram
ESI	Electrospray ionization
eV	Electron volts
GC	Gas chromatography
HRMS	High-resolution mass spectrometry
IMS	Ion mobility spectrometry
LC	Liquid chromatography
m/z	Mass to charge ratio
MeOH	Methanol
MS	Mass spectrometer
MS/MS	Tandem mass spectrometry
MW	Molecular weight
OECD	Organization for Economic Co-operation and Development
POPs	Persistent organic pollutants
PP	Polypropylene
QTOF	Quadrupole time-of-flight
RT	Retention time
TF	Total fluorine
TIC	Total ion chromatogram
TOF	Total organic fluorine
TOF-MS	Time-of-flight mass spectrometry
TOP assay	Total oxidisable precursor assay
SMILES	Simplified molecular input line entry system
SPE	Solid phase extraction
STD	Standard
U.S.EPA	United States Environmental Protection Agency

Per- and polyfluoroalkyl substances (PFASs)

FASAAs	Perfluoroalkyl sulfonamide acetic acids
FASAs	Perfluoroalkyl sulfonamides
FHxSA	Perfluorohexane sulfonamide
FOSA	Perfluorooctane sulfonamide
FTCAs	Fluorotelomer carboxylic acids
FTOHs	Fluorotelomer alcohols
FTSs	Fluorotelomer sulfonic acids
FTUCAs	Fluorotelomer unsaturated carboxylic acids
PAPs	Polyfluoroalkyl phosphate esters
PFAAs	Perfluoroalkyl acids
PFASs	Per- and polyfluoroalkyl substances
PFCAs	Perfluoroalkyl carboxylic acids
PFECAs	Per- and polyfluoroether carboxylic acids
PFESAs	Per- and polyfluoroether sulfonic acids
PFHxA	Perfluorohexanoic acid
PFHxS	Perfluorohexane sulfonic acid
PFOA	Perfluorooctanoic acid
PFOS	Perfluorooctane sulfonic acid
PFSAs	Perfluoroalkyl sulfonic acids

Chapter 1

Introduction

1.1 Introduction of PFASs

Per- and polyfluoroalkyl substances (PFASs) (**Fig. 1.1**) are a group of anthropogenic organic fluorinated compounds that have been widely used in various industrial, commercial, and consumer products, such as carpet protector sprays, food containers, cosmetics, and firefighting foam (Kotthoff et al., 2015; Ye et al., 2015; Zabaleta et al., 2017; Fujii et al., 2013; Barzen-Hanson et al., 2017). PFASs have been globally detected in environmental and wildlife samples owing to their high persistence due to their C–F chemical structures (Pan et al., 2018; Sedlak et al., 2017; Liu Ye et al., 2017). The toxicity of PFASs has been reported (e.g., hepatotoxicity, endocrine-disrupting activity, reproductive toxicity, and developmental toxicity (Sheng et al., 2018; Kar et al., 2017; Lee et al., 2016; Shi et al., 2018). For the reason, Stockholm convention 2009 listed perfluorooctane sulfonic acid (PFOS) and related compounds as persistent organic pollutants (Stockholm Convention, 2009). In 2014, perfluorooctanoic acid (PFOA) was classified as being a suspected carcinogen in humans (group 2B) (IARC Monographs on the Evaluation of Carcinogenic Risk to Humans, 2018). The concerns about bioaccumulation and

(A) Perfluorooctane sulfonic acid (PFOS)

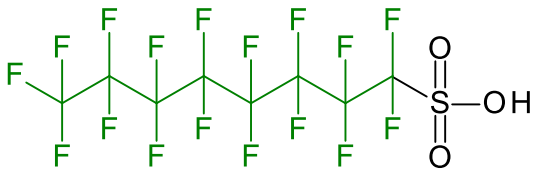

(B) Perfluorooctanoic acid (PFOA)

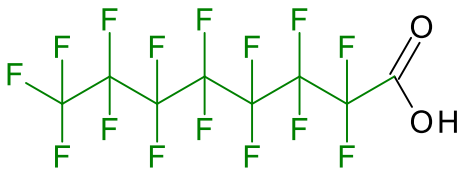

(C) Perfluorohexane sulfonic acid (PFHxS)

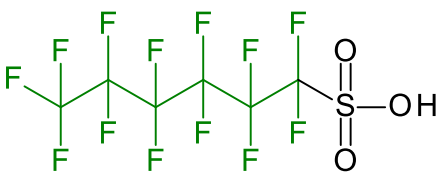

(D) Perfluorohexane slufonamide (FHxSA)

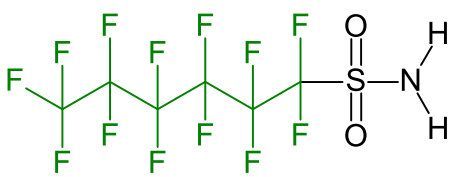

Fig. 1.1 Per- and polyfluoroalkyl substances (PFASs)

the adverse effects of long-chain PFASs in waters and human health have grown. For this reason, PFOA, perfluorohexane sulfonic acid (PFHxS), and its homologs were proposed as candidate persistent organic compounds under the Stockholm Convention (Stockholm Convention, 2018). However, as regulations restrict the use only of legacy PFASs, it is likely that industry has shifted toward the use of alternative PFASs including their precursors with poorly known chemical structures (Wang et al., 2017).

1.2 Objective of this study

The research motivations and main objective of this study were shown in **Fig. 1.2**. The use of firefighting foam has been suspected as a major cause of PFAS contamination in environmental waters. The PFASs are used in firefighting training areas (e.g., airport, military area), and untreated water may be discharged to the environments. In addition, the risk of human exposure through drinking water sourced from fire-fighting foam impacted waters is a global concern. High levels of PFOS contamination from firefighting foam in river water, groundwater, and drinking water were also reported in Okinawa, Japan. However, the characteristics of PFASs contamination other than representative and legacy PFASs (e.g., PFOS, PFOA) were not well known. Therefore, previous studies examined qualitative analysis using high-resolution mass spectrometry (HRMS) to discover unknown PFASs in firefighting foam impacted waters (D'Agostino et al., 2013; Barzen-Hanson et al., 2017). However, it is necessary to examine profile analysis of PFASs for the environments by qualitative analysis for the next step. Moreover, recently, ion mobility mass spectrometry has been started developing in the qualitative analysis field. However, there has been not well known for the application of ion mobility mass spectrometry for the suspect and non-target screening in the environmental research field. The research motivation of this study are as follows;

Question 1: What are the characteristics of PFASs contamination in firefighting foam impacted waters?

Question 2: How to apply the ion mobility mass spectrometry for suspect and non-target screening?

The main objective of this study is to examine suspect and non-target screening for PFASs by ion mobility mass spectrometry. The specific objectives are as follows;

Objective I: To examine a profile analysis with suspect screening of PFASs in firefighting foam impacted waters in Okinawa, Japan (Chapter 4: *Paper I*)

Objective II: To develop a data-independent method linking precursor and fragment ions of PFASs by drift time using ion mobility mass spectrometry (Chapter 5: *Paper II*)

Objective III: To develop a method to search for PFASs by linking fragmentation flags with their precursor ions by drift time using ion mobility mass spectrometry (Chapter 6: *Paper III*)

The framework of this study was shown in **Fig. 1.3**. In previous studies, the investigation of PFASs contamination in the environment were conducted to understand their occurrence and characteristics. Almost these studies were performed the quantitative analysis with authentic standard chemicals. However, in 2019, the Organization for Economic Co-operation and Development (OECD) reported a new comprehensive Global Database of 4,730 PFAS with CAS numbers (OECD, 2019). Therefore, recently, the qualitative analysis has been performed to understand unknown PFASs contamination. There are three approaches; 1. Target screening, 2. Suspect screening, 3. Non-target screening. When the information of targeted substances (database or suspect screening lists) can be obtained, target screening or suspect screening should perform. In contrast, when any information of target substances can not be obtained, non-target screening should perform. Most of the previous studies in the qualitative analysis field were target MS/MS using HRMS to provide more confidence level of identification and updating to the database. This thesis has three chapters; a profile analysis with the suspect screening of PFASs was examined to understand the characteristics of PFASs contamination in firefighting foam impacted waters (Chapter 4), a data-independent method linking precursor and fragment ions by drift time was developed using ion mobility mass spectrometry to improve identification confidence level (Chapter 5), and the linking method based on fragmentation flagging to search for the precursor ions of unknown PFASs were developed (Chapter 6).

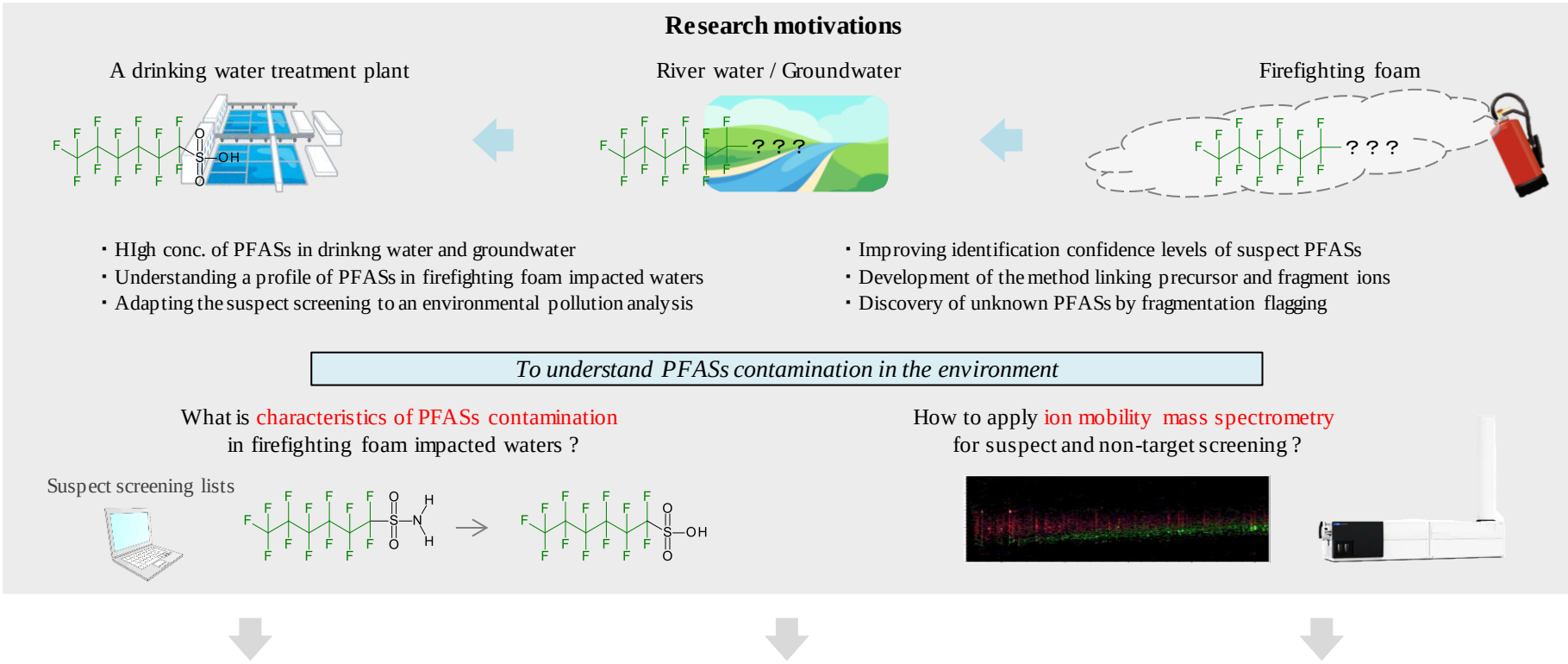

Fig. 1.2 Research motivations and main objective of this study

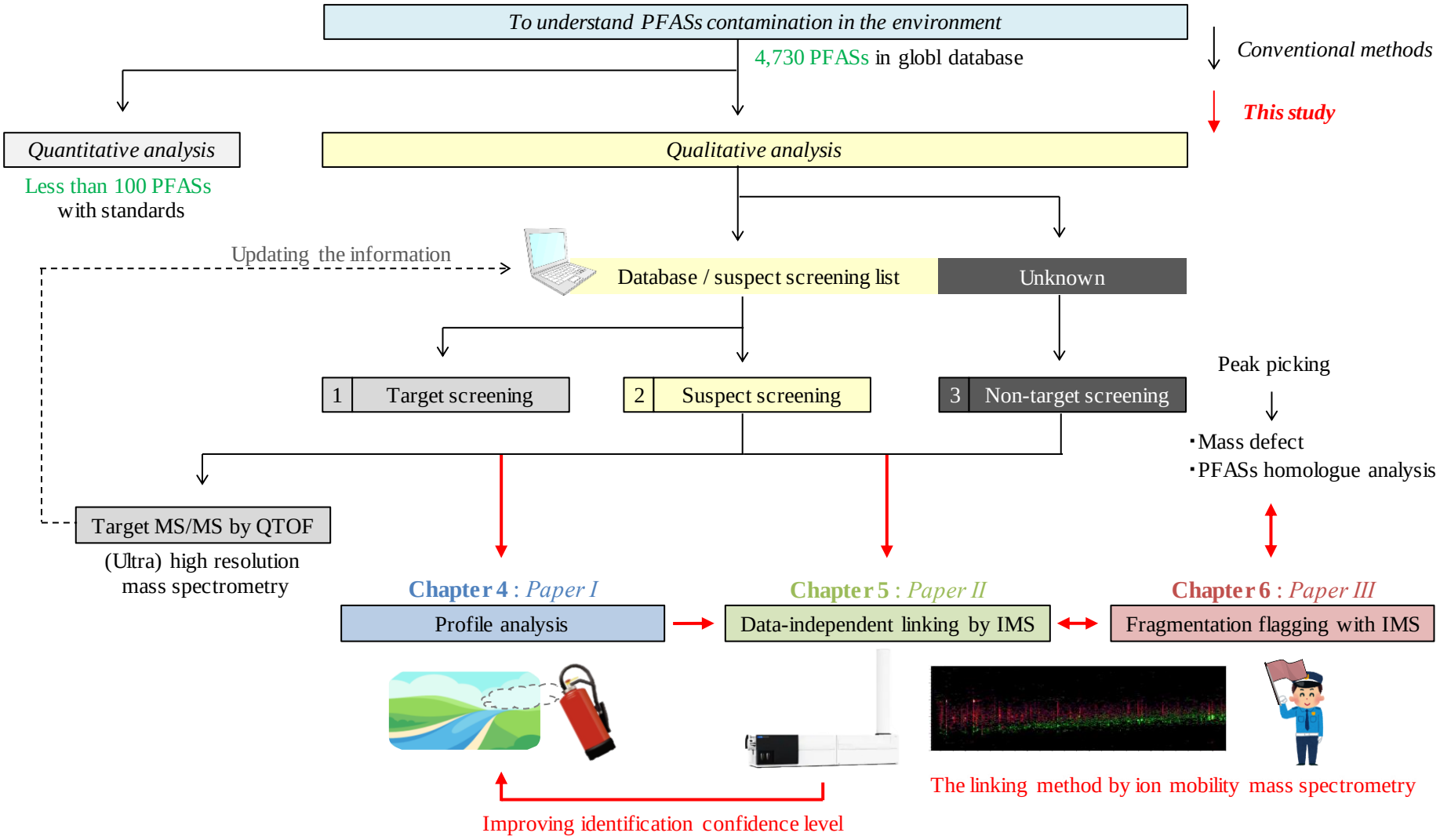

Fig. 1.3 Scope of this study in the qualitative analysis field of PFASs

The framework of this study was shown in **Fig. 1.4**. The frame work of this thesis has Introduction (Chapter 1), Literature Review (Chapter 2), Materials and Methods (Chapter 3), Results and Discussion (Chapter 4, 5, 6), and Conclusion and Future Perspective (Chapter 7).

Study on Suspect and Non-Target Screening of Per- and polyfluoroalkyl substances (PFASs) by Ion Mobility Mass Spectrometry

Chapter 1	Introduction
Chapter 2	Literature Review
Chapter 3	Materials and Methods

Paper I

Chapter 4	A profile analysis with suspect screening of PFASs in firefighting foam impacted waters in Okinawa, Japan

- 4.1. Suspect screening of PFASs in firefighting foam impacted waters
- 4.2 Profile analysis of PFASs in firefighting foam impacted environment waters
- 4.3 Behavior of PFASs in drinking water treatment processes

Paper II

Chapter 5	A new data-independent method linking precursor and fragment ions of PFASs by drift time using ion mobility mass spectrometry

- 5.1 Suspect screening of PFASs for firefighting foam impacted groundwater
- 5.2 A data-independent method linking precursor and fragment ions by drift time using ion mobility mass spectrometry
- 5.3 Evaluation of linking method with focus on the intensity of co-eluting ions

Paper III

Chapter 6	A method to search for PFASs by linking fragmentation flags with their precursor ions by drift time using ion mobility mass spectrometry

- 6.1 Classification of fragment ions and selection of fragmentation flags
- 6.2 Fragmentation flagging for Standards and a product
- 6.3 Linking fragmentation flags with their molecular ions by drift time using ion mobility mass spectrometry for PFAS standards mixture solution
- 6.4 Practical example of the linking method for a household fire extinguisher liquid

Chapter 7	Conclusion and Future Perspective

Fig. 1.4 Framework of this thesis

Chapter 2

Literature Review

2.1 Classification and scope of PFASs

PFASs are a group of anthropogenic organic fluorinated compounds that have been widely used in various industrial, commercial, and consumer products. In 2019, the OECD reported a new comprehensive Global Database of 4,730 PFAS with CAS numbers (OECD, 2019). More than 3,000 PFASs have been manufactured on the global market (KEMI (Swedish Chemicals Agency), 2015). Therefore, there have been concerns that various types of PFAS may be present in the environments. The classification of PFASs was shown in **Fig. 2.1** (Wang et al., 2017; Sha et al., 2019). PFASs have categorized perfluoroalkyl acids (PFAAs), PFAA precursors, and others. In addition, PFAAs divided into perfluoroalkyl sulfonic acids (PFSAs), perfluoroalkyl carboxylic acids (PFCAs), perfluoroalkyl phosphoric acids (PFPAs), and per- and polyfluoroether sulfonic/carboxylic acids (PFESAs / PFECAs). The precursor of PFAAs divided into perfluoroalkane sulfonyl fluoride (PASF)-based substances and fluorotelomer-based substances. PASF-based substances are PFSA precursors (e.g., perfluoroalkyl sulfonamides (FASAs)). The fluorotelomer-based substances are PFCA precursors (e.g., fluorotelomer alcohols (FTOHs), fluorotelomer sulfonic acids (FTSs)). To understand their different types of PFASs in the environments, it is necessary to perform quantitative/qualitative analysis using several types of analytical instruments and evaluations [e.g., liquid chromatography (LC), tandem mass spectrometry (MS/MS), time-of-flight mass spectrometry (TOF-MS), combustion ion chromatography (CIC), Total oxidizable precursors (TOP) assay]. The scope of PFASs was shown in **Fig. 2.2** (McDonough et al., 2019; Koch et al., 2019). The PFASs categorized such as; total fluorine (TF) > total organic fluorine (TOF) > extractable organic fluorine (EOF) [analyzed by CIC] > LC-amenable PFASs [analyzed by LC-HRMS] > precursors to targeted PFASs [evaluated by TOP assay] > targeted PFASs [analyzed by

LC-MS/MS]). A previous study analyzed TOF in environmental samples by CIC (Miyake et al., 2007). The proportion of PFAAs among EOF in fish samples ranged from 10% to 12%, therefore, a significant proportion of PFASs might remain unidentified (Loi et al., 2011). A previous study reported that TOP assay which precursors change to PFAAs by an experimental oxidative decomposition is effective to understand unknown the potential of PFAAs precursors. (Houtz et al., 2012). This evaluation method can comprehensively understand the amount of PFAA precursors. It is important to understand PFASs contamination from multiple perspectives using various types of analytical instruments and evaluations.

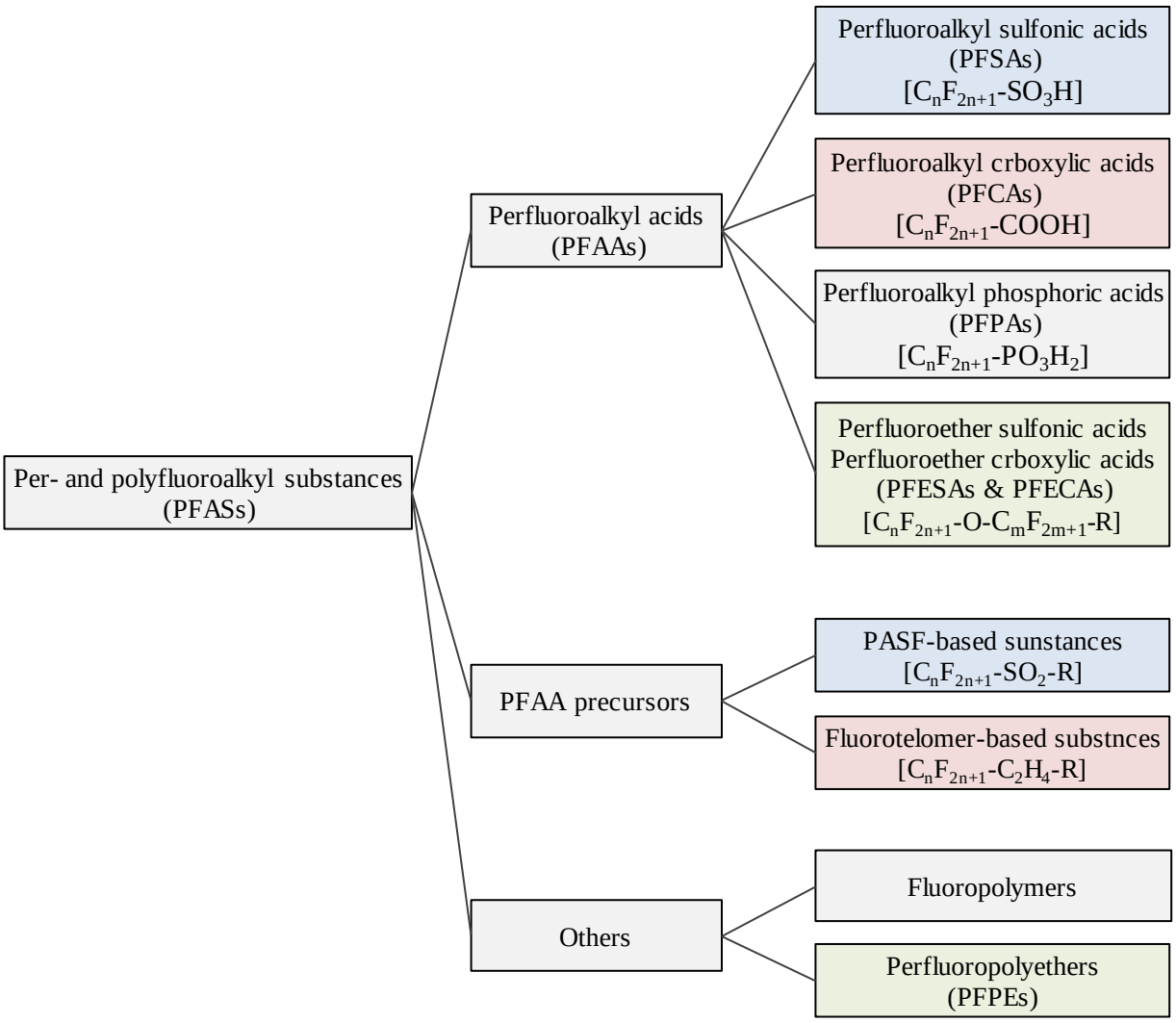

Fig. 2.1 Classfication of PFASs (Wang et al, 2017; Sha et al, 2019)

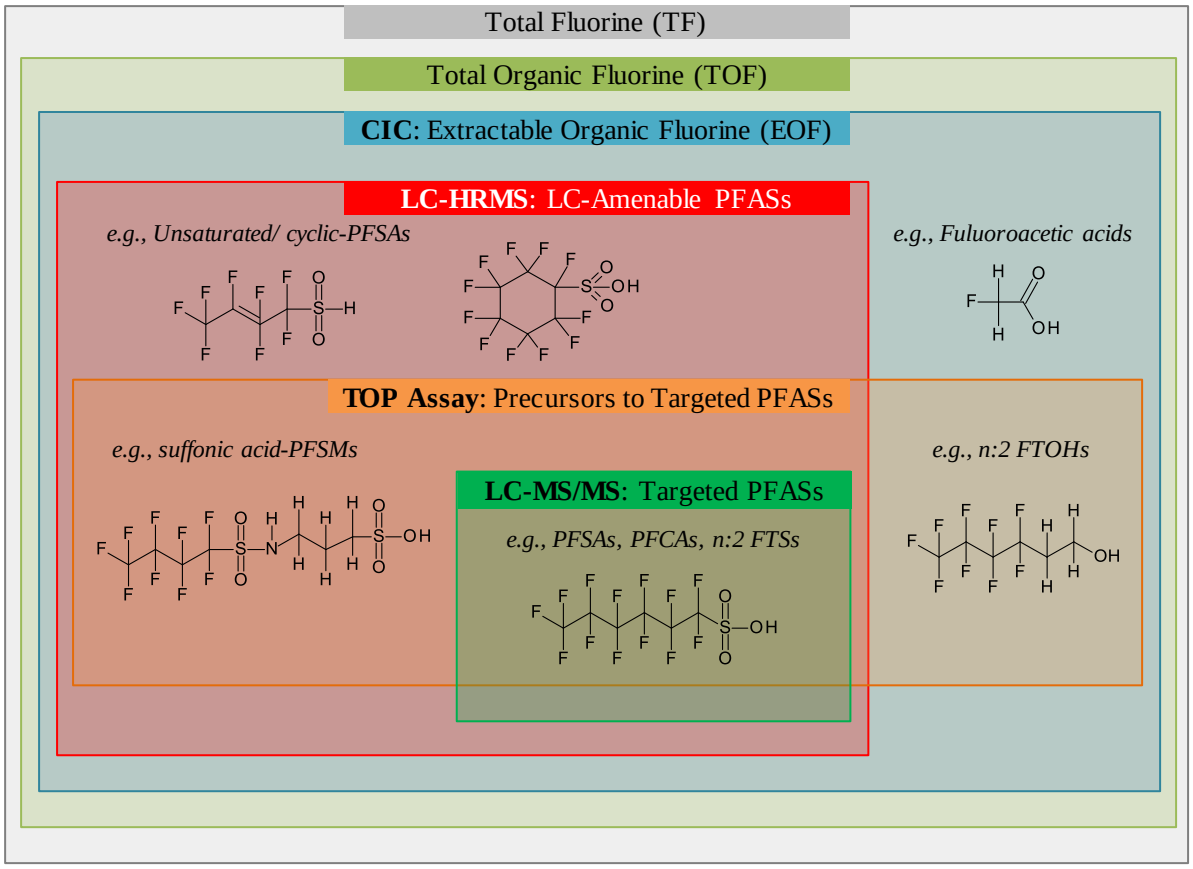

Fig. 2.2 Scope of PFASs (McDonough et al, 2019; Koch et al, 2019)

2.2 PFASs in firefighting foam impacted waters

The use of firefighting foam has been suspected as an important cause of PFASs contamination in environmental waters. The previous studies of PFASs in firefighting foam impacted environments were shown in **Table 2.1**. Some kinds of firefighting foam are aqueous film-forming foams (AFFF). They are used in firefighting training areas (e.g., airport, military area), and untreated water may be discharged to the environments. In a previous report, there were ten PFASs classes (perfluoroalkyl chain lengths ranging from 4 to 12) in the US military-certified AFFF (Place et al., 2012). In addition, 22 PFAS classes of AFFF and commercial fluorinated surfactant concentrates (perfluoroalkyl chain lengths ranging from 3 to 15 for a total of 103 compounds) were identified (D'Agostino et al., 2013). It was expected that leaching and transport of PFASs derived from AFFF in the unsaturated soil at firefighting training area according to experimental tests (Høisæter et al., 2019). It was shown that, in particular, ultra-short-chain PFSAs released into the environment from the firefighting training area through groundwater (Björnsdotter et al., 2019). The result shows considerable potential for PFAAs to expand from the source either due to leaching or uptake into biota. This may be a potential entry route into the terrestrial food web (Bräunig et al., 2019). It was expected that much of the mass of precursors released at the site was converted to PFCAs and PFSAs in groundwater. Thus, one of the critical points is the occurrence and behavior of precursors of PFAAs to understand PFASs contamination (**Fig. 2.3**) (Harding-Marjanovic et al., 2015; Joudan et al., 2019). For example, perflurohexane sulfonamide (FHxSA) formed PFHxS, and 6:2 FTS formed perflurohexanoic acid (PFHxA) by environmental influences. Suspected intermediate transformation products of PFAA precursors in AFFF accounted for approximately half of the total precursor concentration in samples from the training site (Houtz et al., 2013). It was confirmed that intermediate substances from PFAA precursors during the biotransformation may accumulate (Harding-Marjanovic et al., 2015). Therefore, it is important to understand PFASs contamination including PFAA precursors and transformation products in firefighting foam impacted waters.

The risk of human exposure through drinking water sourced from firefighting foam impacted waters is a global concern. For the PFASs exposure risk of humans, the highest total PFAS concentrations were recorded in the monitoring wells around the firefighter training area (Dauchy et al., 2019). In a previous report, the drinking water supplies for 6 million residents around private airports exceed US Environmental Protection Agency's PFOA and PFOS drinking water health advisory of 70 ng/L were found. (Hu et al., 2016). The childhood exposure to PFOA, PFHxS, and PFOS is a determinant of child serum levels and may have the greatest impact on younger ages. It was concluded that drinking water with perfluorobutanesulfonic acid (PFBS), PFHxS, PFOS, and PFOA contamination is an essential source of exposure for children there (Gyllenhammar et al., 2019). Therefore, it is necessary to investigate PFASs contamination derived from firefighting foam in drinking water to understand human health risk. However, quantitative analysis on target analysis has been still mainstream, and it is necessary to understand deeply including unknown PFASs in the future.

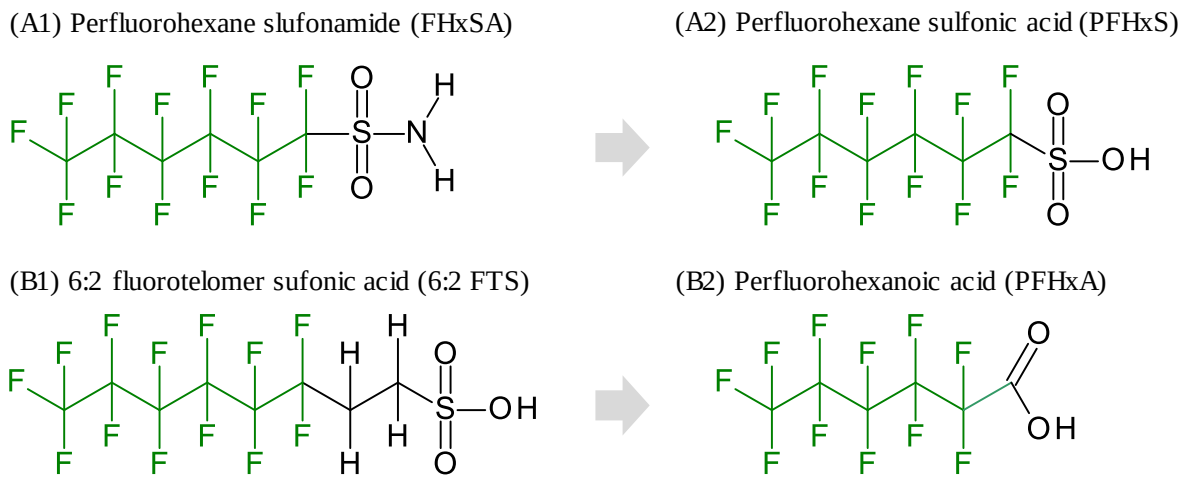

Fig. 2.3 Examples of degradation pathways from the precursors to PFAAs (Harding-Marjanovic et al, 2015; Joudan et al, 2019)

Table 2.1 Previous studies of PFAS in firefighting foam impacted environments

Samples	Country	Contents	Reference
AFFF surfactants	China	PFOS alternatives target analysis (EPA537), TOP assay	Mumtaz et al, 2019
AFFF surfactants, water	France	Target analysis, TOP assay	Dauchy et al, 2017
Surface water	Canada	Estimating the contaminated sites	Milleyr et al, 2018
Surface water	Canada	Target analysis, EOF	D'Agostino et al, 2017
Freshwater, aquatic invertebrates	Sweden	Target analysis, EOF	Koch et al, 2019
Grouundwater	Canada	Target analysis, TOP assay	Martin et al, 2019
Groundwater	United States	Target analysis, TOP assay, vertical profil	Weber et al, 2017
Groundwater	Australia	Fate and redistribution	Bräunig et al, 2017
Groundwater, sediments, soil	Italy	Target analysis	Sammut et al, 2019
Groundwater, soil	France	Target analysis, TOP assay	Dauchy et al, 2019
Groundwater, surface water, landfill leachate	Sweden	Target analysis, ultra-short-chain PFCAs	Björnsdotter et al, 2019
Groundwater surface water, soil	United States	Target analysis, field validation of critical fate and transport properties	Anderson et al, 2016
Groundwater, lake soild, fish	Sweden	Target analysis	Filipovic et al, 2015
Water, sediment, fish	Sweden	Target analysis	Ahrens et al, 2015
Freshwater fish, sediments	Canada	Target analysis	Munoz et al, 2017
Soil	Canada	Optimization of extraction methods, profiling of PFASs	Munoz et al, 2018
Soil	Canada	Target analysis	Mejiao et al, 2017
Unsaturated soil	-	Column study, sorption	Høisæter et al, 2019
Soil	-	Sorption, apparent Log(K_{oc}) estimation	Anderson et al, 2019
Soil	-	Target analysis, sorption	Li et al, 2018
Biopile soil	-	Biotransformation, target analysis	Li et al, 2019
Soil, earthworms	-	Exposure test, bioaccumulation	Rich et al, 2015
Groundwater, soil	-	In sity chemical oxidation(ISCO) treatment	Eberle et al, 2017
AFFF surfactants	-	Sonochemical degradation	Rodriguez et al, 2016
Groundwater	-	Electrochemical treatment	Schaefer et al, 2018

2.3 Qualitative analysis by high-resolution mass spectrometry

As mentioned above, target analysis can be used to quantify known PFASs when authentic standards are available, but standard chemicals are not provided for all substances. Therefore, most recent studies in the qualitative analysis field have used three screening methods—target screening, suspect screening, and non-target screening to cover the various type of PFASs (Fig. 1.3) (Hollender et al., 2017). For example, when the database of target substances with the information (e.g., precursor ion, fragment ions, or retention time (RT)) was obtained, target screening should be performed. When the suspect screening list of target substances with the molecular formulas was obtained, suspect screening should be conducted. When no information of target substances, such as database or suspect screening list, were obtained, non-target screening should be performed. Therefore, recently suspect and non-target screening has been developed to discover the unknown PFASs in the environments. The number of articles regarding the analysis of PFASs using high-resolution mass spectrometry was shown in **Fig. 2.4**. From 2015, the number of articles was getting increased. This study focused on fragmentation flagging and ion mobility mass spectrometry. Their explanations are described in detail in the next part. Previous studies of the suspect and non-target screening for PFASs were shown in **Table 2.2**. Recently, novel PFASs have been reported by using suspect screening against a database in AFFF (Barzen-Hanson et al., 2017), airborne particulate matter (Yu et al., 2018), and wastewater (Wang et al., 2018). Therefore, nowadays some of the suspect screening lists could be obtained in the NORMAN suspect list exchange or the U.S.EPA CompTox Chemistry Dashboard (NORMAN network, 2019). However, it is challenging to discover unknown PFAS homologs by the screening of known molecular formulas based on the external database. The development of a quick and simple method is needed to understand the occurrence of unknown PFASs in the environment. A “non-target” R script approach was examined for AFFF and/ or AFFF-impacted groundwater (Barzen-Hanson et al., 2017). Non-target screening based on a unique mass defect (exact mass − nominal mass, >0.85 or <0.15 unit of CF_2) was developed for filtering and classification of PFASs (Yu et al., 2018). These methods targeted on the precursor ions

of unknown PFASs. PFCAs generate perfluoroalkyl anion fragments (e.g., $[CF_3]^-$, $[C_2F_5]^-$) in LC-MS/MS (Arsenault et al., 2007). Such perfluoroalkyl fragment ions might be used as flags for non-target screening. In 2015, a new non-target screening method using in-source fragmentation flagging to discover unknown PFASs was used in the first report of fragmentation flagging (Liu et al., 2015). The method identifies common fragment ions—fluoroalkyl groups ($[C_2F_5]^-$, *m/z* 118.9920; $[C_3F_7]^-$, *m/z* 168.9888) and others ($[SO_4H]^-$, *m/z* 96.9596; $[Cl]^-$, *m/z* 34.9689)—for prediction of chemical formulas. In fish liver samples, it found over 330 PFASs (Liu et al., 2018). Thus, non-target screening based on fragmentation flagging makes it possible to detect unknown PFASs. Xiao et al. also reported a high resolution precursor ion search to identify PFASs in commercial surfactants (Xiao et al., 2017). Here are examples of substances that generate common fragment ions other than PFASs. Beilawski et al. reported that the novel bioactive sphingolipids have common fragment ions (Beliawski et al., 2006). Xiao et al. observed that biotransformation of the organochlorine pesticide chlordane has common fragment ions (Xiao et al., 2011). In the proteomics field, a previous report suggested that MSFragger was ultrafast and comprehensive peptide identification method (Kong et al., 2017) Therefore, it is necessary to develop the fragmentation flagging approach to discover unknown persistent organic pollutants.

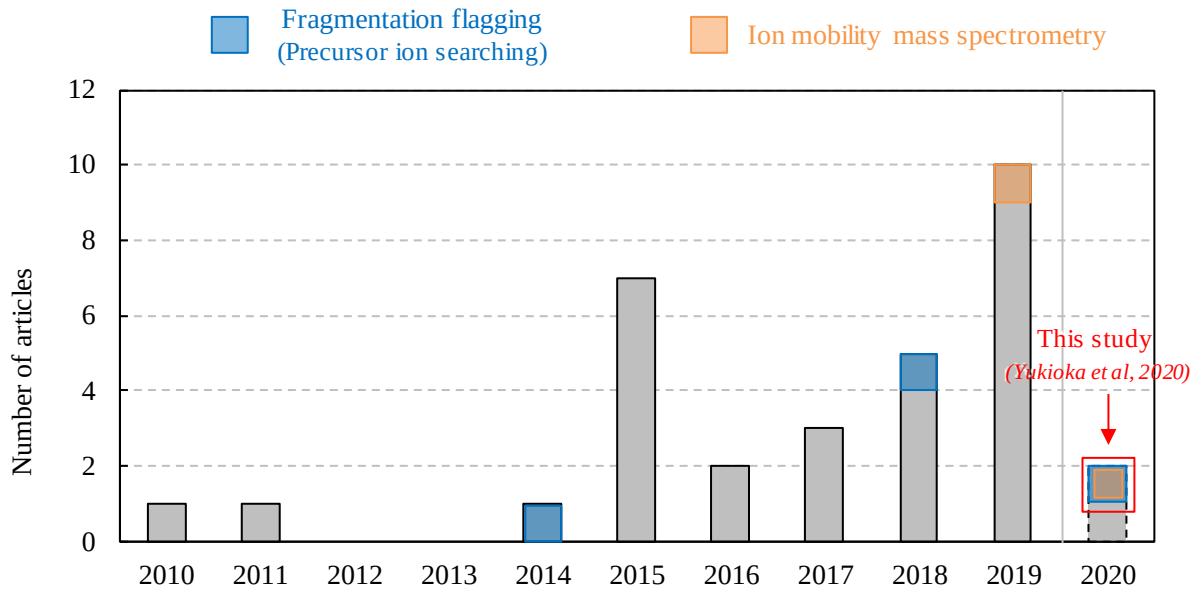

Fig. 2.4 The number of articles regarding qualitative analysis of PFASs using high resolution mass spectrometry (searched in Jan. 2020)

Table 2.2 Suspect and non-target screening of PFASs by using high resolution mass spectrometry

Target PFASs/ products	LC/GC	HRMS	Approaches	Reference
20 PFAS standards AFFF surfactants	LC	IMS-QTOF-MS	Fragmentation flagging Linking by IMS	This study (Yukioka et al, 2020)
PFAS isomers	LC	FAIMS-MS	Separation of PFASs isomers	Ahmed et al, 2019
AFFF surfactants	LC	QTOF-MS	Non-target screening	Dubocq et al, 2019
AFFF surfactants (hydrocarbon surfactants)	LC	QTOF-MS	Suspect screening	Garcia et al, 2019
PFECAs, PFESAs	LC	QTOF-MS	Non-target screening	McCord et al, 2019
125 PFASs	LC	QTOF-MS	Suspect screening Non-target screening PFASs homologue analysis	Yu et al, 2018
90 PFASs	LC	QTOF-MS	Suspect screening Non-target screening	Wang et al, 2018
Over 330 other fluorinated analytes	LC	QTOF-MS (Orbitrap)	Non-target screening fragmentation flagging	Liu et al, 2018
24 PFAS standards	LC	IMS-QTOF-MS	Precursor ion searching	Xiao et al, 2017
PFECAs, other PFASs	LC	QTOF-MS	Non-target screening	Newton et al, 2017
AFFF surfactants	LC	QTOF-MS	Suspected screeeinig Non-target screening Mass defect Non-target Rscript	Barzen-Hanson et al, 2017
PFCAs, PFSAs, PFSiAs, PFSAs-Ketone, FTSs, FASAs, FASEs, Cl-PFSAs, Cl_2-PFSAs	LC	QTOF-MS	Mass defect	Baduel et al, 2017
PFECAs, PFESAs	LC	TOF-MS	Non-target screening Mass defect	Strynar et al, 2015
PFSAs, Cl-PFOS, Ketone-PFOS, Ether-PFHxS, Cl-PFHxS	LC	QTOF-MS	Target screening Non-target screening	Rotander et al, 2015
HPFCAs, Cl-PFCAs, PFSs, H-PFE/As, Cl-PFE/As	LC	QTOF-MS (Orbitrap)	In-Source Fragmentation flagging	Liu et al, 2015
AFFF surfactants	LC	QTOF-MS FTICR-MS	Non-target screening Mass defect	D'Agostino et al, 2013

QTOF-MS: Quadrupole-time-of-flight mass spectrometry
IMS: Ion mobility mass spectrometry
FAIMS-MS: High-field asymmetric waveform ion mobility mass spectrometry
FTICR-MS: Fourier transform ion cyclotron resonance mass spectrometry

2.4 Ion mobility mass spectrometry

In this study, a new linking method uses ion mobility spectrometry, which separates ions by size, shape, charge, and mass (**Fig. 2.5**) (Borsdorf et al., 2006; Creaser et al., 2004; Lanucara et al., 2014). The number of peer-reviewed papers of ion mobility mass spectrometry has been increasing from 2000 (Lanucara et al, 2014). Especially, the application toward biomolecules is the current hot topic. There are three types of ion mobility spectrometry; drift time ion mobility spectrometry (DTIMS), traveling wave ion mobility spectrometry (TWIMS), and field asymmetric ion mobility spectrometry (FAIMS). This study focused on drift time ion mobility spectrometry is evaluated by the "collision cross section (CCS)" calculated from drift time. Substances are separated in a LC column, and their ions are further separated in a drift tube by ion mobility spectrometry. Their drift times can explain by CCS which is one of the molecular structure properties. The Mason-Schamp equation provided the relation between the mobility of ions and CCS. The CCS is a value of molecular information in three-dimensional space on a two-dimensional plane and the average value of the projected area for each plane (Borsdorf et al, 2006). The CCS is an index of ion size and shape. Thus, it is effective to separate the isomers of precursor ions by the difference of drift times (Wu et al, 2000). For an example of PFASs, Ahmed et al suggested that rapid separation for isomers of PFOS using the ion mobility-based method using field asymmetric ion mobility spectrometry (Table 2.2) (Ahmed et al, 2019). In addition, after precursor ions passed into a drift tube, fragment ions are generated in a collision cell, and the switching collision energy (CE) (μs) is faster than the drift time (ms). Therefore, the precursor ion and the fragment ions are linked because they can be observed in the same drift time range (Steiner et al., 2001; Steiner et al., 2003). However, there has been not well known for the application of ion mobility for mass spectrometry the suspect and non-target screening in the environmental research field. Therefore, this study suggested that a new method to search PFASs by linking common fragment ions with their precursor ions using drift time ion mobility mass spectrometry (Table 2.2) (Yukioka et al, 2020).

$$\frac{L}{t_{drift}} = v = KE$$

$$K = \left(\frac{3q}{16N}\right)\left(\frac{2\pi}{\mu k_B T}\right)^{1/2}\left(\frac{1}{\Omega}\right)$$

- L : drift tube length
- t_{drift} : drift time
- v : drift velocity
- K : measured mobility at 273.15 K, 101325 Pa
- E : electric field
- q : charge of analyze ion
- N : density of the drift gas
- μ : (1/mass of the analyte ion)+(1/mass of the drift gas)
- k_B : the Boltzmann constant
- T : gas temperature
- Ω : collision cross section (CCS)

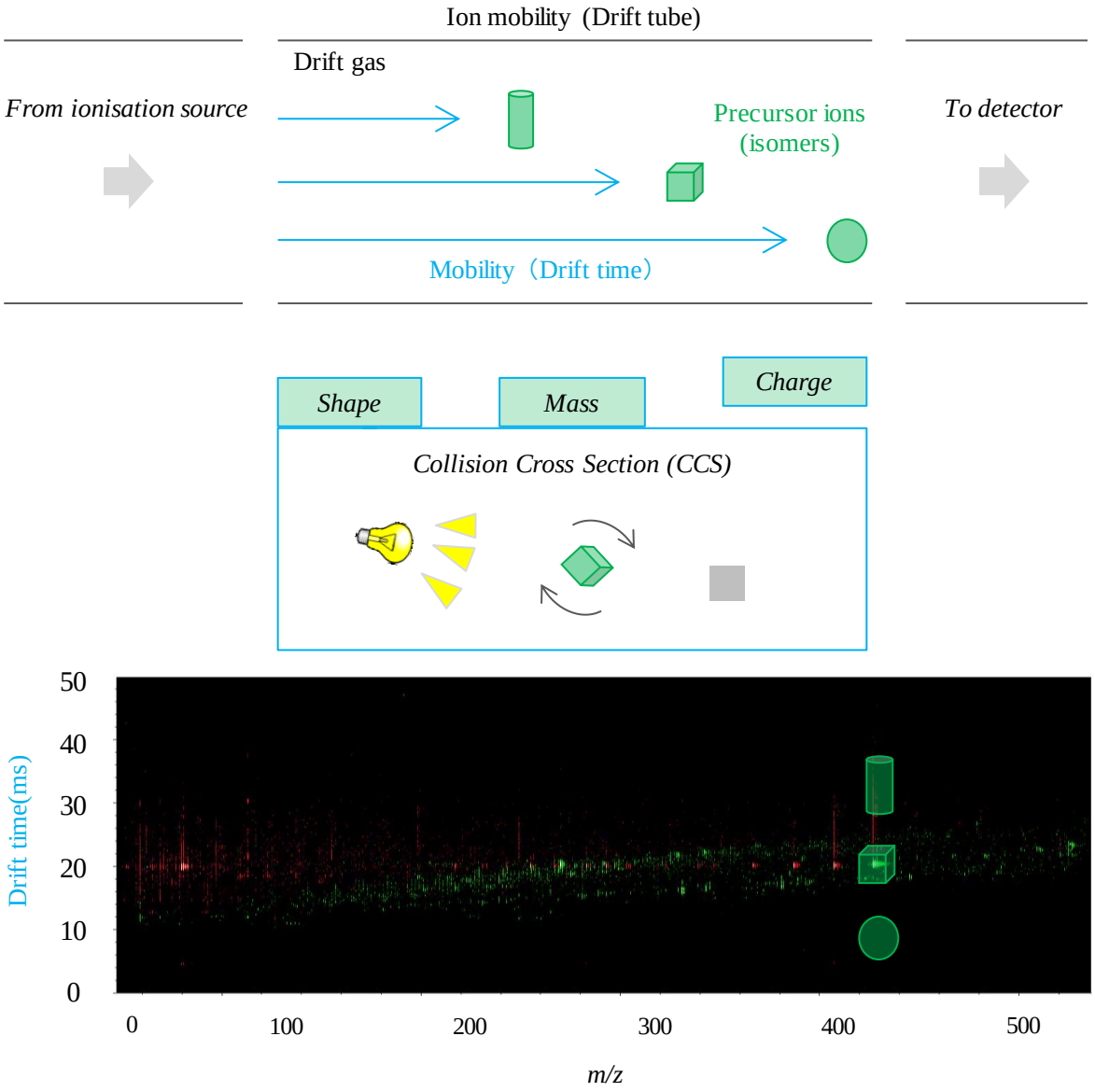

Fig. 2.5 Separation of precursor ions (e.g. isomers) by ion mobility mass spectrometry (Borsdorf et al., 2006; Creaser et al., 2004; Lanucara et al., 2014)

Chapter 3

Materials and Methods

3.1 Chemicals and Standards

All chemicals used for PFAS analysis were LC-MS grade unless otherwise specified. Methanol (MeOH), acetonitrile (ACN), and 1 M ammonium acetate solution were purchased from Wako Pure Chemical (Japan). Two samples were prepared comprising standard mixture solution with 34 PFASs and a household fire extinguisher liquid which was purchased at the Japanese local market in 2016. The product is mainly composed of potassium carbonate and contains a wetting agent. All standards were purchased from Wellington Laboratories, Tokyo Kasei, Wako Pure Chemical, or Sigma-Aldrich. The standard solution spiked with PFASs comprised 12 PFCAs, 3 PFSAs, 3 PAPs (polyfluoroalkyl phosphate esters), 5 FTCAs (fluorotelomer carboxylic acids), 3 FTUCAs (fluorotelomer unsaturated carboxylic acids), 3 FTSs, 3 FASAs, and 2 FASAAs (perfluoroalkyl sulfonamide acetic acids). All standards in the solution were adjusted to 10 ng/mL in MeOH. The household fire extinguisher liquid sample was diluted 1:100 in MeOH.

3.2 Sample collection of firefighting foam impacted waters in Okinawa, Japan

Water samples were collected from a DWTP, rivers, and belowground in Okinawa on 8 April 2019 (**Fig. 3.1**, **Fig. 3.2**, and **Table 3.1**). DWTP samples were collected at each stage of treatment: influent water (river or dam water), ozonation tank effluent, biological activated carbon (BAC) filtration effluent, groundwater treated by hardness reduction, and treated water). The groundwater treated by hardness reduction (about 15% of the total water volume in the DWTP) was mixed with BAC effluent (about 75%) at the tank because of a water shortage in the area. River water samples were collected in the Nagata river (R1), the Hijya river (R2–R4), and the Dakujyaku river (R5). The DWTP takes in source waters from R1

(about 15% of the total water volume) and R2 (about 75%). Groundwater was collected from wells around the firefighting training area (e.g., G1–G8).

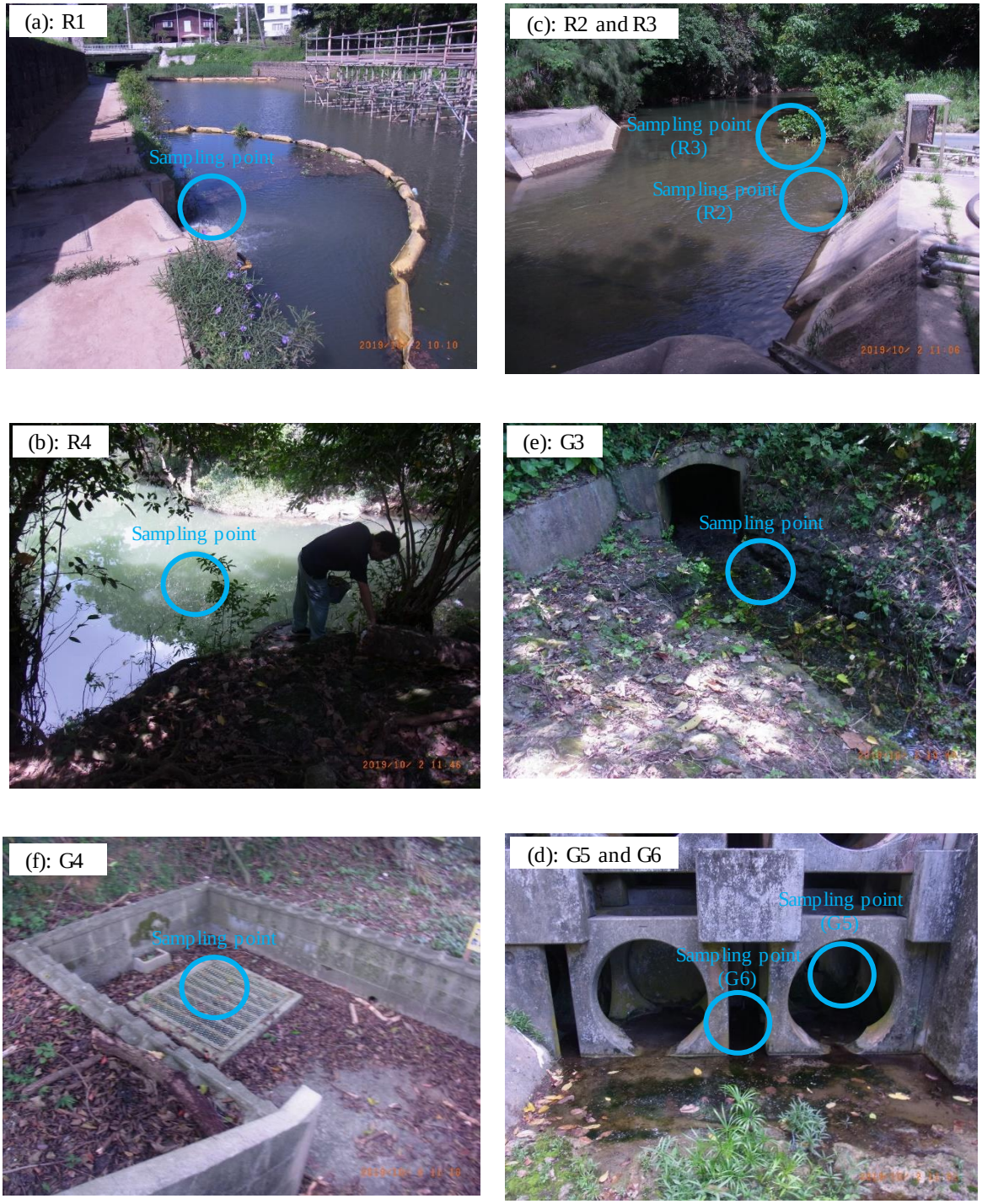

Fig. 3.1 The photos of sampling points in Okinawa, Japan

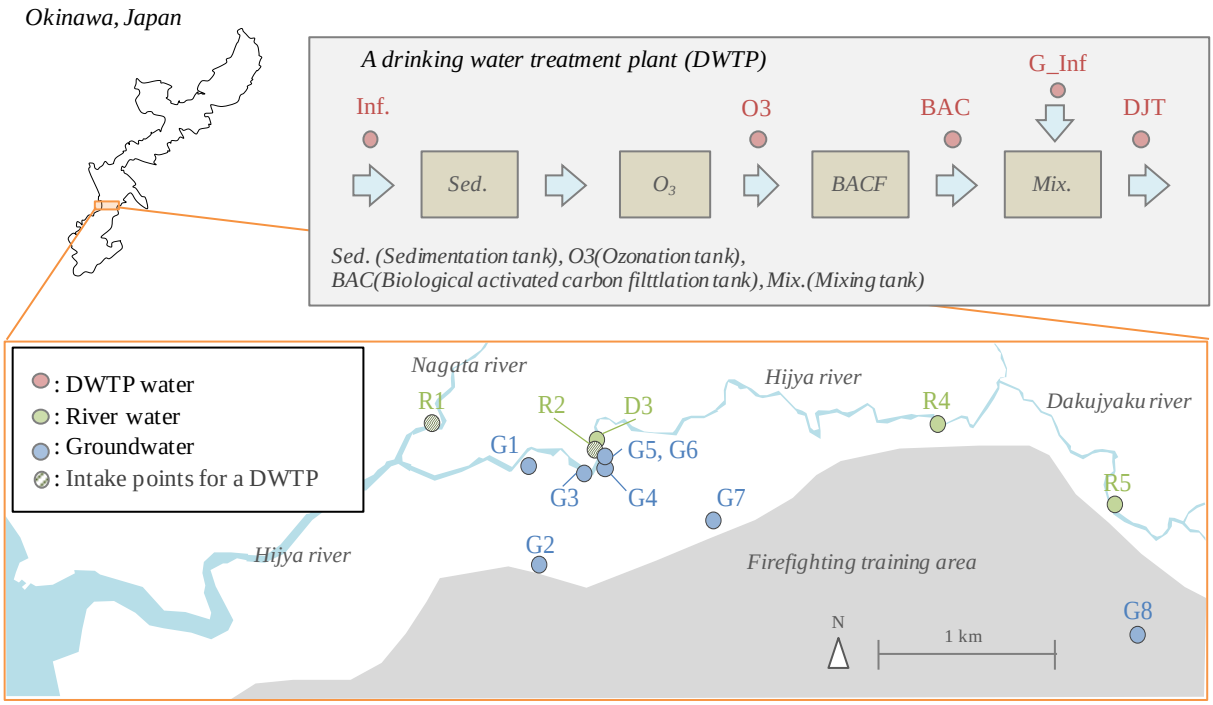

Fig. 3.2 Sampling points in Okinawa, Japan

Table 3.1 The information of sampling points in Okinawa, Japan

No.	Types	ID	Sample Name	Filtering	GPS
1	DWTP water	Inf.	Influent (river/dam water)	Yes	-
2		O3	Ozonation tank effluent water	No	-
3		BAC	Biological activated carbon filtration tank effluent water	No	-
4		G_Inf	Influent (groundwater) treated by hardness reduction process	No	-
5		Eff.	Treated water	No	-
6	River water	R1	Nagata river	Yes	N 26°22'09.696",E 127°45'24.094"
7		R2	Hijya river (the pump station)	Yes	N 26°22'06.052",E 127°45'51.926"
8		R3	Hijya river (upstream of the pump station)	Yes	N 26°22'06.362",E 127°45'51.444"
9		R4	Hijya river (Yaramuruchi)	Yes	N 26°22'09.8",E 127°46'49.5"
10		R5	Dakujyaku river	Yes	N 26°21'58.0",E 127°47'18.7"
11	Groundwater	G1	Groundwater (Nuruga)	No	N 26°22'03.543",E 127°45'40.046"
12		G2	Groundwater (An observation hole around Yara bus stop)	Yes	N 26°21'48.596",E 127°45'42.714"
13		G3	Groundwater (Yarahijyaga)	No	N 26°22'03.712",E 127°45'50.752"
14		G4	Groundwater (Ubuga)	No	N 26°22'06.369",E 127°45'53.247"
15		G5	Groundwater (Around Hijya river pump station) Ishigaki effluent water (pipe)	No	N 26°22'06.308",E 127°45'51.893"
16		G6	Groundwater (Around Hijya river pump station) Ishigaki effluent water (gap)	No	N 26°22'06.308",E 127°45'51.893"
17		G7	Groundwater (An observation hole at Yara park No.2)	Yes	N 26°21'56.840",E 127°46'11.560"
18		G8	Groundwater	No	N 26°21'38.656",E 127°47'22.271"

3.3 Pretreatments

To avoid contamination with PFASs, all *Milli-Q* water were purified through PresepC-Agri (C18) cartridges (Wako, Japan) and Oasis HLB cartridges (Waters) and used an experimental blank (n = 1). Some collected samples were pre-filtered through glass fiber filter (1 μm, Whatman) to remove the solid particles (**Fig. 3.3**). Dissolved-phase samples (1000 mL) in polypropylene bottles were solid-phase extracted by passage with a concentrator (Waters) through an Oasis WAX cartridge (Waters). Chemicals were eluted from the cartridge with 2 mL methanol and then 3 mL methanol + 0.1% ammonium. The insides of the bottles were rinsed with 5 mL MeOH and the remaining chemicals were collected and added to the extracts. The extracts were concentrated to 1 mL with a nitrogen purge (40°C).

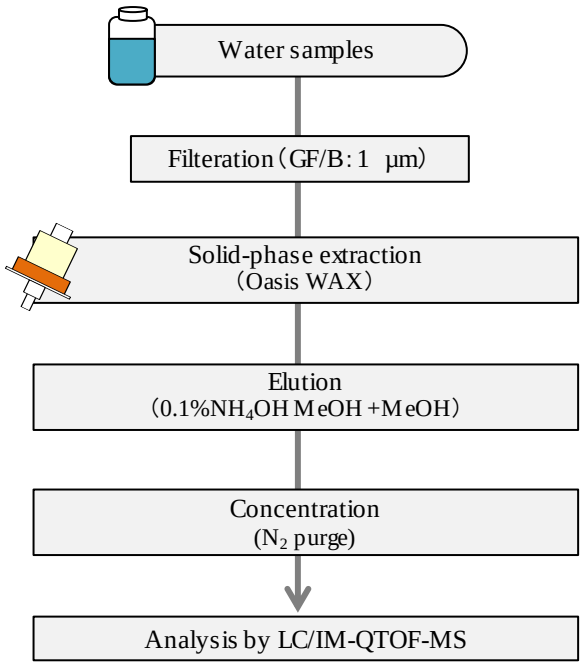

Fig. 3.3 Procedure of pretreatment of water samples

3.4 Analytical conditions

The extracts were concentrated to 1 mL with a nitrogen purge (40°C) and analyzed by LC/IM-QTOF-MS in full scan mode (*m/z* = 50–1700) on an Agilent 1200 SL with Agilent 6560 IM-QTOF system (**Fig. 3.4**). *Milli-Q* water containing ammonium acetate (5 mM) and acetonitrile were used as LC mobile phase. The compounds were separated in a Zorbax Eclipse Plus C18 column (2.1 mm × 100 mm, 1.8 µm, Agilent) and analyzed in dual Agilent Jet Stream mode with negative and positive electrospray ionization (ESI). The instrument was tuned with 85001 solution (Agilent) for mass calibration and confimation of TOF resolution before every batch, and mass-calibrated in real-time by using lock mass chemicals (trifluoroacetic acid, 1H, 1H, 3H-tetrafluoropropoxy, and phosphazine). The TOF resolutions were 9460 at *m/z* 112.9855, 13800 at *m/z* 301.9981, 16800 at 601.9789, and 20160 at 1333.9689 in negative mode, and 9460 at *m/z* 112,9855, 13800 at *m/z* 301.9981, 16800 at 601.9789, and 20160 at 1333.9689 in positive mode. Nitrogen was used as buffer gas in the IMS drift tube for ion separation.

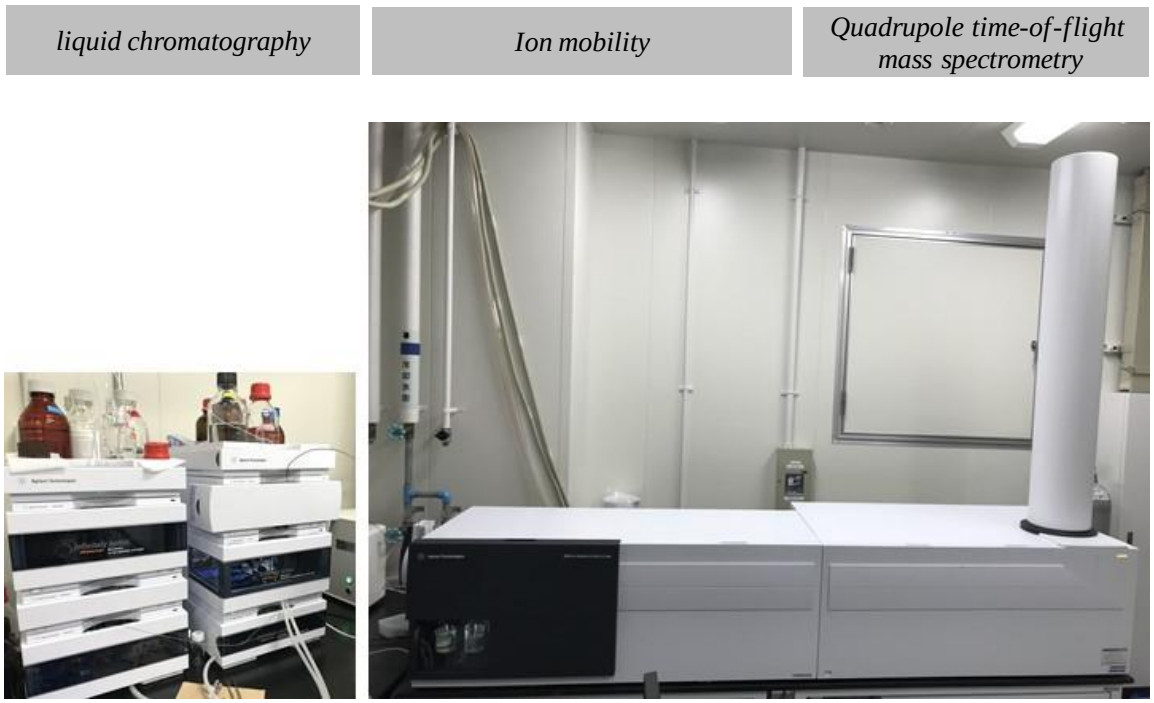

Fig. 3.4 Liquid Chromatography / Ion mobility – Quadrupole Time-of-Flight Mass Spectrometry

3.5 Suspect screening workflow and profile analysis

A PFASs suspect screening workflow was designed for the samples (*n* =18) (**Fig. 3.5**). First, the chromatograms were time-aligned in Profinder 8.0 software (Agilent) (**Table 3.2**). Suspects were screened against molecular formulas in the NORMAN Suspect List Exchange (Nos. 25, 46), a list of PFASs in the OECD PFASs global database compiled by the U.S. EPA (No. 25, 2019), and a list of PFASs discovered by non-target HRMS (No. 46, Liu et al., 2019). The combined list of 4455 PFASs groups had 3236 different molecular formulas because of isomers. Peaks were compared against the combined list (details in **Table 3.3**). Charge carriers [M-H] for negative mode and [M+H] for positive mode were targeted. The match tolerance was ±10 ppm, and the expansion of values for chromatogram extraction was symmetric *m/z* ±0.01. Excluding blank contamination and decarboxylation peaks were conducted. The calculation of identification scores with consideration of mass, isotope abundance, and isotope spacing is described in Supplemental Data. The compound groups were selected with identification scores of >75% in four or more samples (**Fig. 3.6**). Then, the compound groups were regrouped in negative and positive modes. The compound groups were matched in the pre-list and the structural information in the original screening lists (name, SMILES, CAS, PubChem ID, Chemspider ID, structure category, functional groups, perfluoroalkyl chain length, PFAS types. When there were candidate structures for each PFAS formula, they were selected according to list No. 46, because they were detected in environmental or human samples (Liu et al., 2019). List of proposed PFASs with confidence level 4 (unequivocal molecular formula) as suggested previously (Schymanski et al., 2014) was obtained.

After the suspect screening, cluster analysis was performed on the characteristics of PFASs contamination of river water and groundwater samples, using information on 116 proposed PFASs peak areas between sampling points. From similarities between variables, the 116 proposed PFAS were classified into five clusters and calculated the Euclidian distance by Ward's method.

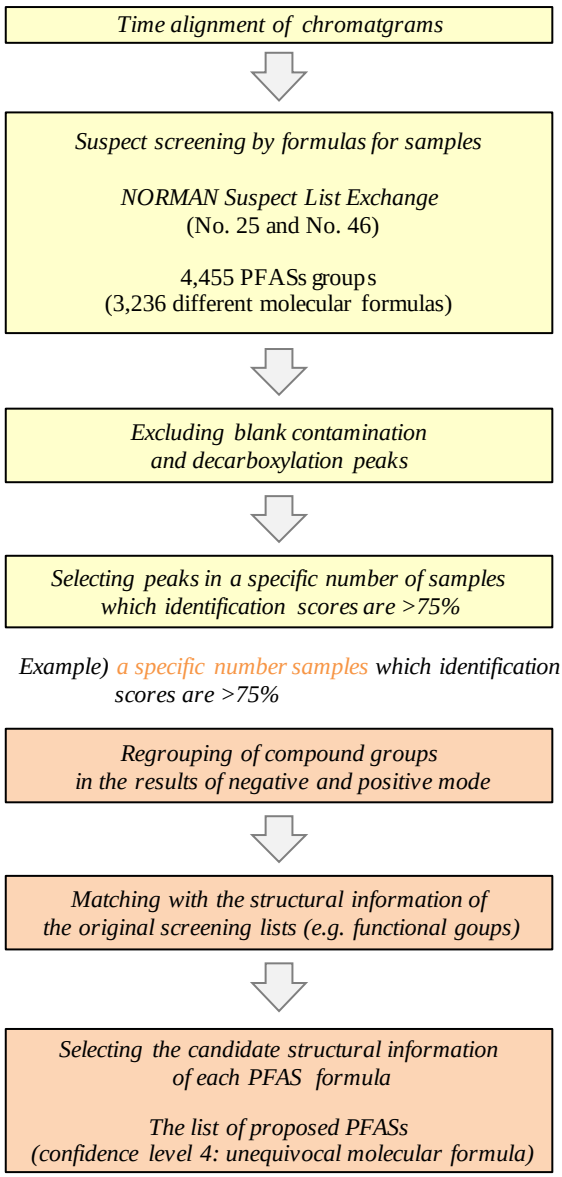

Fig. 3.5 Suspect screening workflow by molecular formulas

Possibility Equations

$P = e^{y}$ $(y = x_2/\sigma_2)$

Score Calculation

$Score = (W_{mass} \times P_{mass} + W_{abundance} \times P_{abundance} + W_{spacing} \times P_{spacing}) / (W_{mass} + W_{abundance} + W_{spacing})$

$W_{mass} = 100.0$

$W_{abundance} = 60.0$

$W_{spacing} = 50.0$

Table 3.2 The condition of time alignment of chromatograms by an analytical software

Suspect screening conditions			The conditions of this study
Time alignment	Time alignment mode	Wtith reference data file	G3
	Time alignment range	Feature extraction for time alignment	Peak heights: >= 1000 counts
		Istope model	Common organic molecules
	Cross-sample variation	Max time shift	±2 min + 0.1%
	Curve-fitting model		Polynominal interpolation

Table 3.3 The detail condition of suspect screening

Suspect screening conditions			Setting of this study
Formula targets	Formula source	Database	"Suspect screening list"
		Matches per formula (Maximum number of matches)	1
		Values to match	Mass
	Negative / Positive Ions	Charge carriers (Negative)	-H
		Charge carriers (Positive)	+H
		Charge states, if not known (charge state range)	1
	Charge state	Isotope grouping (Isotope model)	Common organic molecules
		Charge state (limit assined charge stae)	1 -2
Matching tolerances and scoring	Formula matching	Match tolerance (Masses)	±10 ppm
		Expansion of values for chromatgram extraction (Possible m/z:)	symmetric (m/z): ± 0.01
	Scoring	Contribution to overall score	Mass score: 100 Isotope abundance score: 60 Isotope spacing score: 50
		Expected data variation	MS mass: 2.0 mDa + 5.6 ppm MS isotope abundance: 7.5%
EIC peak integration and filtering	Integration	Integrater selection	Agile 2
	Smoothing	Chromatogram smoothing	Smooth EIC before integration
		Smooting function	Gaussian Function width: 9 points Gaussian width: 5 points
	Peak filters	Filter on peak heights	Height filters: absolute height >= 1000 counts
		Maximum number of peaks (limit by height to the largest)	5
	Chromatogram format	Chromatogram data format	Centroid when available, otherwise profile
Spectrum extraction and centroiding	Peak spectrum	Spectra to include	Average scans >10% of peak height
		TOF spectra	Exclude if above 20% of saturation In the m/z ranges used in the chromatogram Never return an empty spectrum
	Centroiding	Peak location	Maximum spike width: 2 Required valley: 0.7
	Spectrum format	Mass spectral data format	Centroid when available, otherwise profile
Post-processing filters	Find by formula filters	Score	>75%
	Minimum filter matches	A compound must satisfy the checked find by formula filter conditions in	A file in at least one sample group

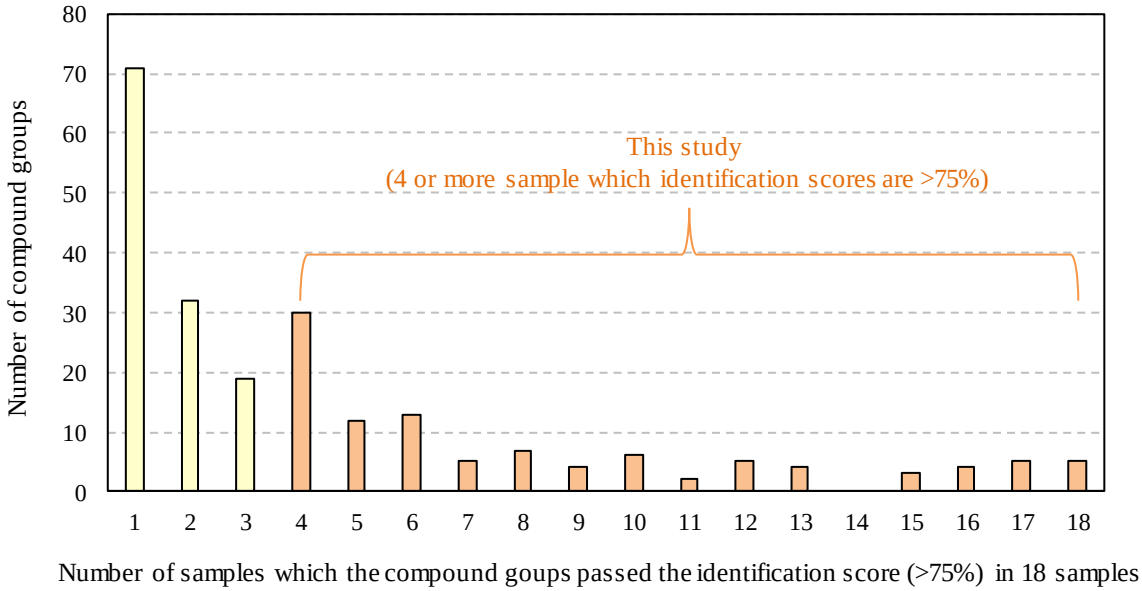

Fig. 3.6 Number of compound groups in different threshold of identification level

3.6 Linking precursors ion with the fragment ions by drift time using ion mobility mass spectrometry

In this study, an ion mobility mass spectrometry was used to link precursor ion with the fragment ions. There are some challenges in conventional analytical methods because many candidates of precursor ions exist in the full-scan spectrum at specific retention time (Liu et al., 2019). It is difficult to link precursor ions with fragment ions according to the information of RT only. Ion mobility mass spectrometry is evaluated by an index, "drift time". The precursor ions which ionized at insource are further separated in a drift tube by ion mobility mass spectrometry. After the precursor ions are passed into a drift tube, fragment ions are generated in a collision cell, and the switching CE (μs) is faster than the drift time (ms) (**Fig. 3.7**). Therefore, the precursor ion and fragment ions can be observed in the same range of drift time, which thus links them (Steiner et al., 2001; Steiner et al., 2003).

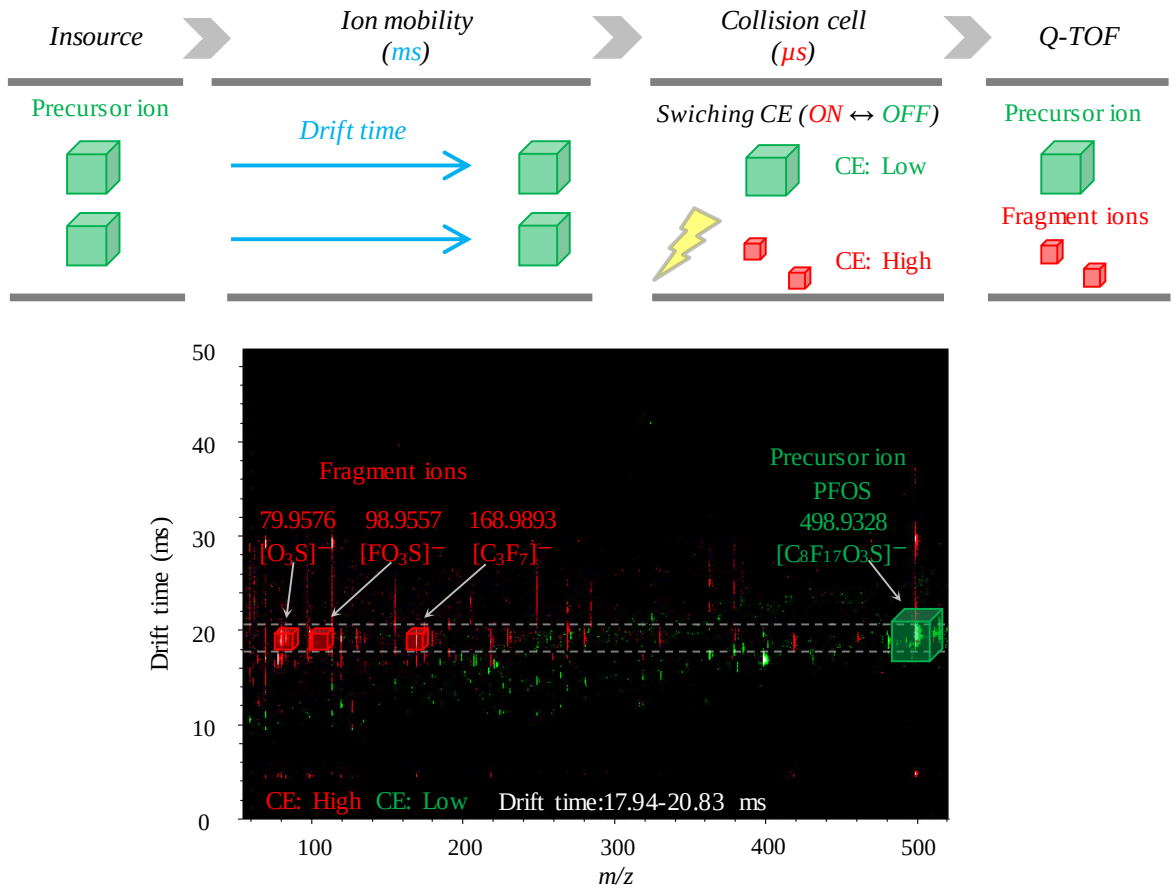

Fig. 3.7 A data-independent method linking precursor and fragment ions by drift time using ion mobility mass spectrometry

3.7 Fragmentation flagging

This study designed an experiment to pick up suspected PFASs peaks by fragmentation flagging of PFAS standards mixture solution and the household fire extinguisher liquid. The samples were analyzed by LC/IM-QTOF in all ions MS/MS mode. The *m/z* of the fragment ions ranged from 50 to 1700 at CE 0, 10, 20, and 40 V. All extracted ion chromatograms (EICs) of fragmentation flags were described in the mass error range of ±10 ppm, and the value of the blank of methanol was subtracted.

The conceptual image of fragmentation flagging to select peaks of suspected PFASs was shown in **Fig. 3.8**. Four EIC of fragment ions: $[C_7F_7]^-$ (*m/z* 216.9888), $[C_7F_9]^-$ (*m/z* 254.9856), $[C_8F_9]^-$ (*m/z* 266.9856), and $[C_7F_{11}]^-$ (*m/z* 292.9824) at 40 V were shown as examples. At a specific RT, multiple fragment ions, i.e. fragmentation flags, were overlapped. These might be fragment ions derived from the same precursor ion, as fragment ions from a specific precursor ion are observed in the same range of RT. For example, $[C_7F_7]^-$, $[C_7F_9]^-$, and $[C_7F_{11}]^-$ might be derived from a precursor ion. The approach has been reported as fragmentation flagging or precursor ion searching (Liu et al., 2015; Liu et al., 2018, Xiao et al., 2017, Liu et al., 2019). It was assumed that peaks of fragmentation flags found within the range of ±0.1 min RT derived from the same precursor ion. Then the EIC peaks of fragmentation flags at each RT were regrouped as fragment sets, making it possible to determine suspected PFASs.

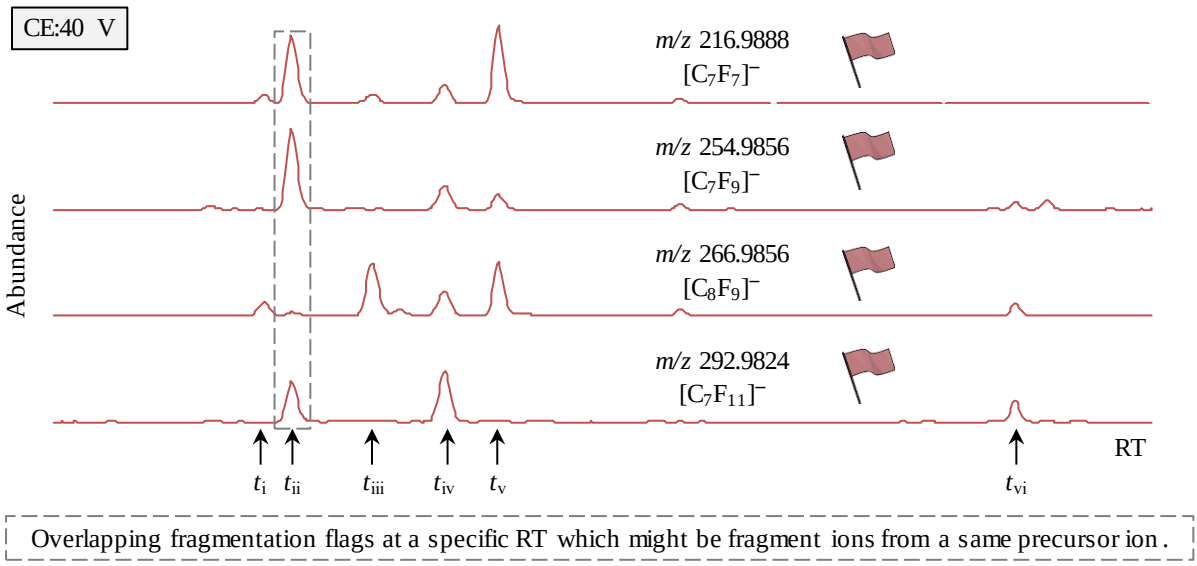

Fig. 3.8 Conceptual image of fragmentation flagging; EICs of fragment ions

Chapter 4

A profile analysis with suspect screening of PFASs in firefighting foam impacted waters in Okinawa, Japan (Paper I)

4.1 A Profile with suspect screening of PFASs

Suspect screening picked up 277 compound groups as [M-H] in negative mode and 111 as [M+H] in positive mode (**Fig. 4.1**). Excluding blank contamination and decarboxylation peaks left 230 compound groups in negative mode and 89 in positive mode. Selecting peaks with identification scores of >75% in four or more samples left 105 negative and 22 positive compound groups. Regrouping in negative and positive modes left 116 compound groups. Examples are shown in **Fig. 4.2**. The candidates were matched with the structural information of the original screening lists. The list of 116 proposed PFASs had a confidence level of 4 (unequivocal molecular formula) (Schymanski et al., 2014).

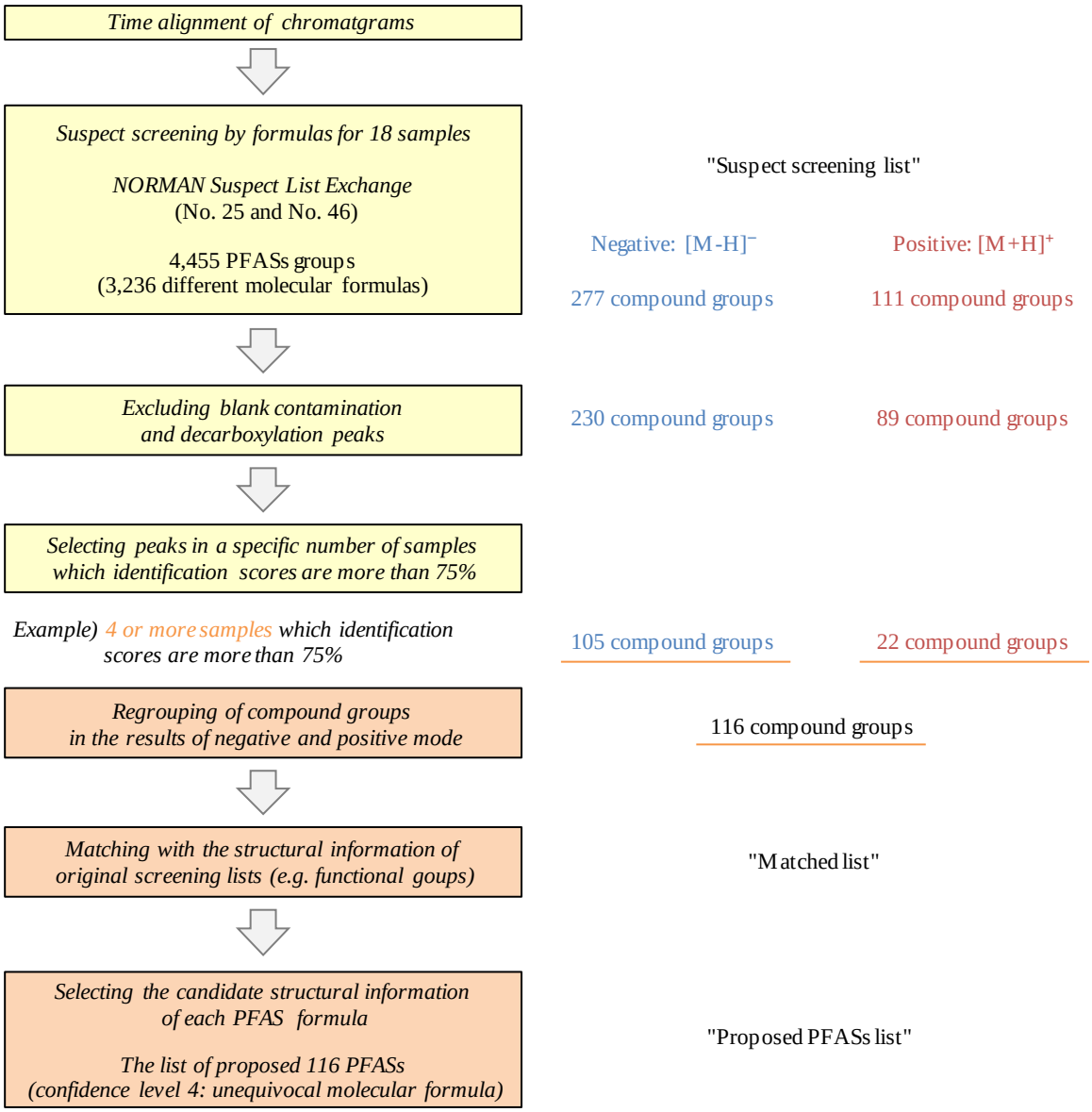

Fig. 4.1 Suspect screening workflow based on molecular formulas.

Fig. 4.2a An example of the result of suspect screening (Neg_Compound group 168, PFOS)

Fig. 4.2b An example of the result of suspect screening (Neg_Compound group 34)

4.2 Profile analysis of PFASs in firefighting foam impacted environment waters

The profiles of the 116 proposed PFASs in each sample are shown in **Fig. 4.3**. The results show proposed PFASs with peak areas of >10000. The numbers of proposed PFASs were 53–65 in DWTP samples, 78–105 in river water samples, and 81–112 in groundwater samples. Supplemental Data B ("Matched list") lists (A) the number of PFASs in firefighting foam impacted waters, and (B–F) profiles of PFASs by (B) molecular weight (MW), (C) functional group, (D) perfluoroalkyl chain length, (E) PFAS type, and (F) PFAS group. The main compositions by MW were 30±3% at 300–400, 27±2% at 400–500, and 19±4% at 500–600. The main compositions by functional group were 13±1% carboxylic acids, 47±2% sulfonic acids, and 24±2% sulfonamides. The main compositions of perfluoroalkyl chain lengths were 10±1% as C4, 14±2% as C5), and 26±3% as C6. The composition of long perfluoroalkyl chain lengths (C8–12; e.g., PFOS and PFOA) was 16% of all proposed PFASs. Some PFASs with defined polyfluoroalkyl chain lengths were categorized as others (e.g., PFECAs) according to their molecular formulas in the original screening lists (Hopkins et al., 2018, detected PFECAs in river water and drinking water). The composition of PFAS types was 28% ± 6% PFSAs and PFCAs, 51% ± 2% PFSA and PFCA precursors, and 21% ± 4% others. The composition of different PFAS groups was 22% ± 2% short-chain PFSA-related compounds, 23% ± 4% PFHxS-related compounds, 7% ± 1% PFOS-related compounds, and 10% ± 1% PFOA-related compounds. Boone et al. (2019) reported that 6 of 25 DWTPs surveyed had specific PFAS profiles (e.g., dominated by PFOA or perfluorobutanoic acid (PFBA)). the results were expected to show similar characteristics of contamination because the PFAS profiles did not differ notably between samples.

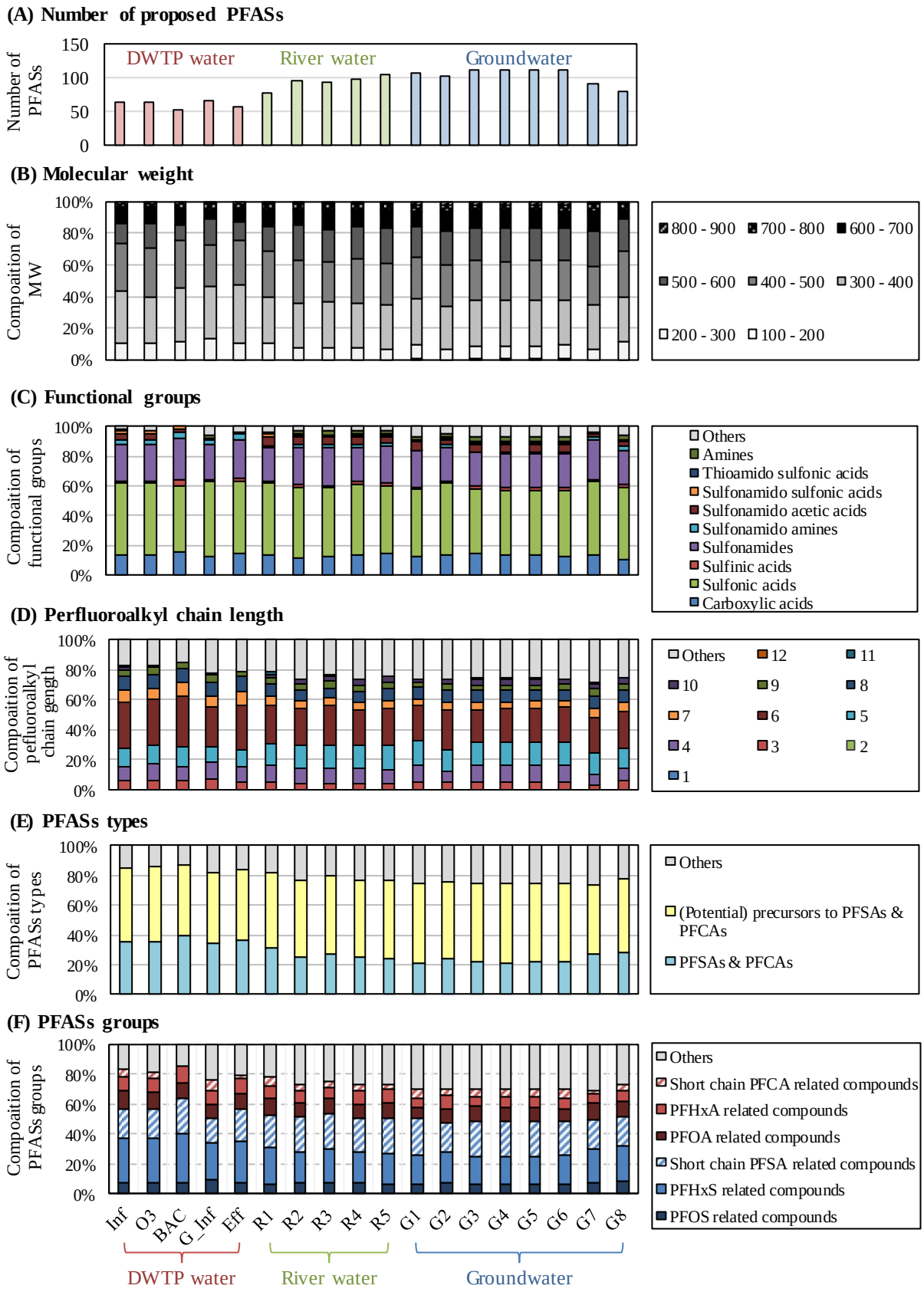

Fig. 4.3 (A) Numbers of proposed PFASs (peak areas > 10 000) in firefighting foam impacted waters. (B–F) Profiles of proposed PFASs by (B) molecular weight, (C) functional group, (D) perfluoroalkyl chain length, (E) PFAS type, (F) PFAS group.

Cluster analysis (**Fig. 4.4**) divided the 116 proposed PFASs into five clusters: cluster 1 (2 PFASs), 2 (5), 3 (15), 4 (49), and 5 (45) (**Fig. 4.5 (A)**). The main factor influencing cluster 1 was R1 (**Fig. 4.5 (B), (C)**), which was collected from the Nagata river. Another source of perfluoroundecanoic acid (PFUnDA) and perfluoroundecanoic acid (PFDoDA) contamination was suspected. The main factors influencing cluster 2 were R5, G7, and G8 around the firefighting training area. The PFASs of cluster 2 had high MWs (500–800) and potential precursors to PFSAs and PFCAs, and it was suspected that they were present in firefighting foam. The main factor influencing cluster 3 was G2, also around firefighting training area. In contrast to cluster 2, the PFASs in cluster 3 had high MWs of 500–700, and there was no major difference between PFAS types. The main PFAAs of cluster 3 were long-chain PFAAs (e.g., perfluoroheptanoic acid (PFHpA), perfluorodecanoic acid (PFDA), linear-perfluorononane sulfonic acid (PFNS), branched-PFNS, and perfluorodecane sulfonic acid (PFDS)). It was suspected that much of the long-chain PFASs used in the firefighting training area might not reach the Hijya River in groundwater because they were concentrated in the soils around the source of contamination. The precursors (e.g., 8:2 FTS) and others (perfluoroalkyl chain structures of 9(1DB), 10(1O), and 10(2O)) also had long-chain structures similar to PFAAs. Most PFASs (94 of 116) were categorized in clusters 4 and 5, and the main factors influencing them were G3–G6, which were close to each other. The main factor at G1, downstream of G3–G6, was stronger in cluster 5 than in cluster 4. PFASs in cluster 4 had high MWs (300–900), and precursors were present in high proportion. Those in cluster 5, in contrast, had low MWs (200–600), and precursors were present in moderate proportion. It was suspected that the precursors in cluster 4 degraded to the PFAAs in cluster 5 in groundwater because G1 lies downstream of the other sampling points, as suggested previously (Dauchy et al., 2019). Testing showed leaching and transport of PFASs derived from AFFFs in unsaturated soil in a firefighting training area (Høisæter et al., 2019). In particular, ultra-short-chain PFSAs can be released in this way (Björnsdotter et al., 2019).

The RTs of most compounds slowed as their MWs increased (**Fig. 4.6**). In contrast, compounds with

two or three water-soluble functional groups (e.g., carboxylic acids, sulfonic acids, amines) had high MWs but early RTs. All these compounds were potential precursors of PFSAs and PFCAs with perfluoroalkyl chain lengths of 4–6. In cluster 1, the PFASs at RT = 6–7 min and MW = 500–700 were C10–11 PFCAs (PFUnDA and PFDoDA), as mentioned above. In cluster 2, the PFASs at RT = 2–5 min and MW = 500–700 were C5–10 PFAA precursors. In cluster 3, the PFASs at RT = 3–7 min and MW = 500–650 were C6–10 PFAAs, C3–8 PFAA precursors, and others (9(1DB), 10(1O), and 10(2O)). In cluster 4, PFASs at RT = 2–4 min and MW = 300–900 were precursors of C4–6 PFAAs with two or three ionized functional groups, as mentioned above. PFASs at RT = 4–6 min and MW = 450–550 were C8–10 PFAAs (e.g., PFOS, PFNS, PFOA, perfluorononanoic acid (PFNA)) and others (6(1O), 8(1O), 8(1=O), 8(1Cl), 8(1H), 9(1O), 9(1=O), and 10(2O)). In cluster 5, the PFASs at RT = 2–6 min and MW = 200–500 were C4–7 PFAAs (e.g., PFBS, perfluoropentane sulfonic acid (PFPeS), PFHxS, perfluoroheptane sulfonic acid (PFHpS), PFHxA, and PFHpA), C3–5 PFAA precursors, and others (4(1Cl), 5(1O), 5(1H=O), 5(1H), 6(1=O), 6(1H), 6(1R/1DB), 8(1), and 8(1R/1DB)). It was suspected that the behavior of PFSAs, PFCAs, and others could be explained by the similarity of their perfluoroalkyl structures. As mentioned above, it was expected that C4–6 PFAA precursors in cluster 4 with two or three ionized functional groups could degrade to C4–7 PFAAs in cluster 5 in groundwater. It was expected that much of the mass of precursors released at the site was converted to PFCAs and PFSAs in groundwater. Suspected intermediate transformation products of PFAA precursors in AFFFs accounted for about half of the total precursor concentration in samples at another training site (Houtz et al., 2013). Intermediate substances from PFAA precursors may accumulate during biotransformation (Harding-Marjanovic et al., 2015). Therefore, our results show that the cluster analysis separated the characteristics of substances by sampling points. In future, it will be necessary to assess PFAS contamination of firefighting foam impacted soils and biota.

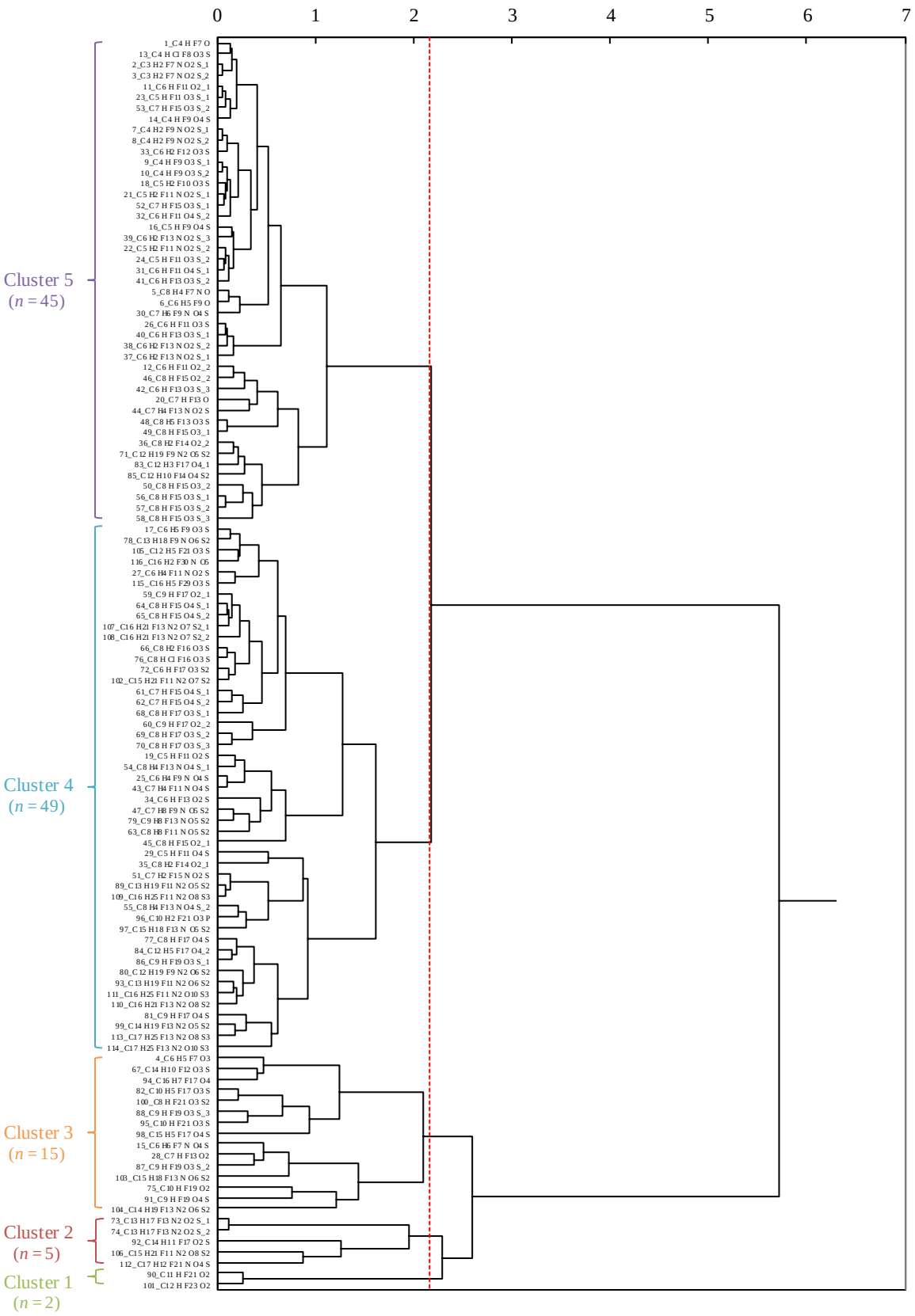

Fig. 4.4 A dendrogram of 116 proposed PFASs by cluster analysis in firefighting foam impacted river waters and groundwater

(A) Summary of clusters

Cluster	Number of PFASs	Sampling points	Characteristics	MW	PFASs types
1	2	R1	Nagata river	500-700	PFUnDA, PFDoDA
2	5	R5, G7, G8	Around firefighting area	500-800	Precursors
3	15	G2	Around firefighting area	500-700	Long chain PFSAs & PFCAs , precursors
4	49	G3, G4, G5, G6	The influential factor of G1 (downstream) is smaller	400-700	Precursors rich
5	45	G1, G3, G4, G5, GC6	The influential factor of G1 (downstream) is larger	200-500	PFSAs & PFCAs rich

(B) Cluster analysis between environmental samples

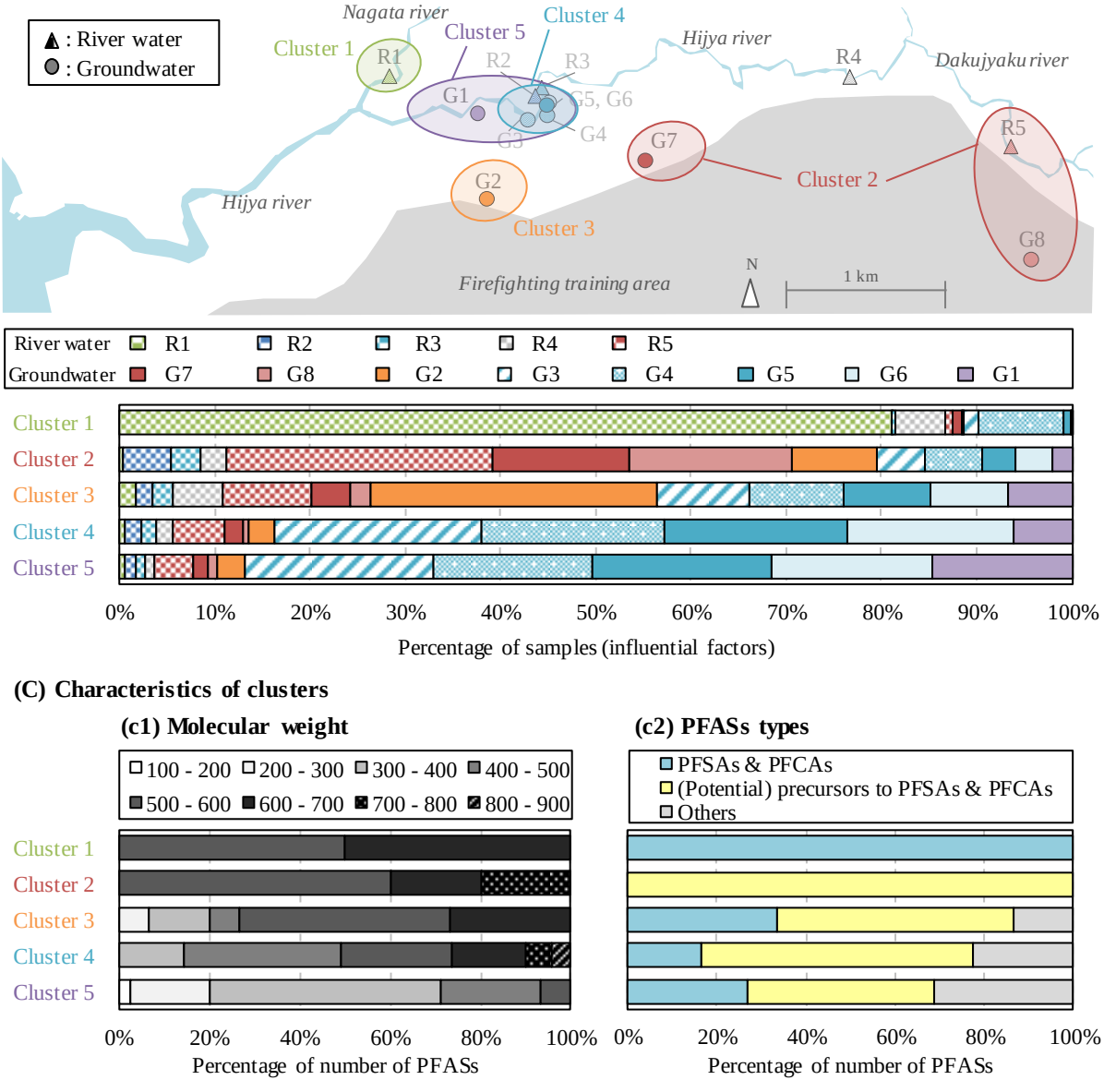

(C) Characteristics of clusters

Fig. 4.5 (A) Summary of results of cluster analysis. (B) Cluster analysis of PFASs in firefighting foam impacted river water and groundwater.
(C) Composition of proposed PFASs by (c1) molecular weight, (c2) PFAS type.

(A) Relation between RTs and MWs

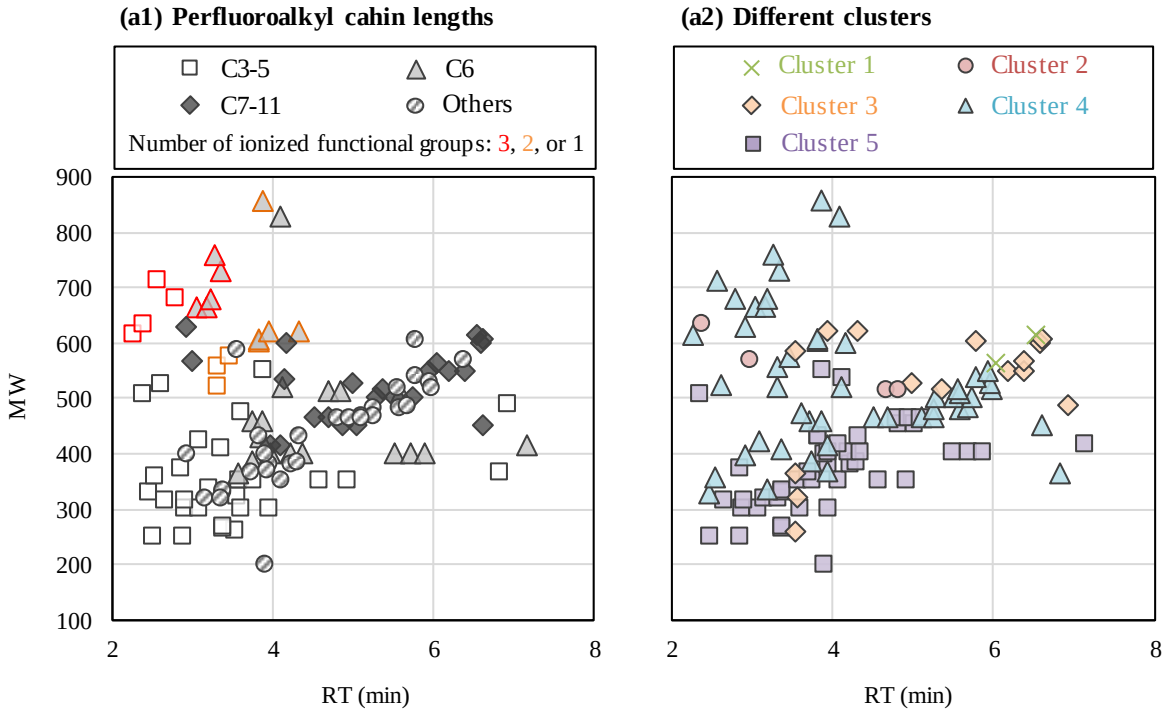

(B) Summary of clusters with PFASs types

Cluster	Number of PFASs	RT	MW	PFASs types		
				PFSAs & PFCAs	PFAA precursors	Others The stuctures of perfluoroalkyl chain
1	2	6-7 min	500-700	C10-11 PFCAs	-	-
2	5	2-5 min	500-700	-	C5-10 PFAA precursors	-
3	15	3-7 min	500-650	C6-10 PFAAs	C3-8 PFAA precursors	9 (1DB), 10 (1O), 10(2O)
4	49	2-4 min	300-900	-	C4-6 PFAA precursors (2 or 3 ionized functional groups)	-
		4-6 min	450-550	C8-10 PFAAs	-	6(1O), 8(1O), 8(1=O), 8(1Cl), 8(1H), 9(1O), 9(1=O), 10(2O)
5	45	2-6 min	200-500	C4-7 PFAAs	C3-5 PFAA precursors	4(1Cl), 5(1O), 5(1H=O), 5(1H), 6(1=O), 6(1H), 6(1R/1DB), 8(1O), 8(1R/1DB)

C*x*-*y*: perfluroalkyl chain lengths

DB: double bond, R: cyclic, O: ether, =O: keton, H: H-substituted, Cl: Cl-substituted

Fig. 4.6 (A) Relation between retention times and molecular weights by (a1) perfluoroalkyl chain lengths and number of ionized functional groups and (a2) clusters. (B) Summary of clusters by PFAS type.

4.3 Behavior of PFASs in drinking water treatment processes

The results of PFSAs, PFCAs, and their precursors differed among the drinking water treatment processes. By BAC filtration, the FASAs (PFSA precursors), with higher peak areas (linear- FHxSA, linear-perfluoro-1-butanesulfonamide (FBSA), branched-FHxSA, and linear-perfluoro-1-pentanesulfonamide (FPeSA)), had positive removal ratios (**Fig. 4.7**). By sedimentation and ozonation, the removal ratios of most PFSAs were −20% to 0%. Ozonation is not effective for PFAS removal (Rahman et al., 2014), and PFAS concentrations are not affected by conventional treatment processes but remain unchanged in the downstream public water supply (Qu et al., 2019). In contrast, by BAC filtration, the removal ratios of PFCAs (e.g., PFOA and PFHxA) were −60% to 0%, because biological degradation reactions formed substances with carboxylic acids. Using high-resolution Orbitrap MS, Shaw et al. (2019) identified 16 biotransformed metabolites (e.g., 6:2 FTS). Rahman et al. (2014) reported that granular activated carbon can remove PFASs but may need frequent reactivation. It difficult to identify the relationships among these PFAS because they depended on peak areas. Therefore, semi-quantification of PFASs without authentic standards will be required next to determine more accurate and detailed profiles of PFASs in firefighting foam impacted waters.

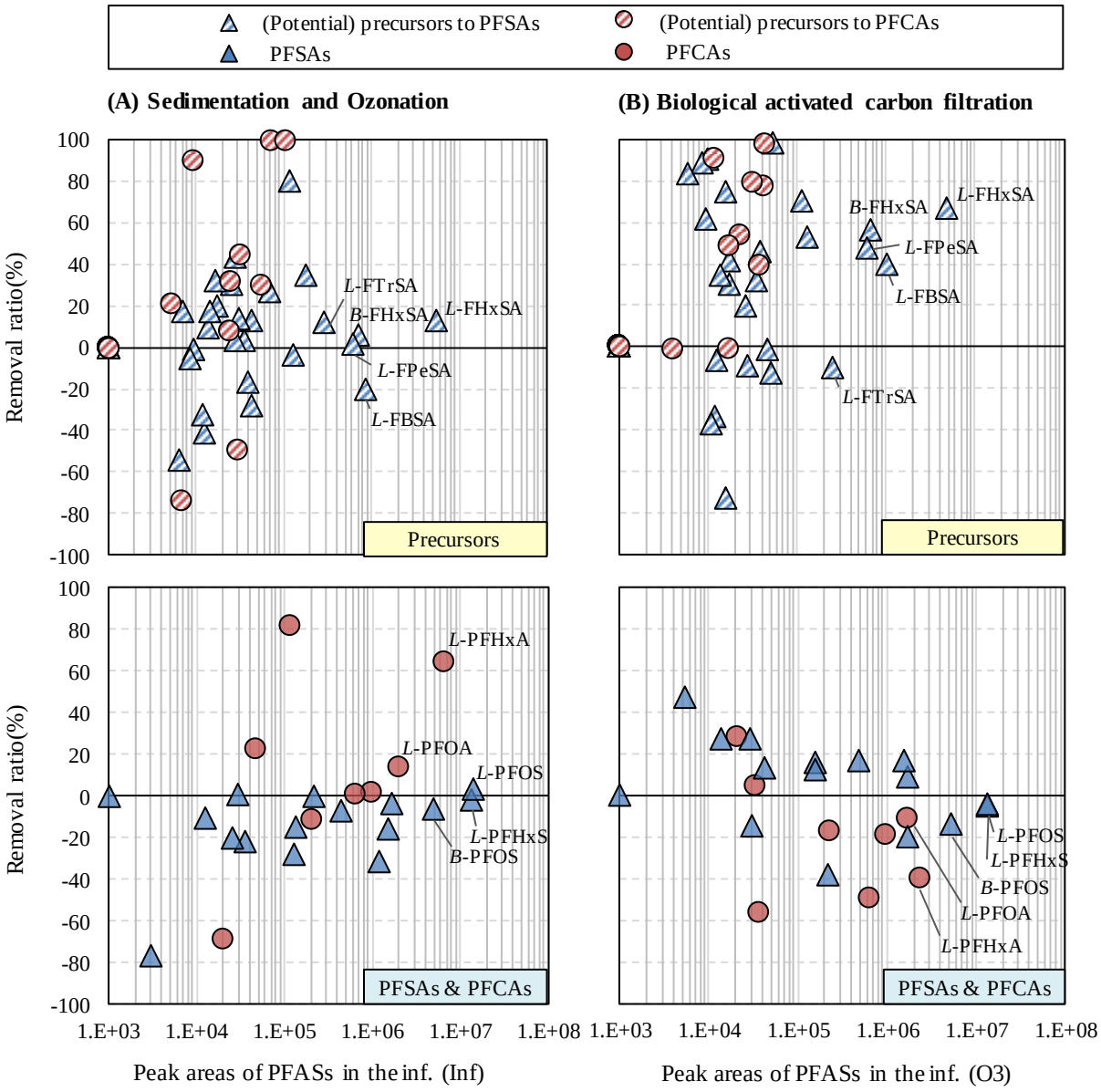

Fig. 4.7 Removal ratios of proposed PFASs in drinking water treatment processes: (A) sedimentation and ozonation, (B) biological activated filtration. Perfluoroalkyl chains: L, linear; B, branched.

Chapter 5

A new data-independent method linking precursor and fragment ions of PFASs by drift time using ion mobility mass spectrometry (Paper II)

5.1 Suspect screening of PFASs in firefighting foam impacted groundwater

The suspects were screened against NORMAN suspect lists (Nos. 25, 46) in firefighting foam impacted groundwater and picked up 175 compound groups as [M-H] in negative mode. Excluding blank contamination and decarboxylation peaks left 141 groups. Selecting peaks in ≥3 samples with identification scores of >75% left 99 groups as suspected PFASs with confidence level 4 (unequivocal molecular formula). (Schymanski et al., 2014)

5.2 A data-independent method linking precursor and fragment ions by drift time

This study used the concept of target MS/MS by quadrupole time of flight (QTOF) and all ions MS/MS with IMS (**Fig. 5.1**) to improve the identification confidence level after suspect or non-target screening to confidence level 4 (unequivocal molecular formula). (Schymanski et al., 2014) All ions MS/MS can rapidly obtain precursor and fragment ions at the same time, because the switching CE (μs) is faster than the RT (s), and is thus useful for target screening. However, for suspect and non-target screening, all ions MS/MS delivers many co-eluting ions in the full-scan spectrum at specific RTs due to matrices derived from environmental samples. Therefore, it is difficult to link a target precursor ion with fragment ions only from the RT. Conventionally, target MS/MS by QTOF is required for each plausible empirical formula after the suspect or non-target screening. (Liu et al., 2015; Liu et al., 2018) However, it takes a long time to enter the information into the instrument, and it depends on screening results of

samples. Therefore, in this study, the data-independent linking method between precursor ion and the fragment ions for PFASs in groundwater by drift time was examined using ion mobility mass spectrometry. Precursor ions passed into a drift tube, and fragment ions are generated in a collision cell, and the switching CE (μs) is faster than the drift time (ms) (**Fig. 5.2**) The precursor ion and the fragment ions are linked because they can be observed in the same drift time range (Steiner et al., 2001; Steiner et al., 2003).

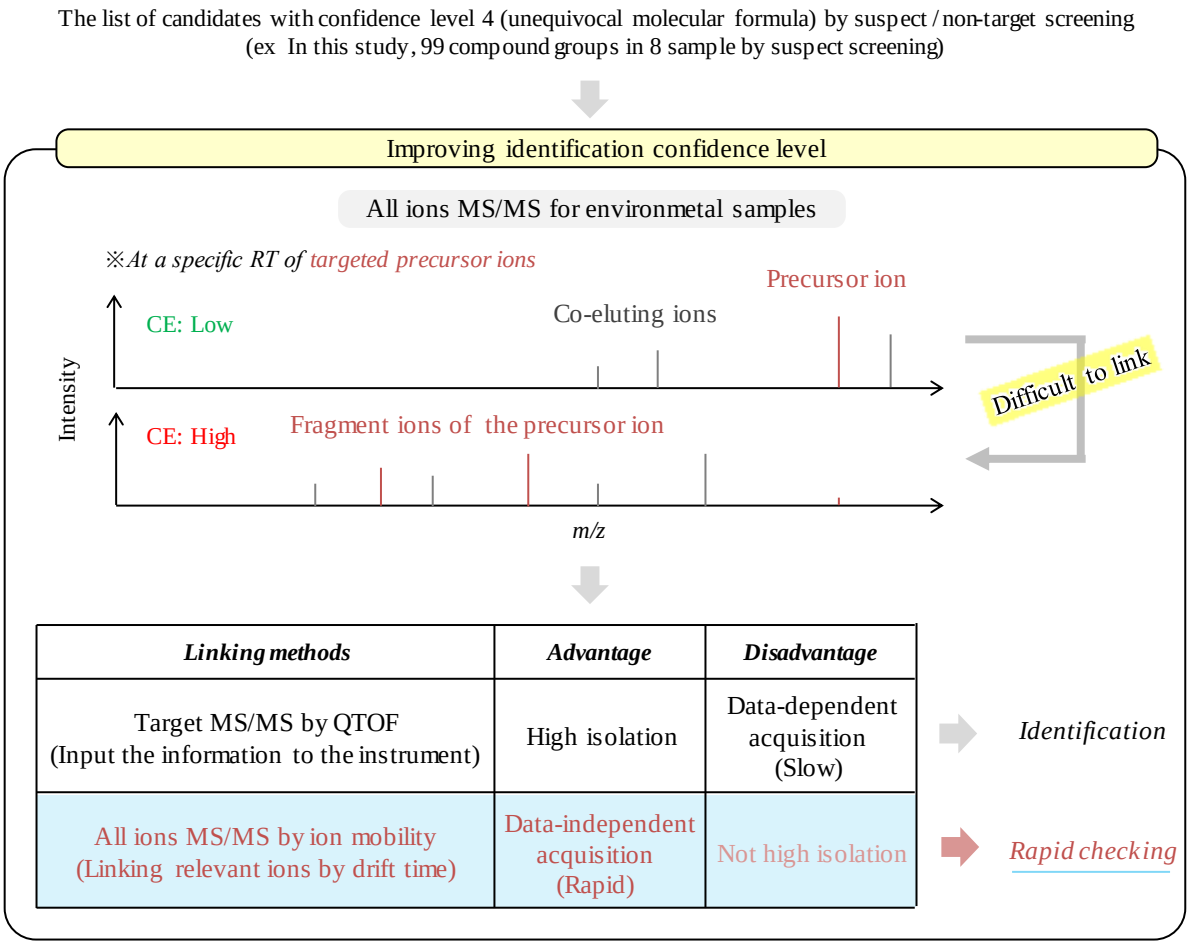

Fig. 5.1 Use of target MS/MS by QTOF and all ions MS/MS with ion mobility mass spectrometry to improve identification confidence level

For PFOS in the STD mixture (RT = 5.359–5.494 min), the spectra of the precursor ion $[C_8F_{17}O_3S]^-$ (*m/z* 498.9328) and the fragment ions $[O_3S]^-$ (*m/z* 79.9578), $[FO_3S]^-$ (*m/z* 98.9560), and $[C_3F_7]^-$ (*m/z* 168.9895) appeared in the same range of drift time (18.54–20.11 ms; **Fig. 5.2a-1**). For FOSA in the STD mixture (RT = 6.826–6.961 min), the spectra of the precursor ion $[C_8HF_{17}NO_2S]^-$ (*m/z* 497.9499) and the fragment ion $[NO_2S]^-$ (*m/z* 77.9668) appeared in the same range of drift time (18.91–19.99 ms; **Fig. 5.2a-2**). On the other hand, the spectra of PFOS and FOSA in groundwater sample G5 appeared in the same range of drift times. For PFOS in G5 (RT = 5.302–5.514 min), the spectra of the precursor ion $[C_8F_{17}O_3S]^-$ (*m/z* 498.9328) and the fragment ions $[O_3S]^-$ (*m/z* 79.9576), $[FO_3S]^-$ (*m/z* 98.9557), and $[C_3F_7]^-$ (*m/z* 168.9893) appeared in the same range of drift time (17.94–20.83 ms; Figure 2b-1). For FOSA in G5 (RT = 6.692–6.866 min), the spectra of the precursor ion $[C_8HF_{17}NO_2S]^-$ (*m/z* 497.9495) and the fragment ion $[NO_2S]^-$ (*m/z* 77.9639) appeared in the same range of drift time (18.91–19.87 ms; **Fig. 5.2b-2**). These results show that data-independent linking can apply to an environmental sample as well as to the STD mixture. The PFOS and FOSA spectra appeared at different RTs (STD mixture: PFOS, 5.359–5.494 min; FOSA, 6.826–6.961 min), in spite of similar *m/z*, because they have different functional groups (PFOS, sulfonic acid; FOSA, sulfonamide). In contrast, their drift times were similar (STD mixture: PFOS, 18.54–20.11 ms; FOSA, 18.91–19.99 ms), because they can be explained by CCS, a value of molecular structure in three-dimensional space on a two-dimensional plane and the average value of the projected area for each plane. (Borsdorf et al., 2006).

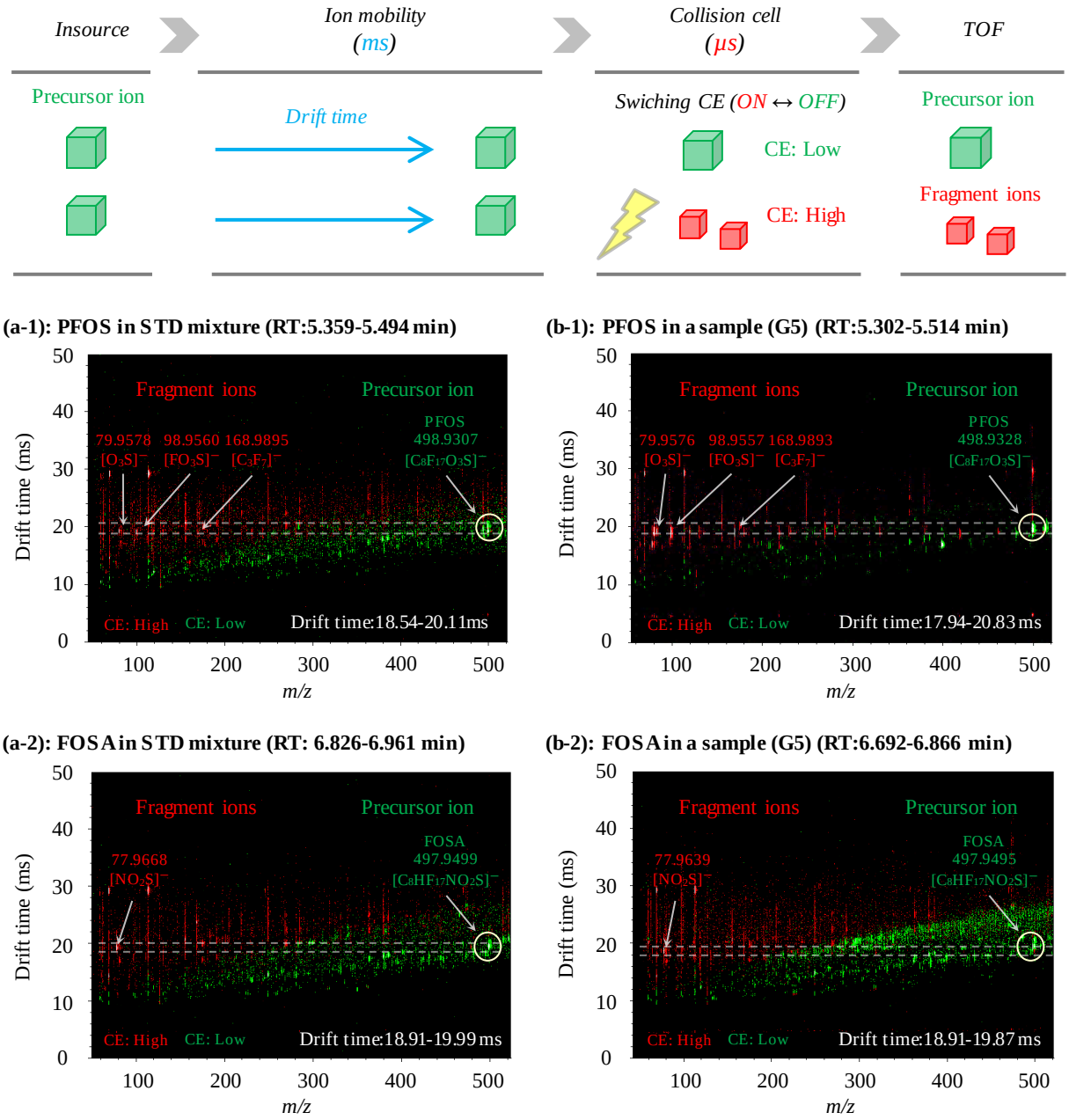

Fig. 5.2 A data-independent linking method between precursor ion and the fragment ions by drift time in (1) a STD mixture and (2) a sample

For PFOS in groundwater sample G4, the fragment ions were $[O_3S]^-$ (*m/z* 79.9578), $[FO_3S]^-$ (*m/z* 98.9557), $[C_2F_5]^-$ (*m/z* 118.9930), $[C_3F_7]^-$ (*m/z* 168.9894), and $[C_4F_9]^-$ (*m/z* 218.9841) (**Fig. 5.3**). In the mass spectrum at a specific RT without drift time, a co-eluting ion (FHxSA $[C_6HF_{13}NO_2S]^-$, *m/z* 397.9551) was observed at CE low, and co-eluting fragment ions at CE high (**Fig. 5.3(a)**). It was suspected that these were co-eluting fragment ions of FHxSA ($[NO_2S]^-$, *m/z* 77.9639) and of hexakis as lock mass chemical for mass calibration (*m/z* 68.9957 and 112.9857). With drift time, the precursor ion of PFOS and the fragment ions were observed in the range of drift time (18.06–20.35 ms; **Fig. 5.3(b)**). The co-eluting ion (FHxSA) was not observed at CE low and fragment ions were not observed at CE high in the range of drift time of PFOS. The fragment ions derived from hexakis were not observed in the same range of drift time either. Thus, the spectra of only the precursor ion of PFOS and the fragment ions were observed clearly in the specific range of drift time. Therefore, the method linked the target precursor ion and the fragment ions by drift time using IMS.

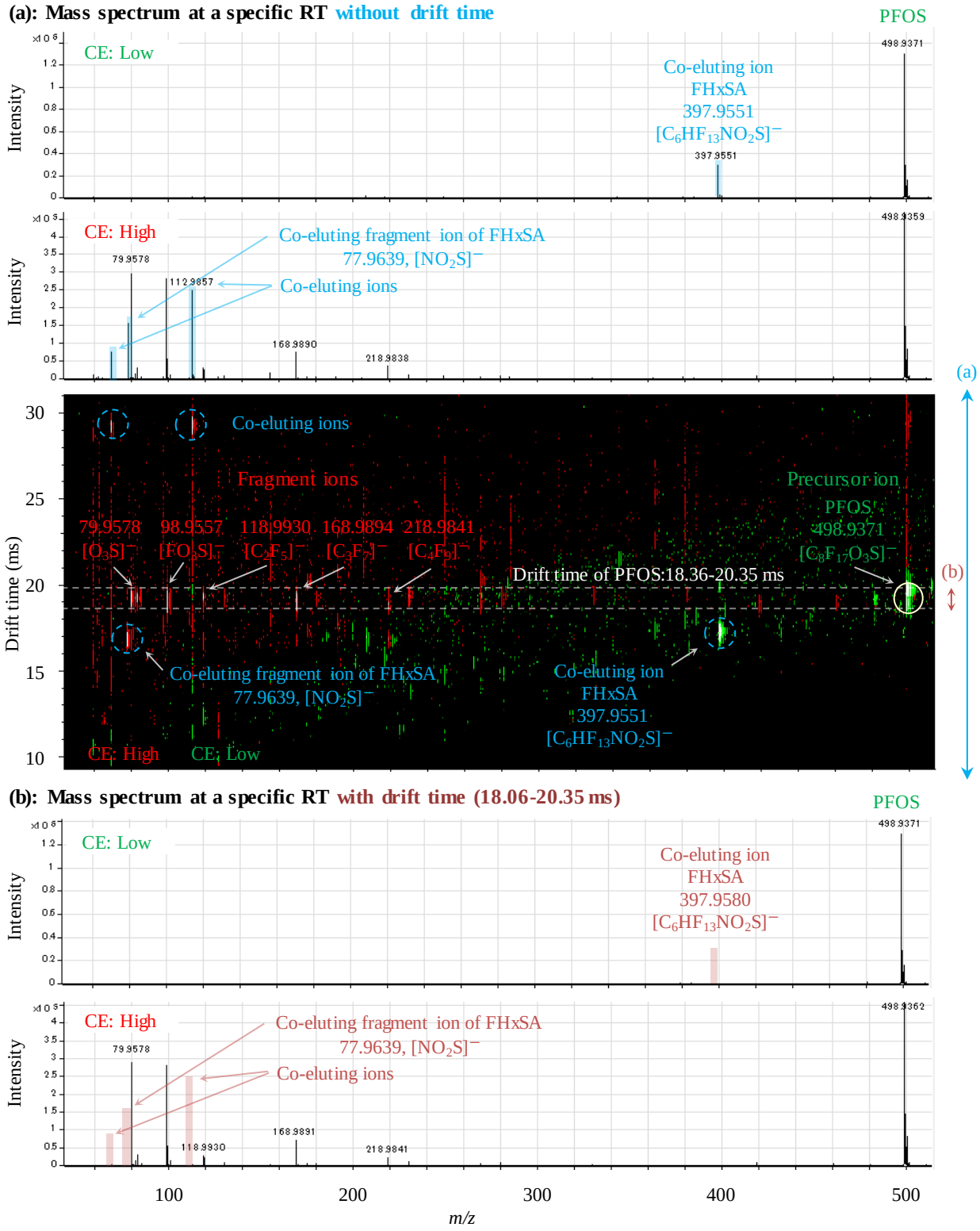

Fig. 5.3 A data-independent linking method between precursor ion and the fragment ions by drift time (DGB3)

5.2 Evaluation of linking method with focus on the intensity of co-eluting ions

The linking method was evaluated by focusing on the intensity of co-eluting ions. Without drift time, 5%–19% of PFASs (4–9 PFASs) were linked. With drift time, 37%–49% of PFASs (15–43 PFASs) were linked (**Fig. 5.4(a)**). It was expected that linking depends on the substances, not the samples. Six PFASs (PFSAs, FASAs) were linked without drift time because of their high intensities compared with co-eluting ions, but 90 PFASs could not be linked without drift time. In contrast, 43 PFASs could be linked with drift time, in particular at short RT or slow drift time (**Fig. 5.4(b)**). The RTs of most compounds slowed as their MWs increased. In contrast, compounds with two or more water-soluble functional groups (e.g., carboxylic acids, sulfonic acids, amines) had high MW but earlier RT (**Fig. 5.5**). The drift times of most compounds slowed as their MWs increased because drift time might depend on CCS, a molecular structural property. (Borsdorf et al., 2006) However, some ions with similar RTs and drift times as PFSAs could not be linked because they overlapped with several PFSAs, which had high intensities.

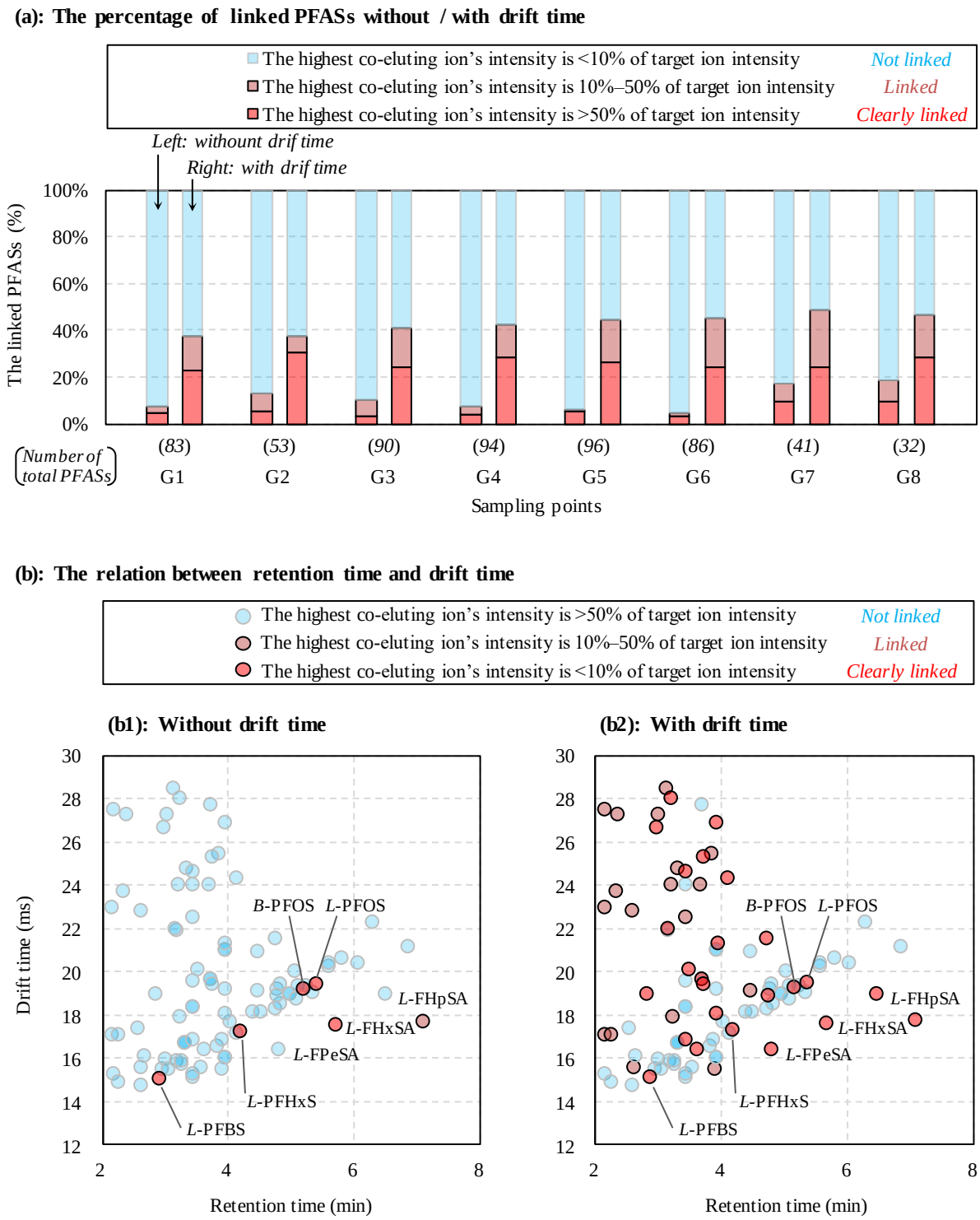

Fig. 5.4 (a) Evaluation of linking method focusing on the intensity of co-eluting ions, and the percentage of 99 linked PFASs in groundwater (left) without and (right) with drift time. (b) Relation between retention times and drift times of 96 suspected PFASs in G5 (b1) without and (b2) with drift time.

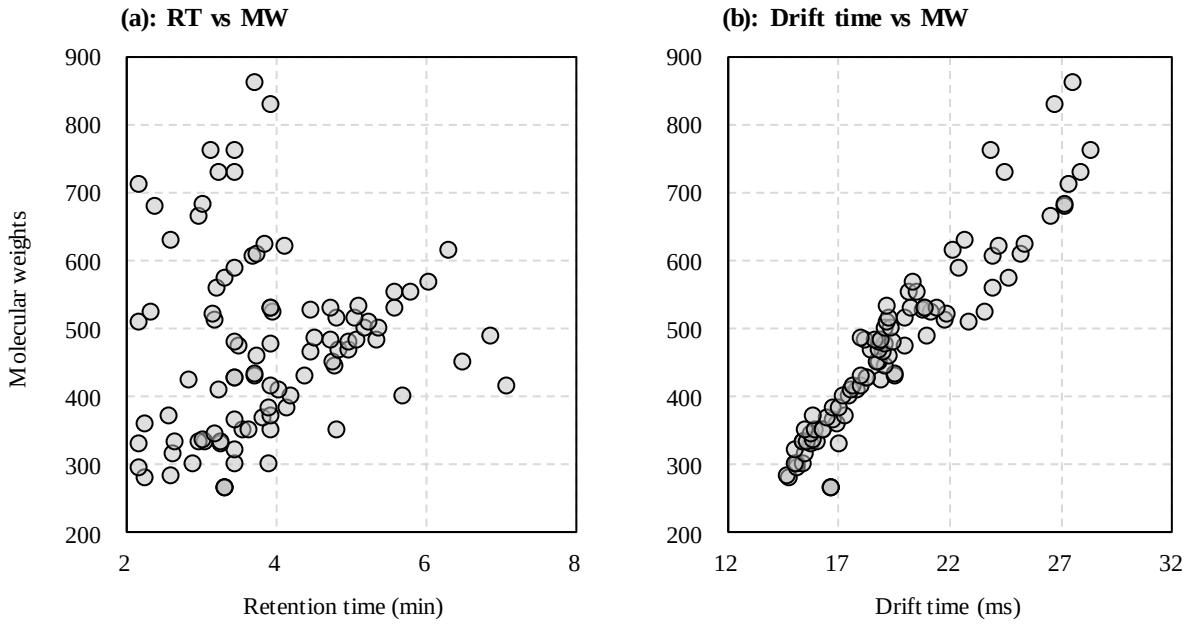

Fig. 5.5 Relation between (a) RT and MW; and (b) drift time and MW of 96 PFASs in groundwater (G5)

The fragment ions of the linked precursor ions were verified. In groundwater sample G5, most precursor ions could be linked probable fragment ions (41/43; **Table 5.1**). However, suspected co-eluting fragment ions of some precursor ions (16/43) were observed at the same RT and drift time. In the case of the fragment ions of $[C_8H_{17}F_{13}NO_3S_2]^-$ (*m/z* 602.0346), it was suspected that the ions with similar RTs as PFASs with high intensities (e.g., PFPeS (*m/z* 348.9410) and 6:2 FTS (*m/z* 426.9726)) could not be linked because their ions overlapped (**Fig. 5.6**). Fragment ions (e.g., *m/z* 68.9957 and *m/z* 112.9850) were also observed from the lock mass chemicals. The result shows that it is necessary to watch these ions carefully when using IMS for linking. From the molecular formulas of the 43 linked PFASs in Table 5.1, it was suspected that 8 C4, 9 C5, 15 C6, 3 C7, and 5 C8 PFASs have different perfluoroalkyl chain lengths, considering the number of fluorines according the original screening lists. It was suspected that the main composition was C4–C6 PFAAs and their precursors. Some of the linked PFASs were found in firefighting foam impacted groundwater. (Barzen-Hanson et al., 2017) It was suspected that these include 4:2 FTS $[C_6H_4F_9O_3S]^-$ (*m/z* 326.9743, RT 2.167 min, drift time 17.03 ms), 6:2 FTS $[C_8H_4F_{13}O_3S]^-$ (*m/z* 426.9679, RT 3.179 min, drift time 19.58 ms), and 8:2 FTS $[C_{10}H_4F_{17}O_3S]^-$ (*m/z* 526.9615, RT 4.746 min,

drift time 21.45 ms), with a linear perfluoroalkyl chain length; and $[C_{12}H_4F_{21}O_3S]^-$ (*m/z* 626.9551, RT 2.619 min, drift time 22.76 ms), $[C_{14}H_4F_{25}O_3S]^-$ (*m/z* 726.9487, RT 3.453 min, drift time 24.56 ms), and $[C_{16}H_4F_{29}O_3S]^-$ (*m/z* 826.9423, RT 3.952 min, drift time 26.78 ms), which are homologs because of their same RTs and drift times, but without a linear perfluoroalkyl chain length, because their RTs were earlier than those of 4:2 FTS, 6:2 FTS, and 8:2 FTS, in spite of higher MWs. Therefore, it will be necessary to increase the confidence level (above level 3) to predict the structures of proposed PFASs. (Schymanski et al., 2014).

Table 5.1 The list of proposed fragment ions of linked precursor ions in a groundwater sample (G5)

No.	Molecular formula	RT (min)	Drift time (ms)	Exact mass of precursor ion (*m/z*)	Proposed perfluoroalkyl cahin length	The evaluation of precursor ions	CE (eV)	Proposed fragment ions [Molecular formula] (observed mass *m/z*)	Number of probable fragment ions	Identification confidence level
1	$C_{12}H_{19}F_9N_2O_5S_2$	2.167	22.89	505.0519	C6	*Linked*	40	$[C_9H_{12}F_9N_2O_2S]^-$ (383.0549), [-]$^-$ (284.9336), $[C_5H_{12}NO_3S]^-$ (166.0574)	2 / 3	3 - 4
2	$C_6H_5F_9O_3S$	2.167	17.03	326.9743	C6	*Linked*	40	$[FO_2S]^-$ (82.9604), $[HO_3S]^-$ (80.9655), $[O_3S]^-$ (79.9570)	3 / 3	3
3	$C_{16}H_{25}F_{11}N_2O_{10}S_3$	2.184	27.41	709.0423	C8	*Linked*	40	$[C_{13}H_{18}F_{11}N_2O_6S_2]^-$ (571.0521), $[C_{10}H_{12}F_{11}N_2O_2S]^-$ (433.0498), $[C_6H_4F_9O_3S]^-$ (326.9781)	2 / 3	3 - 4
4	$C_6H_4F_9NO_4S$	2.268	16.98	355.9644	C8	*Linked*	40	$[C_4HF_9NO_2S]^-$ (297.9574), $[C_4F_9]^-$ (218.9841)	2 / 2	3
5	$C_{12}H_{19}F_9N_2O_6S_2$	2.351	23.63	521.0468	C7	*Linked*	40	$[C_3F_7O_3S]^-$ (248.9639), $[C_5H_{12}NO_4S]^-$ (182.0513), [-]$^-$ (154.9760)	1 / 3	3 - 4
6	$C_{16}H_{25}F_{11}N_2O_8S_3$	2.385	27.19	677.0524	C6	*Linked*	40	$[C_6F_{13}]^-$ (318.9772), $[C_4F_9O_3S]^-$ (298.9441), $[C_5H_{12}NO_3S]^-$ (166.0538)	2 / 3	3 - 4
7	$C_{12}H_5F_{21}O_3S$	2.619	22.76	626.9551	C8	*Linked*	40	$[C_5F_{11}]^-$ (268.9827), [-]$^-$ (284.9327), $[C_2F_5]^-$ (118.9917)	2 / 3	3 - 4
8	$C_6HF_{11}O_2$	2.635	15.53	312.9728	C8	*Linked*	10	$[C_5F_{11}]^-$ (268.9879)	1 / 1	3
9	$C_7H_8F_9NO_5S_2$	2.853	18.93	419.9627	C6	*Clearly linked*	40	$[C_4HF_9NO_2S]^-$ (297.9627), $[O_3S]^-$ (79.9619), $[NO_2S]^-$ (77.9656)	3 / 3	3
10	$C_4HF_9O_3S$	2.903	15.05	298.9430	C7	*Clearly linked*	40	$[FO_3S]^-$ (98.9560), $[O_3S]^-$ (79.9580)	2 / 2	3
11	$C_{16}H_{21}F_{13}N_2O_7S_2$	2.986	26.56	663.0510	C6	*Clearly linked*	40	$[C_6F_{13}]^-$ (318.9770), $[C_4F_9O_3S]^-$ (298.9443), $[C_5H_{12}NO_3S]^-$ (166.0538)	2 / 3	3 - 4

※Probable fragment ions of targeted precursor ion, suspected co-eluting fragment ions

(Continued)

Table 5.1 The list of proposed fragment ions of linked precursor ions in a groundwater sample (G5)

No.	Molecular formula	RT (min)	Drift time (ms)	Exact mass of precursor ion (*m/z*)	Proposed perfluoroalkyl cahin length	The evaluation of precursor ions	CE (eV)	Proposed fragment ions [Molecular formula] (observed mass *m/z*)	Number of probable fragment ions	Identification confidence level
12	$C_{16}H_{21}F_{13}N_2O_8S_2$	3.036	27.22	679.0459	C6	*Linked*	40	$[C_{14}H_{18}F_{13}N_2O_5S_2]^-$ (605.0502), $[C_{11}H_{12}F_{13}N_2O_2S]^-$ (483.0458), $[C_3F_7O_3S]^-$ (248.9625)	2 / 3	3 - 4
13	$C_{17}H_{25}F_{13}N_2O_{10}S_3$	3.153	28.37	759.0391	C6	*Linked*	40	$[C_{14}H_{18}F_{13}N_2O_6S_2]^-$ (621.0422)	1 / 1	3
14	$C_{13}H_{18}F_9NO_6S_2$	3.170	21.92	518.0359	C4	*Clearly linked*	40	$[C_7H_{12}NO_4S]^-$ (206.0501), $[-]^-$ (154.9761), $[C_4H_{10}NO_3S]^-$ (152.0385)	2 / 3	3 - 4
15	$C_{13}H_{19}F_{11}N_2O_5S_2$	3.220	23.96	555.0487	C5	*Linked*	40	$[C_{11}H_{12}F_{13}N_2O_2S]^-$ (433.0469), $[C_3F_7O_3S]^-$ (248.9620), $[-]^-$ (126.9052)	1 / 3	3 - 4
16	$C_{17}H_{25}F_{13}N_2O_8S_3$	3.236	27.97	727.0492	C6	*Clearly linked*	40	$[C_{14}H_{18}F_{13}N_2O_6S_2]^-$ (621.0430), $[C_{14}H_{18}F_{13}N_2O_5S_2]^-$ (605.0486), $[C_{11}H_{12}F_{13}N_2O_2S]^-$ (483.0455)	3 / 3	3
17	$C_7H_4F_{11}NO_4S$	3.253	17.83	405.9612	C5	*Linked*	40	$[C_5HF_{11}NO_2S]^-$ (347.9585), $[HO_4S]^-$ (96.9591), $[NO_2S]^-$ (77.9661)	2 / 3	3 - 4
18	$C_{13}H_{19}F_{11}N_2O_6S_2$	3.336	24.68	571.0436	C5	*Linked*	40	$[-]^-$ (378.9198), $[C_3F_7O_3S]^-$ (248.9623), $[-]^-$ (126.9050)	0 / 3	4
19	$C_{14}H_5F_{25}O_3S$	3.453	24.56	726.9487	-	*Clearly linked*	40	$[C_6F_{13}]^-$ (318.9789), $[C_3F_7]^-$ (168.9889), $[C_2F_5]^-$ (118.9911)	3 / 3	3
20	$C_{16}H_7F_{17}O_4$	3.453	22.44	585.0000	C7	*Linked*	40	$[-]^-$ (284.9296), $[C_5F_{11}]^-$ (268.9510), $[C_3F_7]^-$ (168.9884)	2 / 3	3 - 4
21	$C_7HF_{13}O_2$	3.453	16.8	362.9696	C6	*Clearly linked*	10	$[C_6F_{13}]^-$ (318.9806), $[C_3F_7]^-$ (168.9900)	2 / 2	3
22	$C_8H_8F_{11}NO_5S_2$	3.520	20	469.9595	C5	*Clearly linked*	40	$[-]^-$ (374.9579), $[-]^-$ (174.9669), $[NO_2S]^-$ (77.9654)	1 / 3	3 - 4

※Probable fragment ions of targeted precursor ion, suspected co-eluting fragment ions

(Continued)

Table 5.1 The list of proposed fragment ions of linked precursor ions in a groundwater sample (G5)

No.	Molecular formula	RT (min)	Drift time (ms)	Exact mass of precursor ion (*m/z*)	Proposed perfluoroalkyl cahin length	The evaluation of precursor ions	CE (eV)	Proposed fragment ions [Molecular formula] (observed mass *m/z*)	Number of probable fragment ions	Identification confidence level
23	$C_5HF_{11}O_3S$	3.636	16.31	348.9398	C5	*Clearly linked*	40	$[C_2F_5]^-$ (118.9930), $[C_8H_4F_{12}NO_2S]^-$ (98.9560), $[O_3S]^-$ (79.9580)	3 / 3	3
24	$C_{15}H_{18}F_{13}NO_5S_2$	3.703	23.97	602.0346	C6	*Linked*	40	$[C_5F_{11}O_3S]^-$ (348.9401), $[C_7H_{14}NO_5S_2]^-$ (256.0340), $[C_3F_7O_3S]^-$ (248.9601)	1 / 3	3 - 4
25	$C_8H_5F_{13}O_3S$	3.719	19.58	426.9679	C6	*Clearly linked*	40	$[C_8H_3F_{12}O_3S]^-$ (406.9664), $[C_8H_2F_{11}O_3S]^-$ (386.9600), $[HO_3S]^-$ (80.9656)	3 / 3	3
26	$C_{14}H_{19}F_{13}N_2O_5S_2$	3.753	25.23	605.0455	C6	*Clearly linked*	40	$[C_{11}H_{12}F_{13}N_2O_2S]^-$ (483.0467), $[C_3F_7]^-$ (168.9885), $[C_5H_{12}NO_3S]^-$ (166.0544)	3 / 3	3
27	$C_8H_4F_{13}NO_4S$	3.753	19.32	455.9580	C6	*Clearly linked*	40	$[C_6HF_{13}NO_2S]^-$ (397.9518), $[C_6F_{13}]^-$ (318.9795), $[C_3F_7]^-$ (168.9887)	3 / 3	3
28	$C_{14}H_{19}F_{13}N_2O_6S_2$	3.869	25.41	621.0404	C6	*Linked*	40	$[C_{11}H_{12}F_{13}N_2O_2S]^-$ (483.0474), $[C_7F_{15}]^-$ (368.9795), $[C_3F_7]^-$ (168.9910)	3 / 3	3
29	$C_4H_2F_9NO_2S$	3.919	15.45	297.9590	C4	*Linked*	40	$[C_2F_5]^-$ (118.9938), $[NO_2S]^-$ (77.9672)	2 / 2	3
30	$C_{16}H_5F_{29}O_3S$	3.952	26.78	826.9423	-	*Clearly linked*	40	$[C_7F_{15}]^-$ (368.9778), $[C_4F_9]^-$ (218.9861), $[C_3F_7]^-$ (168.9896)	3 / 3	3
31	$C_8HF_{15}O_2$	3.952	18.03	412.9664	C7	*Clearly linked*	10	$[C_7F_{15}]^-$ (368.9823), $[C_4F_9]^-$ (218.9910), $[C_3F_7]^-$ (168.9931)	3 / 3	3
32	$C_9H_8F_{13}NO_5S_2$	3.968	21.24	519.9563	C6	*Clearly linked*	40	$[C_6HF_{13}NO_2S]^-$ (397.9559), $[-]^-$ (154.9735), $[NO_2S]^-$ (77.9644)	2 / 3	3 - 4

※Probable fragment ions of targeted precursor ion, suspected co-eluting fragment ions

(Continued)

Table 5.1 The list of proposed fragment ions of linked precursor ions in a groundwater sample (G5)

No.	Molecular formula	RT (min)	Drift time (ms)	Exact mass of precursor ion (*m/z*)	Proposed perfluoroalkyl cahin length	The evaluation of precursor ions	CE (eV)	Proposed fragment ions [Molecular formula] (observed mass *m/z*)	Number of probable fragment ions	Identification confidence level
33	$C_{15}H_{18}F_{13}NO_6S_2$	4.134	24.28	618.0295	C6	*Clearly linked*	40	$[-]^-$ (378.9155), $[C_3F_7O_3S]^-$ (248.9603), $[HO_4S]^-$ (96.9583)	0 / 3	4
34	$C_6HF_{13}O_3S$	4.200	17.21	398.9366	C6	*Clearly linked*	40	$[C_2F_5]^-$ (118.9939), $[FO_3S]^-$ (98.9576), $[O_3S]^-$ (79.9599)	3 / 3	3
35	$C_9HF_{17}O_2$	4.482	19.08	462.9632	C8	*Linked*	20	$[C_8F_{17}]^-$ (418.9721), $[C_4F_9]^-$ (218.9853), $[C_3F_7]^-$ (168.9886)	3 / 3	3
36	$C_{10}H_5F_{17}O_3S$	4.746	21.45	526.9615	C8	*Clearly linked*	40	$[C_{10}H_3F_{12}O_3S]^-$ (506.9594), $[HO_3S]^-$ (80.9660), $[O_3S]^-$ (79.9577)	3 / 3	3
37	$C_7HF_{15}O_3S$	4.779	18.8	448.9334	C7	*Clearly linked*	40	$[C_3F_7]^-$ (168.9894), $[FO_3S]^-$ (98.9547), $[O_3S]^-$ (79.9564)	3 / 3	3
38	$C_5H_2F_{11}NO_2S$	4.812	16.33	347.9558	C6	*Clearly linked*	40	$[C_2F_5]^-$ (118.9913), $[NO_2S]^-$ (77.9654)	2 / 2	3
39	$C_8HF_{17}O_3S$	5.191	19.17	498.9302	C8	*Clearly linked*	40	$[C_3F_6O_3S]^-$ (229.9484), $[FO_3S]^-$ (98.9546), $[O_3S]^-$ (79.9567)	3 / 3	3
40	$C_8HF_{17}O_3S$	5.388	19.39	498.9302	C8	*Clearly linked*	40	$[C_3F_7]^-$ (168.9905), $[FO_3S]^-$ (98.9565), $[O_3S]^-$ (79.9581)	3 / 3	3
41	$C_6H_2F_{13}NO_2S$	5.699	17.53	397.9526	C6	*Clearly linked*	40	$[C_2F_5]^-$ (118.9927), $[NO_2S]^-$ (77.9686)	2 / 2	3
42	$C_7H_2F_{15}NO_2S$	6.500	18.9	447.9494	C7	*Clearly linked*	40	$[HO_4S]^-$ (96.9579), $[NO_2S]^-$ (77.9642)	1 / 2	3 - 4
43	$C_7H_4F_{13}NO_2S$	7.103	17.7	411.9682	C6	*Clearly linked*	40	$[-]^-$ (190.9455), $[C_2F_5]^-$ (118.9921), $[HO_4S]^-$ (96.9584)	1 / 3	3 - 4

Mass spectrum at a specific RT (3.564-3.738 min) with drift time (23.36-23.84 ms) for targeted $[C_{15}H_{17}F_{13}NO_3S_2]^-$ *m/z* 602.0346

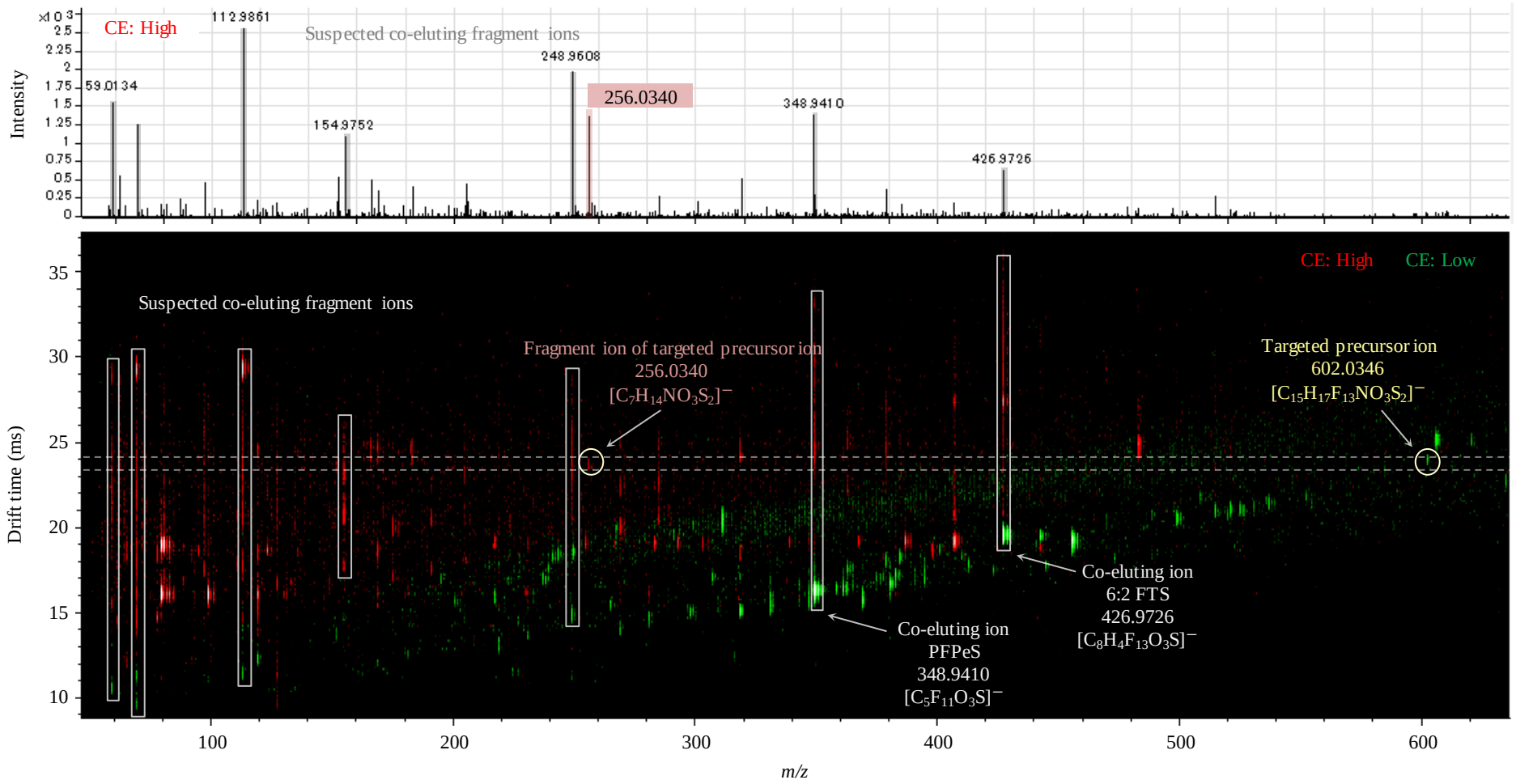

Fig. 5.6 The mass spectrum ar a specific RT with drift time for targeted $[C_8H_{17}F_{13}NO_3S_2]^-$ (*m/z* 602.0346) in a groundwater sample (G5)

Finally, this study explored a data-independent method for linking precursor and fragment ions of PFASs by drift time using IMS (Fig. 5.1). This study evaluated it on PFASs in firefighting foam impacted groundwater by considering the intensity of co-eluting ions to see how many ions could be excluded. Because the method uses all ions MS/MS mode, a single run can acquire a lot of MS/MS information independent of sample or data analysis (**Fig. 5.7**). This means that if the original database, screening list, or statistical filtering / data cleaning approach changes, reanalysis is not required. Therefore, this method will be particularly effective for environmental research with large numbers of samples. The resolution of IMS will need to be improved in order to link PFASs which have similar properties.

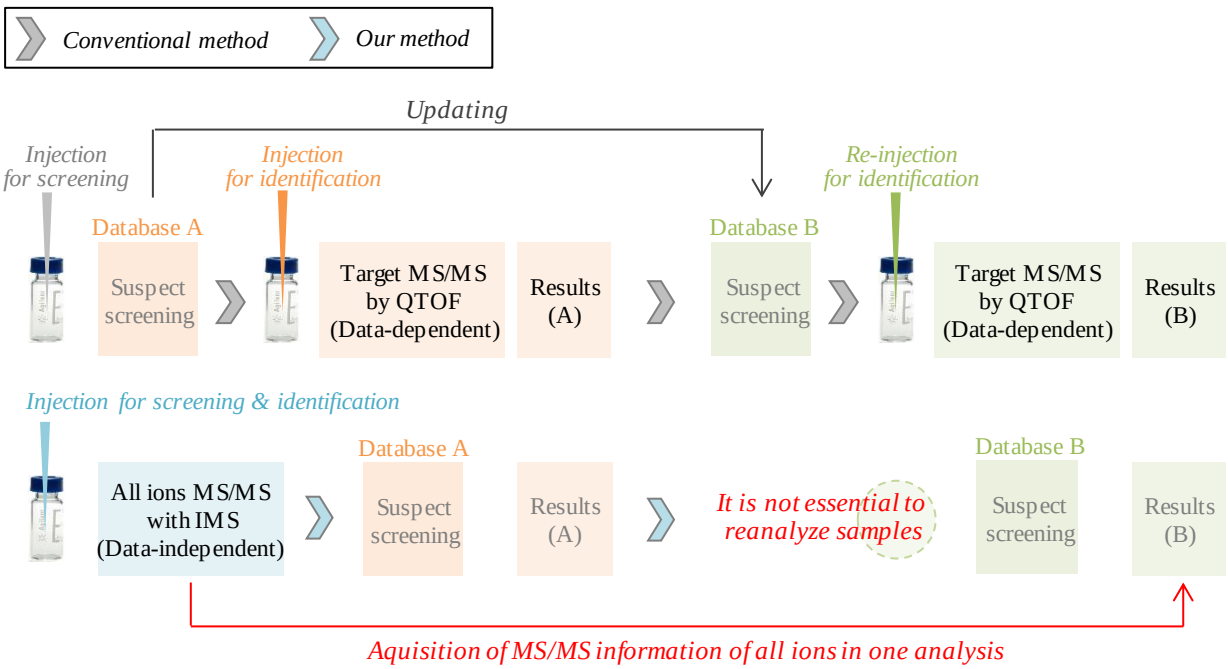

Fig. 5.7 Advantage of new data-independent linking method

Chapter 6

A method to search for PFASs by linking fragmentation flags with their precursor ions by drift time using ion mobility mass spectrometry (Paper III)

6.1 Classification of fragment ions and selection of fragmentation flags

Target analysis of 34 PFASs by LC/IM-QTOF detected 33 PFASs (12 PFCAs, 3 PFSAs, 3 di-PAPs, 3 FTSs, 4 FTCAs, 3 FTUCAs, 3 FASAs, 2 FASAAs). As a result, 68 PFASs with *m/z* of fragment ions were archived by referring to previous reports (**Table 6.1**) (Barzen-Hanson et al., 2017; Rotander et al., 2015; Baduel et al., 2017; Newton et al., 2017; Lang et al., 2016; Ruan et al., 2015). The search resulted in 122 types of fragment ions, 90 with C and F atoms and 32 without them. Some of 68 PFASs had common fragment ions; for example, 43% of them had $[C_2F_5]^-$ (*m/z* 118.9920), 46% had $[C_3F_7]^-$ (*m/z* 168.9888), 21% had $[C_4F_9]^-$ (*m/z* 218.9856), 13% had $[C_5F_{11}]^-$ (*m/z* 268.9824), 24% had $[C_6F_{13}]^-$ (*m/z* 318.9792), and 6% had $[C_7F_{15}]^-$ (*m/z* 368.9760). The data showed that the fragment ions $[C_nF_{2n+1}]^-$ were useful as flags to discover suspected PFASs. Other fragment ions were also detected frequently: $[CF_2O_3S]^-$ (*m/z* 129.9536), $[C_2F_4O_3S]^-$ (*m/z* 179.9504), and $[C_3F_6O_3S]^-$ (*m/z* 229.9472). However, some kinds of PFASs did not generate fluoroalkyl common fragment ions, such as diPAPs and fluorotelomer thioamido sulfonates owing to those fragmentation patterns (Baduel et al., 2017).

Table 6.1 Classification of PFASs fragment ions used for fragmentation flagging (***Class 1*** $[C_xF_y]^-$, ***Class 2*** $[C_xF_yO]^-$, ***Class 3*** $[C_xF_yO_3S]^-$, ***Class X*** Others)

No.	Compunds	$[M - H]^-$ Chemical formula	$[M - H]^-$ Exact mass *m/z*	Fragment ions	Reference
1	PFBA	$C_4F_7O_2$	212.9787	$[C_3F_7]^-$	This study
2	PFPeA	$C_5F_9O_2$	262.9755	$[C_4F_9]^-$, $[C_2F_5]^-$	This study
3	PFHxA	$C_6F_{11}O_2$	312.9723	$[C_5F_{11}]^-$, $[C_2F_5]^-$	This study
4	PFHpA	$C_7F_{13}O_2$	362.9691	$[C_6F_{13}]^-$, $[C_3F_7]^-$, $[C_2F_5]^-$	This study
5	PFOA	$C_8F_{15}O_2$	412.9659	$[C_7F_{15}]^-$, $[C_4F_9]^-$, $[C_3F_7]^-$, $[C_2F_5]^-$	This study
6	PFNA	$C_9F_{17}O_2$	462.9627	$[C_8F_{17}]^-$, $[C_5F_{11}]^-$, $[C_4F_9]^-$, $[C_3F_7]^-$	This study
7	PFDA	$C_{10}F_{19}O_2$	512.9595	$[C_9F_{19}]^-$, $[C_6F_{13}]^-$, $[C_5F_{11}]^-$, $[C_4F_9]^-$, $[C_3F_7]^-$, $[C_2F_5]^-$	This study
8	PFUnDA	$C_{11}F_{21}O_2$	562.9563	$[C_{10}F_{21}]^-$, $[C_6F_{13}]^-$, $[C_5F_{11}]^-$, $[C_4F_9]^-$, $[C_3F_7]^-$, $[C_2F_5]^-$	This study
9	PFDoDA	$C_{12}F_{23}O_2$	612.9531	$[C_{11}F_{23}]^-$, $[C_7F_{15}]^-$, $[C_6F_{13}]^-$, $[C_5F_{11}]^-$, $[C_4F_9]^-$, $[C_3F_7]^-$, $[C_2F_5]^-$	This study
10	PFTrDA	$C_{13}F_{25}O_2$	662.9499	$[C_{12}F_{25}]^-$, $[C_9F_{19}]^-$, $[C_8F_{17}]^-$, $[C_7F_{15}]^-$, $[C_6F_{13}]^-$, $[C_5F_{11}]^-$, $[C_4F_9]^-$, $[C_3F_7]^-$, $[C_2F_5]^-$	This study
11	PFTeDA	$C_{14}F_{27}O_2$	712.9467	$[C_{13}F_{27}]^-$, $[C_6F_{13}]^-$, $[C_5F_{11}]^-$, $[C_4F_9]^-$, $[C_3F_7]^-$, $[C_2F_5]^-$	This study
12	PFHxDA	$C_{16}F_{31}O_2$	812.9403	$[C_{15}F_{31}]^-$, $[C_{11}F_{23}]^-$, $[C_{10}F_{21}]^-$, $[C_9F_{19}]^-$, $[C_8F_{17}]^-$, $[C_7F_{15}]^-$, $[C_6F_{13}]^-$, $[C_5F_{11}]^-$, $[C_4F_9]^-$, $[C_3F_7]^-$, $[C_2F_5]^-$	This study
13	PFBS	$C_4F_9O_3S$	298.9424	$[FO_3S]^-$, $[O_3S]^-$	This study
14	PFPeS	$C_5F_{11}O_3S$	348.9392	$[C_3F_6O_3S]^-$, $[C_2F_5]^-$, $[FO_3S]^-$, $[O_3S]^-$, $[CF_3]^-$	Rotander *et al*, 2015
15	PFHxS	$C_6F_{13}O_3S$	398.9361	$[C_2F_5]^-$, $[FO_3S]^-$	This study
16	PFHpS	$C_7F_{15}O_3S$	448.9329	$[C_3F_7]^-$, $[CF_2O_3S]^-$, $[C_2F_5]^-$, $[FO_3S]^-$, $[O_3S]^-$	Rotander *et al*, 2015
17	PFOS	$C_8F_{17}O_3S$	498.9297	$[C_3F_7]^-$, $[C_2F_5]^-$, $[FO_3S]^-$, $[O_3S]^-$	This study
18	PFNS	$C_9F_{19}O_3S$	548.9265	$[C_3F_6O_3S]^-$, $[C_3F_7]^-$, $[CF_2O_3S]^-$, $[FO_3S]^-$, $[O_3S]^-$	Rotander *et al*, 2015
19	6:2 diPAP	$C_{16}H_8F_{26}O_4P$	788.9745	$[C_8H_5F_{13}O_4P]^-$, $[C_8H_4F_{12}O_4P]^-$, $[H_2O_4P]^-$, $[O_3P]^-$	This study
20	8:2 diPAP	$C_{20}H_8F_{34}O_4P$	988.9617	$[C_{10}H_5F_{17}O_4P]^-$, $[C_{10}H_4F_{16}O_4P]^-$, $[H_2O_4P]^-$, $[O_3P]^-$	This study
21	6:2/8:2 diPAP	$C_{18}H_8F_{30}O_4P$	888.9681	$[C_{10}H_5F_{17}O_4P]^-$, $[C_8H_5F_{13}O_4P]^-$, $[C_8H_4F_{12}O_4P]^-$, $[H_2O_4P]^-$, $[O_3P]^-$	This study
22	4:2 FTS	$C_6H_4F_9O_3S$	326.9737	$[C_6H_3F_8O_3S]^-$, $[HO_3S]^-$, $[O_3S]^-$	This study
23	6:2 FTS	$C_8H_4F_{13}O_3S$	426.9674	$[C_8H_3F_{12}O_3S]^-$, $[C_7F_9]^-$, $[HO_3S]^-$, $[O_3S]^-$	This study
24	8:2 FTS	$C_{10}H_4F_{17}O_3S$	526.9610	$[C_{10}H_3F_{16}O_3S]^-$, $[C_9F_{11}]^-$, $[HO_3S]^-$	This study
25	6:2 FTCA	$C_8H_2F_{13}O_2$	376.9847	$[C_7F_{11}]^-$, $[CFO_2]^-$	This study
26	8:2 FTCA	$C_{10}H_2F_{17}O_2$	476.9783	$[C_9F_{15}]^-$	This study
27	5:3 FTCA	$C_8H_4F_{11}O_2$	341.0036	$[C_7HF_8]^-$, $[C_7F_7]^-$, $[CFO_2]^-$	This study
28	7:3 FTCA	$C_{10}H_4F_{15}O_2$	440.9972	$[C_9H_2F_{13}]^-$, $[C_9HF_{12}]^-$, $[C_9F_{11}]^-$, $[C_8F_9]^-$, $[CFO_2]^-$	This study

Class 1 $[C_xF_y]^-$, ***Class 2*** $[C_xF_yO]^-$, ***Class 3*** $[C_xF_yO_3S]^-$, ***Class X*** Others ***(Continued)***

Table 6.1 Classification of PFASs fragment ions used for fragmentation flagging (***Class 1*** $[C_xF_y]^-$, ***Class 2*** $[C_xF_yO]^-$, ***Class 3*** $[C_xF_yO_3S]^-$, ***Class X*** Others)

No.	Compunds	[M - H]⁻ Chemical formula	[M - H]⁻ Exact mass *m/z*	Fragment ions	Reference
29	6:2 FTUCA	$C_8HF_{12}O_2$	356.9785	$[C_7F_{11}]^-$, $[C_6F_9]^-$	This study
30	8:2 FTUCA	$C_{10}HF_{16}O_2$	456.9721	$[C_9F_{15}]^-$	This study
31	10:2 FTUCA	$C_{12}HF_{20}O_2$	556.9657	$[C_{11}F_{19}]^-$	This study
32	FOSA	$C_8HF_{17}NO_2S$	497.9456	$[C_3F_7]^-$, $[FO_2S]^-$, $[NO_2S]^-$	This study
33	*N*-Me-FOSA	$C_9H_3F_{17}NO_2S$	511.9613	$[C_4F_9]^-$, $[C_3F_7]^-$, $[C_2F_5]^-$, $[FO_2S]^-$, $[CF_3]^-$, $[O_2S]^-$	This study
34	*N*-Et-FOSA	$C_{10}H_5F_{17}NO_2S$	525.9769	$[C_8F_{17}]^-$, $[C_8F_{14}]^-$, $[C_5F_{11}]^-$, $[C_4F_9]^-$, $[C_3F_7]^-$, $[C_2H_5FNO_2S]^-$, $[C_2H_4NO_2S]^-$, $[HO_2S]^-$, $[C_2H_3O_2]^-$	This study
35	FOSAA	$C_{10}H_3F_{17}NO_4S$	555.9511	$[C_8HF_{17}NO_2S]^-$, $[C_8F_{17}]^-$, $[C_4F_9]^-$, $[C_3F_7]^-$, $[C_2H_2NO_4S]^-$, $[NO_2S]^-$	This study
36	*N*-Et-FOSAA	$C_{12}H_7F_{17}NO_4S$	583.9824	$[C_{10}H_5F_{17}NO_2S]^-$, $[C_8F_{17}]^-$, $[C_4F_9]^-$, $[C_3F_7]^-$, $[C_2F_5]^-$, $[FO_2S]^-$, $[NO_3]^-$	This study
37	FHxSE	$C_8H_5F_{13}NO_3S$	441.9783	$[C_3F_7]^-$, $[C_2H_4NO_3S]^-$, $[C_2F_5]^-$, $[CH_2NO_2S]^-$, $[NO_2S]^-$, $[HO_2S]^-$, $[O_2S]^-$	Baduel, C., *et al*., 2017
38	*N*-SP-FHxSA	$C_9H_7F_{13}NO_5S_2$	519.9558	$[C_6HF_{13}NO_2S]^-$, $[NO_2S]^-$	Barzen-Hanson *et al*, 2017
39	*N*-SPAmP-FHxSA	$C_{14}H_{18}F_{13}N_2O_5S_2$	605.0449	$[C_{11}H_{12}F_{13}N_2O_2S]^-$, $[C_6F_{13}]^-$, $[C_5H_{12}FN_2O_2S]^-$, $[C_3F_7]^-$, $[C_5H_{12}NO_3S]^-$, $[C_2F_5]^-$, $[O_3S]^-$	Barzen-Hanson *et al*, 2017
40	*N*-SHOPAmP-FHxSA	$C_{14}H_{18}F_{13}N_2O_6S_2$	621.0399	$[C_{11}H_{12}F_{13}N_2O_2S]^-$, $[C_5H_{12}NO_4S]^-$, $[C_3F_7]^-$, $[CH_3O_3S]^-$, $[O_3S]^-$	Barzen-Hanson *et al*, 2017
41	*N*-SPAmP-FHxSAPS	$C_{17}H_{24}F_{13}N_2O_8S_3$	727.0487	$[C_{14}H_{18}F_{13}N_2O_5S_2]^-$, $[C_{11}H_{12}F_{13}N_2O_2S]^-$, $[C_6F_{13}]^-$, $[C_5H_{12}FN_2O_2S]^-$, $[C_3F_7]^-$, $[C_2F_5]^-$	Barzen-Hanson *et al*, 2017
42	*N*-diHOPAmHOB-FHxSA	$C_{15}H_{20}F_{13}N_2O_5S$	587.0885	$[C_{12}H_{14}F_{13}N_2O_3S]^-$, $[C_{11}H_{12}F_{13}N_2O_2S]^-$, $[C_6F_{13}]^-$, $[C_5H_{12}FN_2O_2S]^-$, $[C_3F_7]^-$, $[C_2F_5]^-$	Barzen-Hanson *et al*, 2017
43	*N*-diHOPAmHOBFHxSAPS	$C_{18}H_{26}F_7N_2O_8S_2$	709.0923	$[C_{15}H_{20}F_{13}N_2O_6S_2]^-$, $[C_{14}H_{18}F_{13}N_2O_5S_2]^-$, $[C_{12}H_{11}F_{13}NO_5S_2]^-$, $[C_{12}H_{14}F_{13}N_2O_3S]^-$, $[C_{11}H_{12}F_{13}N_2O_2S]^-$, $[C_9H_5F_{13}NO_2S]^-$, $[C_7H_3F_{13}NO_2S]^-$, $[C_6F_{13}]^-$, $[C_3F_7]^-$, $[C_2F_5]^-$	Barzen-Hanson *et al*, 2017
44	*N*-CMAmPFBSA	$C_{11}H_{14}F_9N_2O_4S$	441.0530	$[C_9H_{12}F_9N_2O_2S]^-$, $[C_8H_8F_9N_2O_2S]^-$, $[C_7H_5F_9NO_2S]^-$, $[C_4F_9O_2S]^-$, $[C_4F_9]^-$, $[C_5H_{11}N_2O_2S]^-$, $[CH_2NO_2S]^-$, $[HO_2S]^-$	Barzen-Hanson *et al*, 2017
45	F5S-PFOS	$C_8F_{21}O_3S_2$	606.8954	$[C_8F_{16}O_3S]^-$, $[C_6F_{12}O_3S]^-$, $[C_5F_{10}O_3S]^-$, $[C_4F_8O_3S]^-$, $[C_3F_6O_3S]^-$, $[C_2F_4O_3S]^-$, $[CF_2O_3S]^-$, $[F_5S]^-$, $[O_3S]^-$	Barzen-Hanson *et al*, 2017
46	F5S-PFHpA	$C_8F_{19}O_2S$	520.9316	$[F_5S]^-$	Barzen-Hanson *et al*, 2017
47	UPFPeS	$C_8F_{15}O_3S$	460.9329	$[C_8F_{15}]^-$, $[C_7F_{13}]^-$, $[C_6F_{11}]^-$, $[C_4F_7]^-$, $[C_3F_7]^-$, $[C_3F_5]^-$, $[CF_2O_3S]^-$, $[C_2F_5]^-$, $[FO_3S]^-$, $[O_3S]^-$	Barzen-Hanson *et al*, 2017
48	H-UPFBS	$C_8HF_{12}O_3S$	442.9423	$[C_8F_{13}O_3S]^-$, $[C_8F_{13}]^-$, $[C_7F_{11}]^-$, $[C_6F_9]^-$, $[C_5F_7]^-$, $[C_4F_5]^-$, $[C_3F_5]^-$, $[FO_3S]^-$, $[O_3S]^-$	Barzen-Hanson *et al*, 2017
49	H-PFHxS	$C_8HF_{16}O_3S$	480.9391	$[C_8F_{15}O_3S]^-$, $[C_7F_{13}O_3S]^-$, $[C_8F_{15}]^-$, $[C_7F_{13}]^-$, $[C_6F_{11}]^-$, $[C_3F_6O_3S]^-$, $[C_4F_7]^-$, $[C_3F_7]^-$, $[CF_2O_3S]^-$, $[C_2F_5]^-$, $[FO_3S]^-$, $[O_3S]^-$	Barzen-Hanson *et al*, 2017

Class 1 $[C_xF_y]^-$, ***Class 2*** $[C_xF_yO]^-$, ***Class 3*** $[C_xF_yO_3S]^-$, ***Class X*** Others ***(Continued)***

Table 6.1 Classification of PFASs fragment ions used for fragmentation flagging (***Class 1*** $[C_xF_y]^-$, ***Class 2*** $[C_xF_yO]^-$, ***Class 3*** $[C_xF_yO_3S]^-$, ***Class X*** Others)

No.	Compunds	$[M - H]^-$ Chemical formula	$[M - H]^-$ Exact mass *m/z*	Fragment ions	Reference
50	7:1 PFAS	$C_8H_2F_{15}O_3S$	462.9485	$[C_8HF_{14}O_3S]^-$, $[C_8F_{13}O_3S]^-$, $[C_8F_{13}]^-$, $[C_7F_{11}]^-$, $[C_6F_9]^-$, $[C_5F_7]^-$, $[C_4F_5]^-$, $[FO_3S]^-$, $[O_3S]^-$	Barzen-Hanson *et al*, 2017
51	O-U-PFPrA	$C_8F_{13}O_3$	390.9640	$[C_6F_{11}]^-$, $[C_5F_9]^-$, $[C_4F_7O]^-$, $[C_4F_7]^-$, $[C_3F_5O]^-$, $[C_2F_5O]^-$, $[C_3F_5]^-$, $[C_2F_5]^-$, $[CF_3O]^-$, $[CF_3]^-$	Barzen-Hanson *et al*, 2017
52	*N*-AHOBFHxSAPS	$C_{15}H_{20}F_{13}N_2O_6S_2$	635.0555	$[C_{12}H_{14}F_{13}N_2O_3S]^-$, $[C_6F_{13}]^-$, $[C_6H_{14}NO_4S]^-$, $[C_3F_7]^-$, $[C_4H_9N_2O_2S]^-$	Barzen-Hanson *et al*, 2017
53	*N*-SPAmP-FHxSAA	$C_{16}H_{20}F_{13}N_2O_7S_2$	663.0504	$[C_{11}H_{12}F_{13}N_2O_2S]^-$, $[C_9H_5F_{13}NO_2S]^-$, $[C_6HF_{13}NO_2S]^-$, $[C_6F_{13}]^-$, $[C_3F_7]^-$, $[C_5H_{12}NO_3S]^-$, $[O_3S]^-$	Barzen-Hanson *et al*, 2017
54	*N*-diHOBAmP-FHxSA	$C_{15}H_{20}F_{13}N_2O_4S$	571.0936	$[C_{12}H_{14}F_{13}N_2O_2S]^-$, $[C_{11}H_{12}F_{13}N_2O_2S]^-$, $[C_6F_{13}]^-$, $[C_6H_{14}FN_2O_2S]^-$, $[C_3F_7]^-$, $[C_5H_{11}N_2O_2S]^-$, $[C_2F_5]^-$, $[C_2H_3O_2]^-$	Barzen-Hanson *et al*, 2017
55	1HO-6:2 FTS	$C_8H_4F_{13}O_4S$	442.9623	$[C_8H_2F_{13}O_3S]^-$, $[C_6F_{13}]^-$, $[C_7F_{11}]^-$, $[C_6F_9]^-$, $[C_5F_7]^-$, $[C_3F_7]^-$, $[C_2H_3O_4S]^-$, $[C_2F_5]^-$, $[CH_3O_3S]^-$, $[HO_3S]^-$, $[O_3S]^-$	Barzen-Hanson *et al*, 2017
56	6:2 FTSO2PA	$C_{11}H_8F_{13}O_4S$	482.9936	$[C_8HF_{10}]^-$, $[C_8H_3F_8S]^-$, $[C_8F_9]^-$, $[C_7F_9]^-$, $[C_7F_7]^-$, $[C_3H_5O_4S]^-$, $[FO_2S]^-$	Barzen-Hanson *et al*, 2017
57	PFOS-Cl	$C_8F_{16}O_3SCl$	514.9001	$[C_2F_5]^-$, $[O_3SCl]^-$, $[FO_3S]^-$, $[O_3S]^-$, $[Cl]^-$	Baduel *et al*, 2017
58	PFOS-Cl_2	$C_8F_{15}O_3SCl_2$	530.8706	$[C_5F_9O_3S]^-$, $[C_4F_7O_3SCl]^-$, $[C_4F_7O_3S]^-$, $[C_3F_6O_3S]^-$, $[C_2F_4O_3S]^-$, $[CF_2O_3S]^-$, $[FO_3S]^-$, $[O_3S]^-$, $[Cl]^-$	Baduel *et al*, 2017
59	PFOS-Keton	$C_8F_{15}O_4S$	476.9278	$[C_7F_{13}O_3S]^-$, $[C_7F_{13}]^-$, $[C_5F_9O_3S]^-$, $[C_6F_{11}O]^-$, $[C_4F_7O_3S]^-$, $[C_5F_9]^-$, $[C_4F_7O]^-$, $[C_4F_7]^-$, $[C_3F_5O]^-$, $[C_3F_5]^-$, $[CF_2O_3S]^-$, $[FO_3S]^-$, $[O_3S]^-$	Baduel *et al*, 2017
60	PFHxSi	$C_6F_{13}O_2S$	382.9411	$[C_3F_7]^-$, $[C_2F_5]^-$, $[FO_2S]^-$	Baduel *et al*, 2017
61	6:2FTSAS	$C_{15}H_{16}F_{13}NO_5S_2$	601.0262	$[C_7H_{14}NO_5S_2]^-$, $[C_7H_{12}NO_4S]^-$, $[C_4H_{10}NO_3S]^-$, $[C_4H_7O_3S]^-$	Baduel *et al*, 2017
62	PFHxSaAm	$C_{11}H_{12}F_{13}N_2O_2S$	483.0412	$[C_6F_{13}]^-$, $[C_5H_{12}FN_2O_2S]^-$, $[C_3F_7]^-$, $[C_5H_{11}N_2O_2S]^-$, $[C_2F_5]^-$	Baduel *et al*, 2017
63	$C_{12}F_{12}H_{12}O_2$	$C_{12}H_{11}F_{12}O_2$	415.0567	$[C_{10}H_6F_{11}]^-$, $[C_{10}H_5F_{10}]^-$, $[C_{10}H_4F_9]^-$	Newton *et al*, 2017
64	*None proposed*	$C_4HF_8O_3S$	280.9519	$[C_4F_7O_2S]^-$, $[C_4F_7]^-$, $[C_3F_5]^-$, $[FO_3S]^-$, $[O_3S]^-$	Newton *et al*, 2017
65	5:2 Cl-PFAES	$C_7F_{14}O_4SCl$	480.8982	$[C_6F_{12}OCl]^-$	Ruan *et al*, 2015
66	8:2 Cl-PFAES	$C_{10}F_{20}O_4SCl$	630.8886	$[C_8F_{16}OCl]^-$, $[FO_3S]^-$, $[FO_2S]^-$	Ruan *et al*, 2015
67	10:2 Cl-PFAES	$C_{12}F_{24}O_4SCl$	730.8823	$[C_{10}F_{20}OCl]^-$	Ruan *et al*, 2015
68	Ether-PFHxS	$C_6F_{13}O_4S$	414.9310	$[C_3F_7O]^-$, $[C_2F_5O]^-$, $[FO_3S]^-$, $[CF_3O]^-$, $[O_3S]^-$	Rotander *et al*, 2015

Class 1 $[C_xF_y]^-$, ***Class 2*** $[C_xF_yO]^-$, ***Class 3*** $[C_xF_yO_3S]^-$, ***Class X*** Others

The fragmentation flags were selected from the fragment ions classification in order to discover suspected PFASs. The fragmentation flags were classified into three classes of fluorinated fragment ions, ***Class 1***, 120 types of $[C_xF_y]^-$ (e.g., $[C_nF_{2n+1}]^-$, n = 2–16); ***Class 2***, 123 types of $[C_xF_yO]^-$ (e.g., $[C_nF_{2n+1}O]^-$, n = 2–16); and ***Class 3***, 131 types of $[C_xF_yO_3S]^-$ (e.g., $[C_nF_{2n+1}O_3S]^-$, n = 1–16) (**Fig. 6.1**). The fragmentation flags had a wide range of fluoroalkyl chain lengths (C_4–C_{16}); as PFASs are often manufactured as chain-length homologs (Lee et al., 2016), it was important to capture both of very-short- and very-long-chain lengths. In ***Class 1*** $[C_xF_y]^-$, 71% of PFASs generated $[C_nF_{2n+1}]^-$ fluoroalkyl ions, and some fluorotelomer acids fragmented saturated fluoroalkyl ions (e.g., $[C_nF_{2n-1}]^-$, $[C_nF_{2n-3}]^-$, $[C_nF_{2n-5}]^-$ from FTCAs, FTUCAs, and FTSs). Among emerging PFASs in industry, perfluoroalkyl dioic acids, hydro-substituted perfluoroalkyl dioic acids, and unsaturated perfluorinated alcohols generated $[C_nF_{2n+1}]^-$, $[C_nF_{2n-1}]^-$, and $[C_nF_{2n-3}]^-$, as previously reported (Yu et al., 2018). In ***Class 2***, $[C_xF_yO]^-$ was associated with polyfluoroalkyl ester carboxylic acids (PFECAs), which have been produced as PFOA replacements; e.g., ADONA (3H-perfluoro-3-[(3-methoxy-propoxy)propanoic acid]) and GenX (hexafluoropropylene oxide dimer acid) (Wang et al., 2017). Previous studies reported that $[C_nF_{2n+1}O]^-$ (n = 1–4, 10, 11, 14) were observed as fragment ions of PFECAs (Yu et al., 2018; McCord et al., 2018). The legacy and emerging PFASs were globally detected in environmental samples and drinking water in recent years (Pan et al., 2018; Gebbink et al., 2017; Sun et al., 2016). In ***Class 3***, $[C_xF_yO_3S]^-$ (e.g., $[C_nF_{2n+1}O_3S]^-$ from (n-pentafluoro(5)sulfide)-perfluorooctane sulfonate (F5S-PFOS, $[C_8HF_{19}O_3S_2]$) (Barzen-Hanson et al., 2017) and dechlorinated perfluoroalkyl sulfonate (PFOS-Cl_2, $[C_8HF_{15}O_3SCl_2]$) (Baduel et al., 2017)) were detected according to the classification. In ***Class X***, 11 types of non-fluorinated fragment ions were classified (e.g., $[O_3S]^-$).

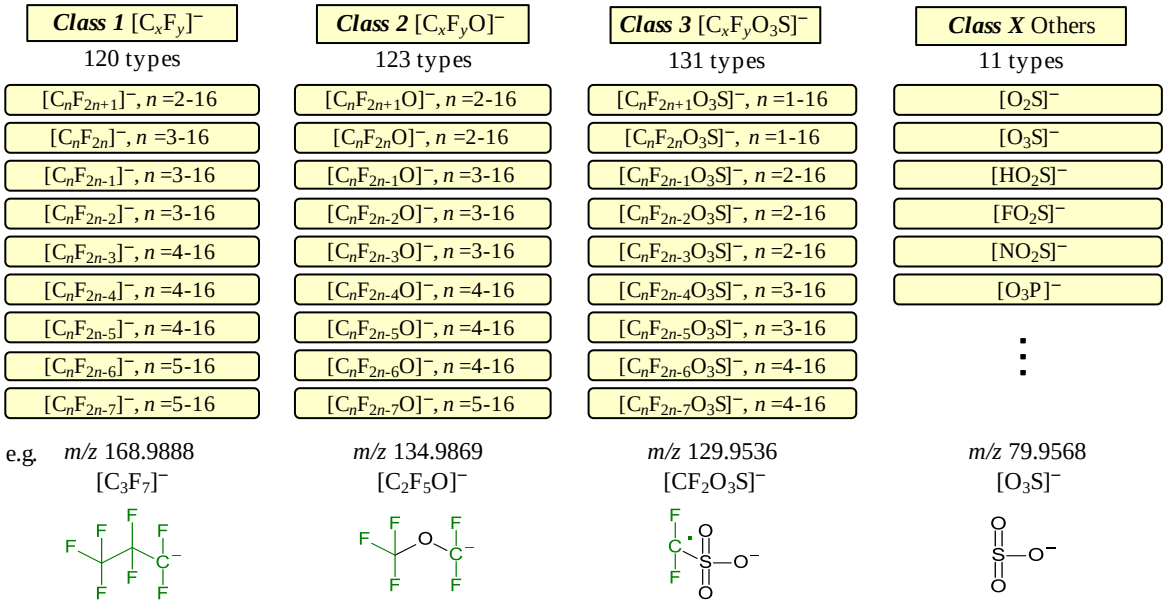

Fig. 6.1 Selection of fragmentation flags

6.2 Fragmentation flagging for Standards and a product

The fragmentation flagging or parent-ion searching approach was examined to discover unknown PFASs in environmental samples or products (Liu et al., 2015; Liu et al., 2018; Xiao et al., 2017; Liu et al., 2019). In this study, the selection of peaks by fragmentation flagging for PFAS standards mixture solution was performed for validation (**Fig. 6.2**). The sample was examined at CE 10, 20, and 40 V to cover a wide range of PFASs. The 385 EICs were classified into four types of fragmentation flags: ***Class 1***, 120 types of $[C_xF_y]^-$; ***Class 2***, 123 types of $[C_xF_yO]^-$; ***Class 3***, 131 types of $[C_xF_yO_3S]^-$; and ***Class X***, 11 types of others (not including C or F). In this study, peaks which were observed above the abundance threshold (1×10^4) were used as fragmentation flags. Firstly, RTs (t_x) with locating overlapped fragmentation flags were named t_1 to t_{20} in ***Class 1***; t_{21} to t_{24} in ***Class 3***; and t_{25} to t_{40} in ***Class X***. In ***Class 2***, no fragmentation flags were observed because the targeted PFASs in this study do not have C_xF_yO fragment ions according to the classification. Secondly, all t_x were regrouped as T_y (T_1 with t_1; T_2 with t_{21} and t_{25}; T_3 with t_2; …; T_{30} with t_{20} and t_{39}; and T_{31} with t_{40}). At this point, T_y derived only from ***Class X*** (T_5, T_{11}, T_{12}, T_{19}, T_{21}, T_{24}, and T_{31}) were excluded in further steps as they have no fluoroalkyl groups. Finally, the obtained T_y were treated s as "Flag Sets" which included fluorinated fragment ions (***Classes 1*** to ***3***). As a result, 20 flag sets were selected by fragmentation flagging as follows; PFHxA (Flag Set S1, T_1 with t_1), PFBS (Flag Set S2, T_2 with t_{21} and t_{25}), 6:2 FTUCA (Flag Set S3, T_3 with t_2), …, *N*-MeFOSA (Flag Set S23, T_{29} with t_{19} and t_{38}), and *N*-EtFOSA (Flag Set S24, T_{30} with t_{20} and t_{39}). However, at this stage, peaks and chemical formulas might disagree because EICs were selected in the range of ±20 ppm. Three diPAPs (Flag Set S17, S20, and S22) were excluded from the results because it was expected that their fragmentation flags (e.g. $[C_{10}F_{17}]^-$, *m/z* 442.9729)) and the actual fragment ions (e.g. $[C_8H_5F_{13}O_4P]^-$, *m/z* 442.9718) were different. As the peaks of suspected PFASs were selected under specific conditions, the results might depend on the range of targeted PFASs. This study targeted 20 PFASs which the abundances of fragment ions were high for validation of the linking method.

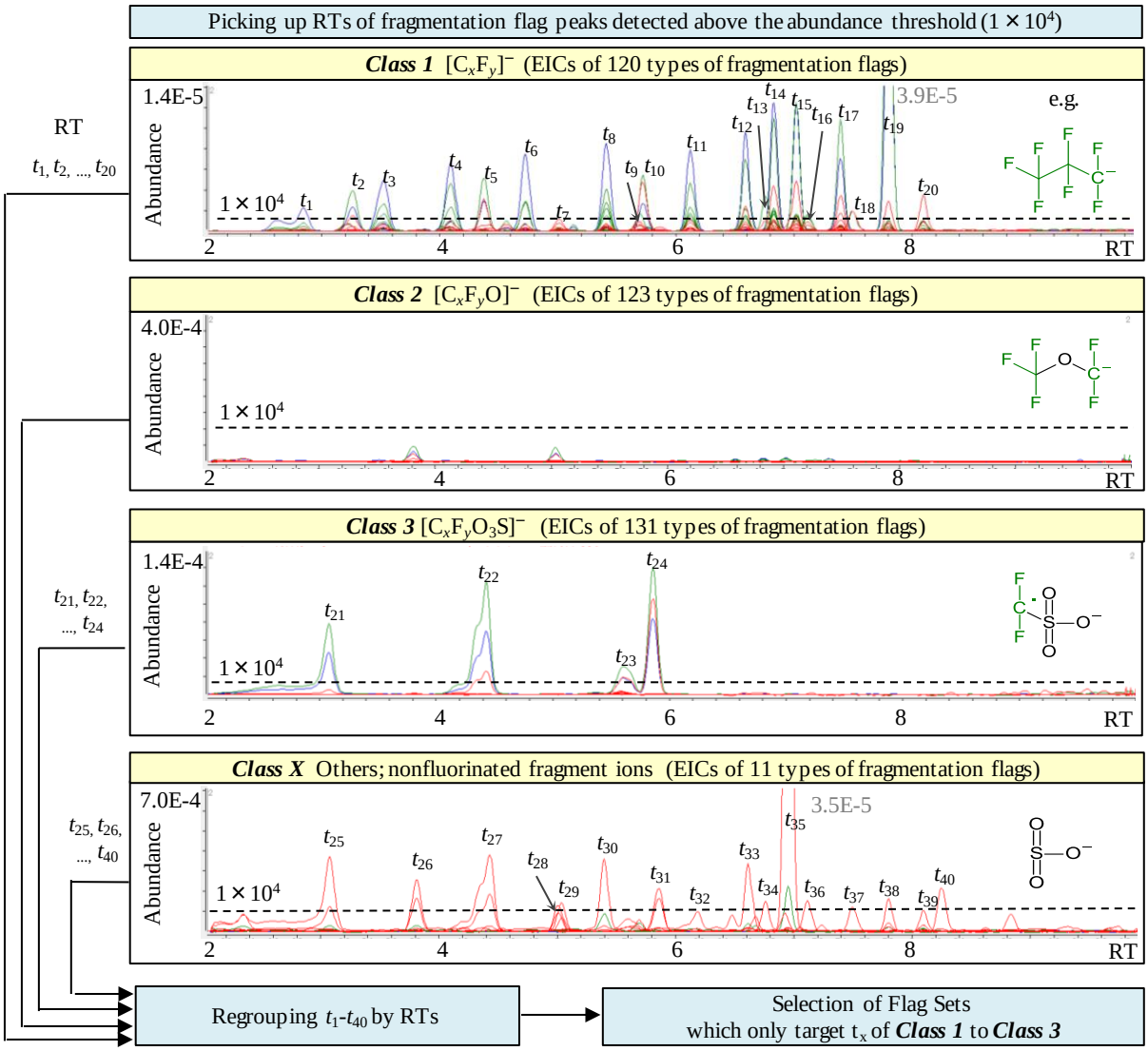

Compounds	Flag Set	T_y	t_x Class 1	2	3	X
PFHxA	S1	T_1	t_1	-	-	-
PFBS	S2	T_2	-	-	t_{21}	t_{25}
6:2 FTUCA	S3	T_3	t_2	-	-	-
PFHpA	S4	T_4	t_3	-	-	-
-	-	T_5	-	-	-	t_{26}
PFOA	S5	T_6	t_4	-	-	-
8:2 FTUCA	S6	T_7	t_5	-	-	-
PFHxS	S7	T_8	-	-	t_{22}	t_{27}
PFNA	S8	T_9	t_6	-	-	-
FOSAA	S9	T_{10}	t_7	-	-	t_{28}
-	-	T_{11}	-	-	-	t_{29}
-	-	T_{12}	-	-	-	t_{30}
PFDA	S10	T_{13}	t_8	-	-	-
(Branched PFOS)	S11	T_{14}	-	-	t_{23}	-
N-EtFOSAA	S12	T_{15}	t_9	-	-	-
10:2 FTUCA	S13	T_{16}	t_{10}	-	-	-

Compounds	Flag Set	T_y	t_x Class 1	2	3	X
PFOS	S14	T_{17}	-	-	t_{24}	t_{31}
PFUnDA	S15	T_{18}	t_{11}	-	-	-
-	-	T_{19}	-	-	-	t_{32}
PFDoDA	S16	T_{20}	t_{12}	-	-	-
-	-	T_{21}	-	-	-	t_{33}
6:2 diPAP	S17	T_{22}	t_{13}	-	-	t_{34}
PFTrDA	S18	T_{23}	t_{14}	-	-	-
-	-	T_{24}	-	-	-	t_{35}
PFTeDA	S19	T_{25}	t_{15}	-	-	-
6:2/8:2 diPAP	S20	T_{26}	t_{16}	-	-	t_{36}
PFHxDA	S21	T_{27}	t_{17}	-	-	-
8:2 diPAP	S22	T_{28}	t_{18}	-	-	t_{37}
N-MeFOSA	S23	T_{29}	t_{19}	-	-	t_{38}
N-EtFOSA	S24	T_{30}	t_{20}	-	-	t_{39}
-	-	T_{31}	-	-	-	t_{40}

Fig. 6.2 Selection of peaks by fragmentation flagging for PFAS standards mixture solution. The EICs were described at 10 V in blue, 20 V in green, and 40 V in red.

6.3 Linking fragmentation flags with their precursor ions by drift time using ion mobility mass spectrometry for PFAS standards mixture solution

Fragmentation flagging itself helped in suggesting the precursor ions which generate F-containing fragment ions by LC/QTOF-MS. However, it was difficult to search for the precursor ions from some co-eluting compounds at a specific RT. This study proposed a new method of linking fragmentation flags with their precursor ions by the drift time of ion mobility spectrometry by validating with the use of PFAS standards mixed solution. The method contains three sub-steps; **Step 1**, searching for mass spectrum of fragmentation flags at 10, 20 or 40 V; **Step 2**, determining the range of drift time of fragmentation flags; **Step 3**, searching for the *m/z* of prospective precursor ions for specific drift time at 0 V. As above mentioned, the switching CE (μs) is faster than the drift time (ms) from ion mobility to collision cell, the precursor ion and fragment ions could be observed in the same range of drift time (Steiner et al., 2001; Steiner et al., 2003). Therefore, the linkage method could narrow down the candidates of precursor ions by drift time using ion mobility spectrometry.

The method was validated by using the data obtained from 20 targeted PFASs in standard mixed solution (Flag Set S1-24, excluding S11, 17, 20, 28). As examples, (a) PFOA (Flag Set S5, RT = 4.003–4.138 min), (b) PFOS (Flag Set S14, RT = 5.788–5.923 min), and (c) FOSAA (Flag Set S9, RT = 4.939–5.074 min) were described (**Fig. 6.3**). For PFOA (Flag Set S5), in **Step 1**, signals of $[C_3F_7]^-$ (*m/z* 168.9877), $[C_4F_9]^-$ (*m/z* 218.9847), and $[C_7F_{15}]^-$ (*m/z* 368.9737) were matched with corresponding fragmentation flags. In **Step 2**, the range of drift time of fragmentation flags was between 18.19 and 19.31 ms. In **Step 3**, the spectrum of *m/z* 412.9627 ($[C_7F_{15}O_2]^-$) was searched between the range of drift time at 0 V, thus, it was the precursor ion of PFOA. The precursor ion was searched by drift time using ion mobility spectrometry. The results of PFOS and FOSAA can be explained in the same manner. For PFOS (Flag Set S14), in **Step 1**, signals of $[O_3S]^-$ (*m/z* 79.9580), $[C_2F_5]^-$ (*m/z* 118.9927), $[C_3F_7]^-$ (*m/z* 168.9904), and $[C_3F_6O_3S]^-$ (*m/z* 229.9434) were searched. In **Step 2**, the range of drift time of fragmentation flags was between 19.03 and 21.32 ms. In **Step 3**, the spectrum of *m/z* 498.9328

($[C_8F_{17}O_3S]^-$) was searched between the range of drift time at 0 V, it was the precursor ion of PFOS. For FOSAA (Flag Set S14), in **Step 1**, signals of $[NO_2S]^-$ (*m/z* 77.9666), $[C_3F_7]^-$ (*m/z* 168.9916), $[C_4F_9]^-$ (*m/z* 218.9878), and $[C_8F_{17}]^-$ (*m/z* 418.9754) were searched. In **Step 2**, the range of drift time of fragmentation flags was between 21.56 and 22.28 ms. In **Step 3**, the spectrum of *m/z* 555.9553 ($[C_{10}H_3F_{17}NO_4S]^-$) was searched between the range of drift time at 0 V, it was the precursor ion of FOSAA. The fragmentation flags and their suspected precursor ion were observed in the same range of drift time. The validity of these methods was confirmed by ion mobility spectrometry of 20 PFASs (Fig. S3a–t). Their precursor ions and fragment ions could also be observed in the same range of drift time comparing with the results of MS/MS experiments. Separation of targeted PFASs from co-eluting peaks by drift time using ion mobility spectrometry for 8:2 FTUCA and *N*-EtFOSAA were shown in **Fig. 6.4** as examples. It was shown that 8:2 FTUCA (Flag Set S6, T_7) and PFHxS (Flag Set S7, T_8) were co-eluting at specific RT (a-1). In addition, branched PFOS (Flag Set S11, T_{14}), *N*-EtFOSAA (Flag Set S12, T_{15}), and 10:2 FTUCA (Flag Set S13, T_{16}) were co-eluting at specific RT as well (b-1). For searching 8:2 FTUCA, PFHxS could be excluded by drift time (19.99-21.32 ms) (a-2). For *N*-EtFOSAA, branched PFOS, 10:2 FTUCA, and some unrelated mass spectrum could be excluded by drift time (23.37-24.57 ms) as well (b-2). The results of other PFASs were shown in Fig. S3a–t. Therefore, the method could quickly associate the fragment ions with the precursor ion by drift time for non-target analysis.

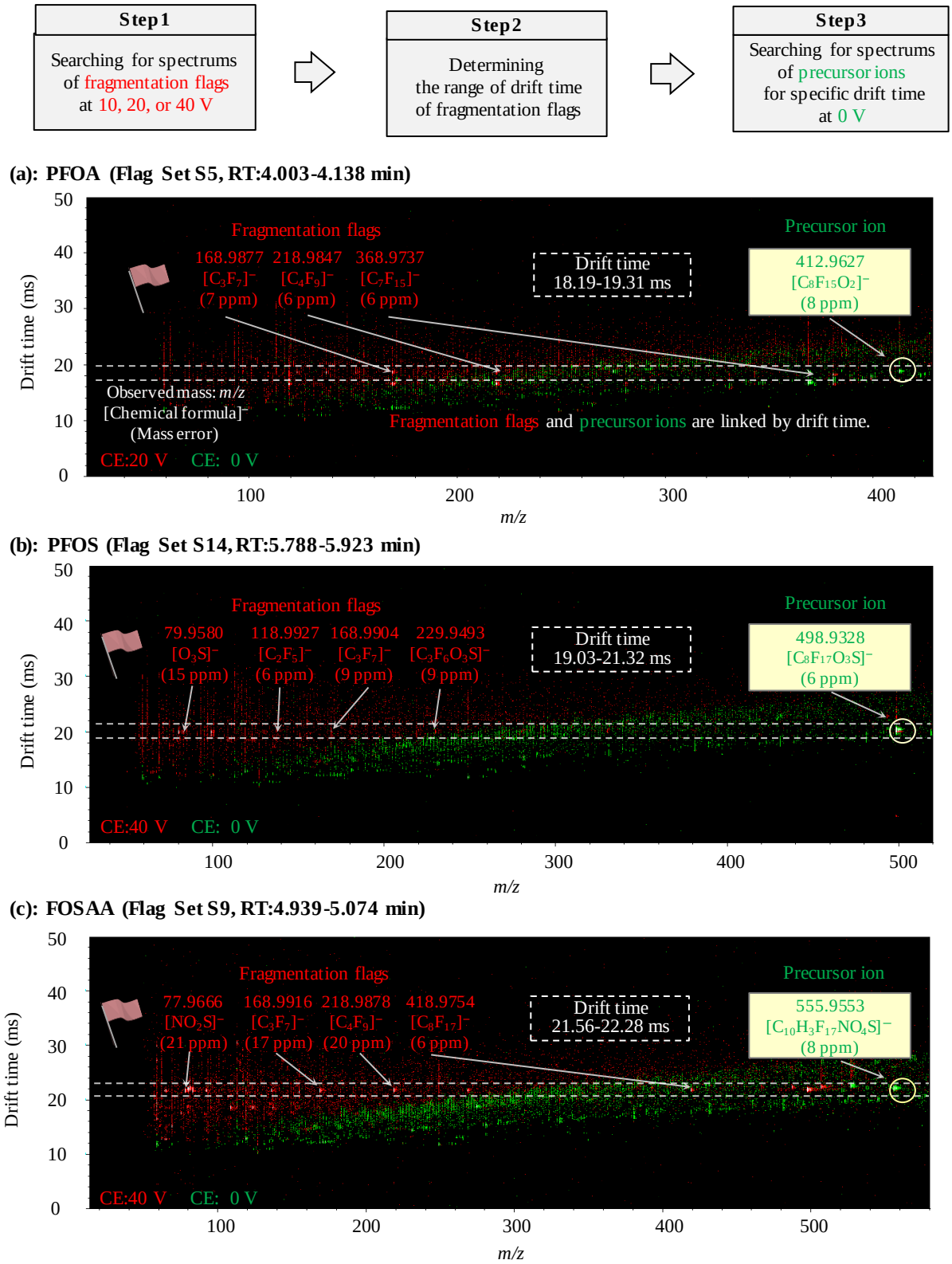

Fig. 6.3 A method of linking fragmentation flags with their precursor ions by drift time using ion mobility mass spectrometry.

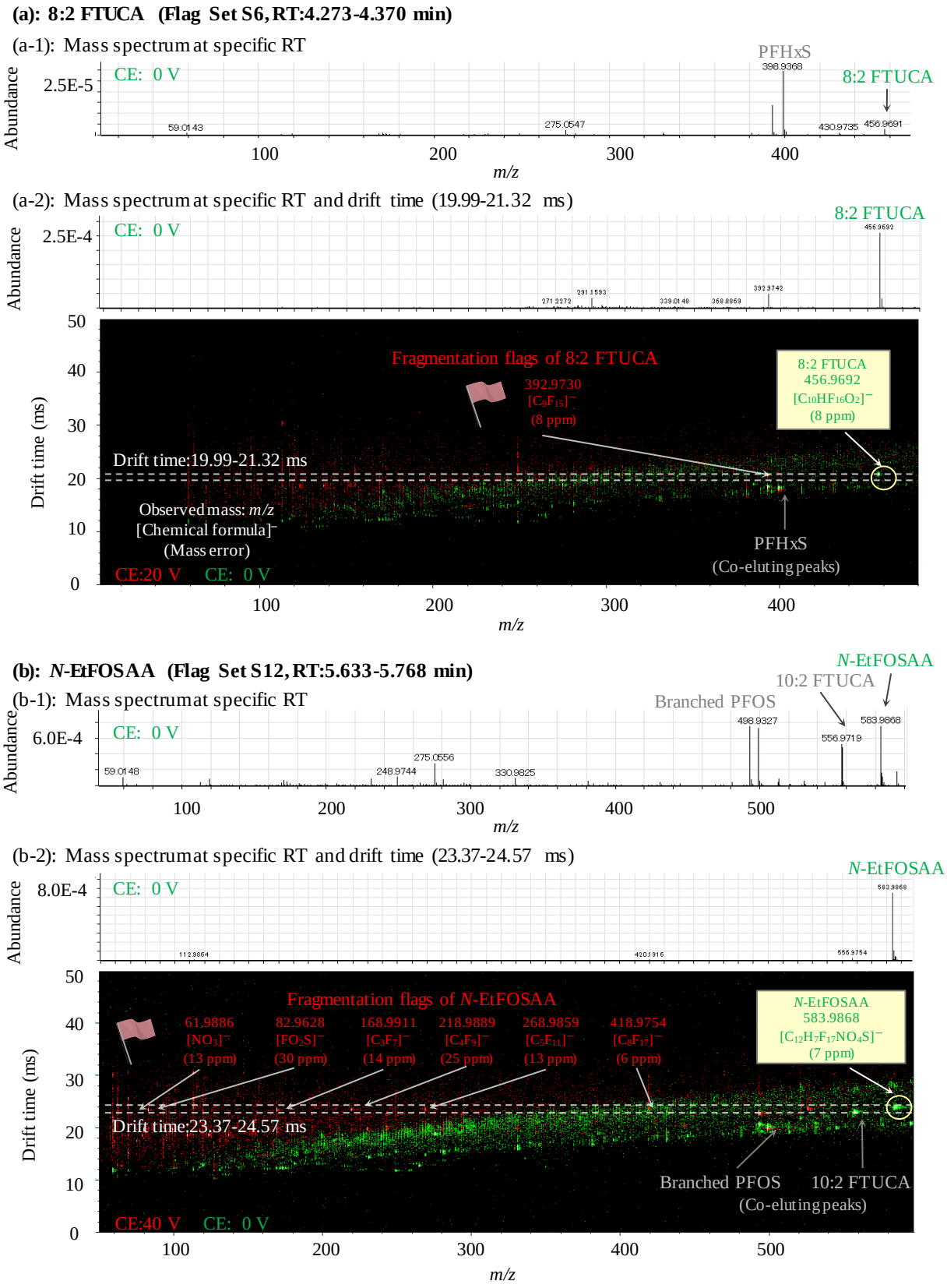

Fig. 6.4 Separation of targeted PFASs from co-eluting peaks by drift time using ion mobility mass spectrometry

6.4 Practical example of the linking method for a household fire extinguisher liquid

The results of a household fire extinguisher liquid were described as a practical example. Selection of peaks by fragmentation flagging for the product is shown in **Fig. 6.5**. Firstly, RTs (t_x) with locating overlapped fragmentation flags were named t_1 to t_9 in ***Class 1***; t_{10} to t_{13} in ***Class 2***, t_{14} in ***Class 3***, and t_{15} to t_{25} in ***Class X***. Secondly, all t_x were regrouped as T_y (T_1 with t_{15}; T_2 with t_1; T_3 with t_{16}; …; T_{13} with t_8; and T_{14} with t_9, t_{13}, and t_{25}). At this point, T_y derived only from ***Class X*** (T_1, T_3, T_4, T_7, T_{10}) were excluded in further steps as they have no fluoroalkyl groups. Finally, nine flag sets were determined: Flag Set 1 (T_2), 2 (T_5), 3 (T_6), 4 (T_8), 5 (T_9), 6 (T_{11}), 7 (T_{12}), 8 (T_{13}), and 9 (T_{14}).

To search for their precursor ions, the method of linking their fragmentation flags with their precursor ions by ion mobility spectrometry applied for the product. For Flag Set 2, RT = 3.707–3.880 min (Fig. S5b), in **Step 1**, signals of $[HO_3S]^-$ (*m/z* 80.9666) $[C_7F_7]^-$ (*m/z* 216.9889), $[C_7F_9]^-$ (*m/z* 254.9856), and $[C_7F_{11}]^-$ (*m/z* 292.9823) were matched with corresponding fragmentation flags. In **Step 2**, the range of drift time of fragmentation flags was between 19.03 and 21.32 ms. In **Step 3**, this range was associated with *m/z* 426.9759 at 0 V. These steps revealed the prospective precursor ions of each flag set: *m/z* 312.9719 (Flag Set 1), *m/z* 426.9759 (2), *m/z* 569.0863 (3), *m/z* 458.9449 (4), *m/z* 511.0743 (5), *m/z* 425.9821 (6), *m/z* 835.9571 (7), *m/z* 907.0223 (8), and *m/z* 771.9868 (9). Therefore, the method could be applied for actual samples, and proposed PFASs were at confidence level 4 (exact mass of interest) (Schymanski et al., 2014). Because these values lie in the range of the unique mass defect (>0.85 or <0.15 unit of CF_2) (Yu et al., 2018), they are all likely PFASs. The advantage of the method makes it possible to detect unknown PFASs without the outernal database. Therefore, applying mass defect filtering-MSMS strategies after the method developed in this study can be effective for searching unknown PFASs.

Finally, their suspected molecular formulas were described according to MS/MS experiments. Flag Set 1 had two candidate precursor ions, *m/z* 312.9719 and *m/z* 268.9807, owing to the suspected loss of $[CO_2]$ (43.9898 Da) by ESI. However, they are commonly used in Q1/Q3 pair for monitoring

perfluorohexanoic acid (PFHxA). Flag Sets 5, 6, and 9 indicated the loss of [HF] (20.0062 Da). Fragmentation led to the neutral loss of HF (e.g., *m/z* 511.0743 and *m/z* 491.0730 in Flag Set 5); fluorotelomer-based PFASs or novel PFASs form with $C_{2n}H_{2n}F_{2n}O_2$ (Newton et al., 2017) showed the same fragmentation. Thus, the precursor ions of Flag Sets 5, 6, and 7 were suggested as fluoroalkyl chain structures including H atoms. As a result, PFHxA $[C_6F_{11}O_2]^-$ (Flag Set 1); 6:2 FTS $[C_8H_4F_{13}O_3S]^-$ (2); 6:2 fluorotelomer sulfonamide alkylbetaine (6:2 FTAB) $[C_{15}H_{18}F_{13}N_2O_4S]^-$ (3); $[C_8H_4F_{13}O_3S_2]^-$ (4); 6:2 fluorotelomer sulfonamide amine (6:2 FTA) $[C_{13}H_{16}F_{13}N_2O_2S]^-$ (5), N-ethyl perfluorohexane sulfonamide (*N*-EtFHxSA) $[C_8H_5F_{13}NO_2S]^-$ (6), $[C_{16}H_8F_{26}NO_4S_2]^-$ (7), $[C_{23}H_{13}F_{26}N_2O_4S]^-$ (8); and $[C_{16}H_8F_{26}NO_2S]^-$ (9) were suggested as proposed formulas in line with the fragment ions classification and previous studies (Barzen-Hanson et al., 2017; D'Agostino et al., 2013; Mejia-Avendaño et al., 2017) (**Table 6.2**). The similar fragmentation patterns were observed between Flag Set 6, 7, and 9, common fragment ions; $[C_8H_5F_{13}NO_2S]^-$ (*m/z* 425.9835), $[C_8H_4F_{12}NO_2S]^-$ (*m/z* 405.9771), …, and $[C_8F_8NO_2S]^-$ (*m/z* 325.9522) were detected. Therefore, it was indicated that the precursor ions of Flag Set 7, and 9 were *N*-EtFHxSA homologs. In addition, fragment ion $[C_{12}H_{14}F_{13}N_2O_2S]^-$ (*m/z* 497.0568) of Flag Set 8 was the same fragment ion of *N*-dihydroxybutyl (diHOB) dimethyl Ammonio PropylperFluoro Alkane SulfonAmide (N-diHOBAmP-FHxSA) $[C_{15}H_{20}F_{13}N_2O_4S]^-$ (*m/z* 571.0936) which were detected in AFFF and/ or AFFF-impacted groundwater (Barzen-Hanson et al., 2017). It was suspected that the precursor ions of Flag Set 7, 8, and 9 were dimer types of C6 PFASs because they have F_{26} and fragmentation patterns were similar to diPAPs. The chemical formulas of fragment ions might be different compared with fragmentation flags, it was same as validation of PFAS standard mixture solution. For example of Flag Set 7, it was expected that their fragmentation flags (e.g. $[C_{10}F_{14}]^-$, *m/z* 385.9776; $[C_7F_{14}O]^-$, *m/z* 365.9726) and the actual fragment ions (e.g. $[C_8H_3F_{11}NO_2S]^-$, *m/z* 385.9709; $[C_8H_2F_{10}NO_2S]^-$, *m/z* 365.9647) were different. Therefore, the prediction of chemical structures from accurate masses, isotopic patterns, and fragmentation rules using ultrahigh-resolution MS are required as an additional step.

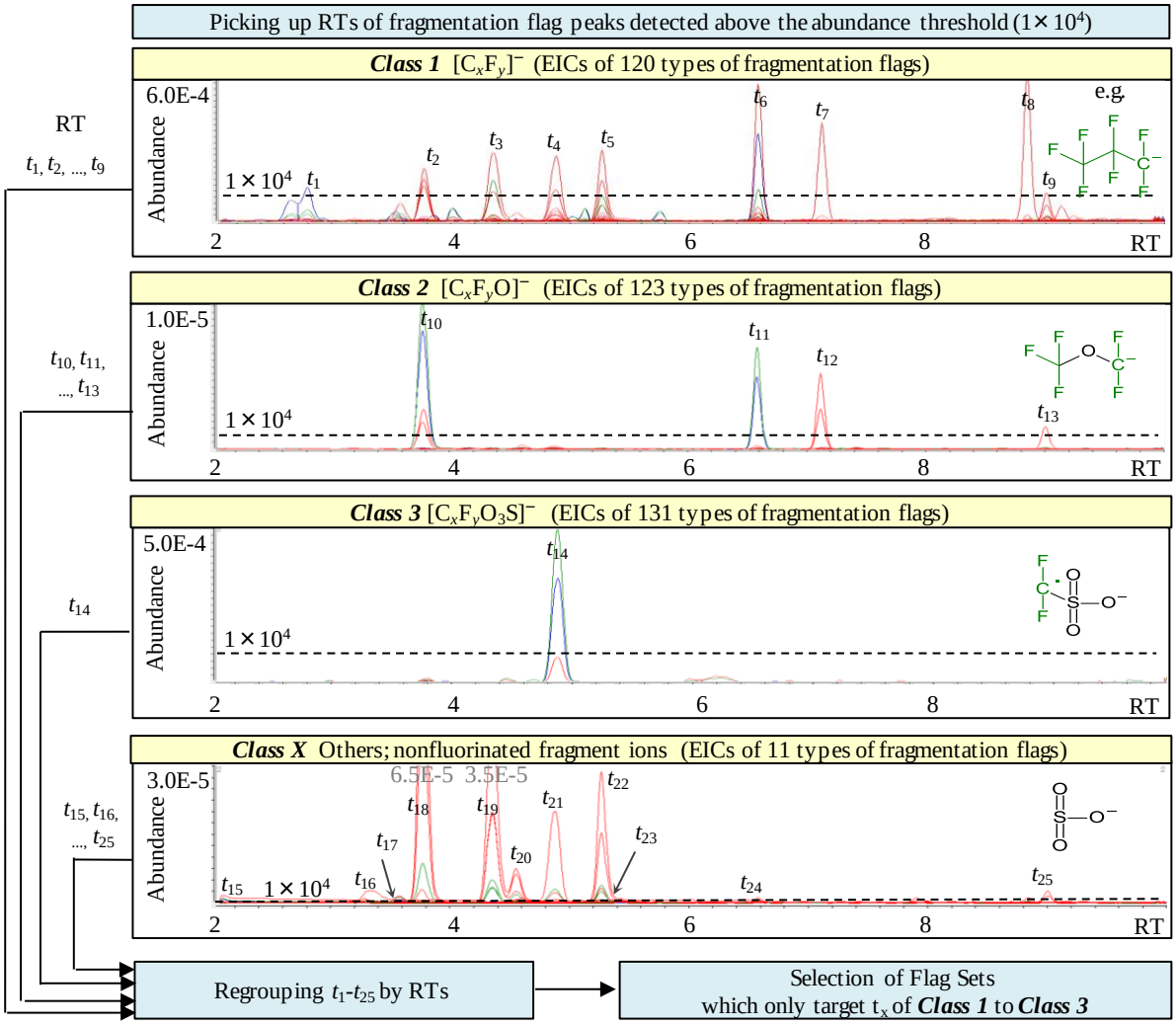

Flag Set	T_y	t_x Class 1	Class 2	Class 3	Class X
-	T_1	-	-	-	t_{15}
1	T_2	t_1	-	-	-
-	T_3	-	-	-	t_{16}
-	T_4	-	-	-	t_{17}
2	T_5	t_2	t_{10}	-	t_{18}
3	T_6	t_3	-	-	t_{19}
-	T_7	-	-	-	t_{20}

Flag Set	T_y	t_x Class 1	Class 2	Class 3	Class X
4	T_8	t_4	-	t_{14}	t_{21}
5	T_9	t_5	-	-	t_{22}
-	T_{10}	-	-	-	t_{23}
6	T_{11}	t_6	t_{11}	-	t_{24}
7	T_{12}	t_7	t_{12}		
8	T_{13}	t_8	-	-	-
9	T_{14}	t_9	t_{13}	-	t_{25}

Fig. 6.5 Selection of peaks by fragmentation flagging for a fire extinguisher liquid. The EICs were described at 10 V in blue, 20 V in green, and 40 V in red.

Table 6.2 The list of proposed PFASs in the household fire extinguisher liquid

Flag Set	RT (min)	drift time (ms)	Proposed formula	Name	Observed mass (*m/z*)	Exact mass (*m/z*)	Mass error (ppm)	Fragment ions (mass error (ppm))
1	2.578-2.752	16.14-17.22	$C_6HF_{11}O_2$	PFHxA (Perfluorohexanoic acid)	312.9702	312.9728	8	$[C_5F_{11}]^-$ (0.0)
2	3.707-3.880	19.03-21.32	$C_8H_5F_{13}O_3S$	6:2 FTS (6:2 fluorotelomer sulfonic acid)	426.9759	426.9679	19	$[C_8H_3F_{12}O_3S]^-$ (0.2), $[C_8H_2F_{11}O_3S]^-$ (1), $[C_7F_{11}]^-$ (0.3), $[C_7F_9]^-$ (12), $[C_7F_7]^-$ (0.5), $[HO_3S]^-$ (25)
3	4.286-4.460	24.81-27.22	$C_{15}H_{19}F_{13}N_2O_4S$	6:2 FTAB (6:2 fluorotelomer sulfonamide alkylbetaine)	569.0863	569.0785	14	$[C_8HF_{10}]^-$ (0.3), $[C_8F_9]^-$ (2), $[C_8HF_8]^-$ (3), $[C_5H_{11}N_2O_2]^-$ (3), $[HO_2S]^-$ (11)
4	4.788-5.000	19.87-21.80	$C_8H_5F_{13}O_3S_2$	-	458.9449	458.9400	11	$[C_7F_{11}]^-$ (6), $[C_8F_9]^-$ (7), $[C_7F_9]^-$ (18), $[C_7F_7]^-$ (4), $[HO_3S_2]^-$ (11), $[HO_3S]^-$ (25)
5	5.213-5.386	22.40-24.45	$C_{13}H_{17}F_{13}N_2O_2S$	6:2 FTA (6:2 fluorotelomer sulfonamide amine)	511.0743	511.0730	2	$[C_6F_{11}]^-$ (20), $[C_8F_9]^-$ (0.4), $[C_8HF_8]^-$ (2), $[FO_3S]^-$ (5)
6	6.526-6.661	19.27-20.96	$C_8H_6F_{13}NO_2S$	*N*-EtFHxSA (*N*-ethyl perfluorohexane sulfonamide)	425.9821	425.9839	4	$[C_6F_9]^-$ (8), $[C_4F_5]^-$ (13), $[H_2NO_2S]^-$ (15)
7	7.066-7.201	28.18-30.23	$C_{16}H_9F_{26}NO_4S_2$	-	835.9571	835.9485	10	$[C_8H_4F_{12}NO_2S]^-$ (4), $[C_8H_3F_{11}NO_2S]^-$ (1), $[C_8H_2F_{10}NO_2S]^-$ (1), $[C_8HF_9NO_2S]^-$ (6)
8	8.765-8.900	28.67-30.23	$C_{23}H_{14}F_{26}N_2O_4S$	-	907.0223	907.0186	4	$[C_{12}H_{14}F_{13}N_2O_2S]^-$ (6), $[C_{12}H_{13}F_{12}N_2O_2S]^-$ (6), $[C_{12}H_{11}F_{10}N_2O_2S]^-$ (8), $[C_{12}H_{10}F_9N_2O_2S]^-$ (6), $[C_6F_{13}]^-$ (7)
9	8.920-9.055	26.62-28.67	$C_{16}H_9F_{26}NO_2S$	-	771.9868	771.9866	0.3	$[C_8H_5F_{13}NO_2S]^-$ (0.0), $[C_8H_4F_{12}NO_2S]^-$ (7), $[C_8H_3F_{11}NO_2S]^-$ (2), $[C_8H_2F_{10}NO_2S]^-$ (1), $[C_8HF_9NO_2S]^-$ (1), $[C_8F_8NO_2S]^-$ (6), $[C_7F_{11}]^-$ (12)

Reference: Barzen-Hanson et al., 2017; D'Agostino et al., 2013; Mejia-Avendaño et al., 2017

Chapter 7

Conclusions and Future Perspectives

7.1 Conclusions

In conclusion, to understand PFASs contamination in the environments, this study examined the profile analysis with suspect screening of PFASs in firefighting foam impacted waters in Okinawa, Japan; and developed the data-independent method linking precursor and fragment ions by drift time using ion mobility mass spectrometry (**Fig. 7.1**). The main objective of this study was to examine suspect and non-target screening for PFASs by ion mobility mass spectrometry.

In Chapter 4, this study used profile analysis with suspect screening to characterize PFAS contamination in waters affected by firefighting training and identified 116 proposed PFASs and their characteristics (e.g., MWs, functional groups, and perfluoroalkyl chain lengths). Some high-MW precursors of PFAAs and long-chain PFAAs were specifically observed in the firefighting training area. On the other hand, we suspect that PFAAs are formed from their precursors in groundwater by environmental influences. In drinking water treatment processes, PFSAs can be formed from precursors such as FASAs, and PFCAs can be formed by BAC filtration. As our methods covered only substances that could be ionized by ESI with LC, other substances must be targeted next. The proposed PFASs, identified only according to their molecular formulas, need a greater identification confidence level, which can be achieved by high-resolution target MS/MS. Furthermore, because we characterized the PFASs by their peak areas, it will be necessary to use semi-quantification to measure concentrations.

In chapter 5, to improve identification confidence level of suspected PFASs after suspect / non-target screening, the study attempted to utilize drift time acquired by ion mobility mass spectrometry for making

linkages between precursor ion and the fragment ions. Furthermore, the linking method for PFASs in firefighting foam impacted groundwater was evaluated with focus on the intensity of co-eluting ions. The 99 compound groups were obtained by suspect screening using NORMAN exchange lists. Without drift time, 5%–19% of PFASs (4–9 PFASs) were linked. With drift time, 37%–49% of PFASs (15–43 PFASs) were linked. This study evaluated it on PFASs in firefighting foam impacted groundwater by considering the intensity of co-eluting ions to see how many ions could be excluded. Because the method uses all ions MS/MS mode, a single run can acquire a lot of MS/MS information independent of sample or data analysis. This means that if the original database, screening list, or statistical filtering / data cleaning approach changes, reanalysis is not required. Therefore, this method will be particularly effective for environmental research with large numbers of samples. The resolution of IMS will need to be improved in order to link PFASs which have similar properties.

In Chapter 6, the study focused on the fragmentation flagging approach with common fragment ion as flags to discovery unknown PFASs. However, there are some challenges due to many candidates of them in the full-scan spectrum at a specific retention time. The study developed a new method of linking fragmentation flags with their precursor ions by drift time using the ion mobility mass spectrometry for searching PFASs. For validating the process, the PFAS standards mixture solution was analyzed by LC/IM-QTOF. As a result, 20 flag sets of spiked PFASs were obtained by fragmentation flagging. The precursor ions and their fragmentation flags were observed at the same range of drift time. The method could link them and separate targeted PFASs from co-eluting compounds by drift time. Moreover, the method was applied to a household fire extinguisher liquid to find nine prospective precursor ions. Therefore, the results showed the utility of ion mobility mass spectrometry to search for precursor ions of suspected PFASs rapidly. Simple analytical methods to predict molecular formulas and structures are required next.

Study on Suspect and Non-Target Screening of Per- and polyfluoroalkyl substances (PFASs) by Ion Mobility Mass Spectrometry

A drinking water treatment plant

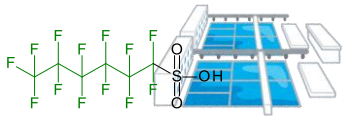

River water / Groundwater

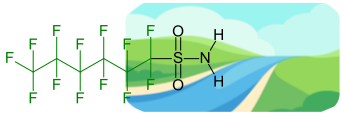

Firefighting foam

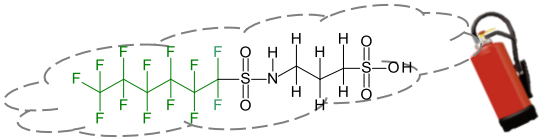

Suspect screening

Non-target screening

Chapter 4 : *Paper I*

A profile analysis with suspect screening of PFASs in firefighting foam impacted waters in Okinawa, Japan

- The profile of proposed 116 PFASs
- The cluster analysis for environmental waters
- The behavior of PFASs in a DWTP treatment processes

Chapter 5 : *Paper II*

A new data-independent method linking precursor and fragment ions of PFASs by drift time using ion mobility mass spectrometry

- A data-independent linking method by drift time (Precursor ion → Fragment ion)
- The evaluation the method considering co-eluting ions

Chapter 6 : *Paper III*

A method to search for PFASs by linking fragmentation flags with their precursor ions by drift time using ion mobility mass spectrometry

- The selection of fragmentation flags
- Fragmentation flagging for standards and a product
- A data-independent linking method by drift time (Fragmentation flags → Precursor ion)

Cluster	Number of PFASs	Sampling points	Characteristics	MW	PFASs types
1	2	R1	Nagata river	500-700	PFUnDA, PFDoDA
2	5	R5, G7, G8	Around firefighting area	500-800	Precursors
3	15	G2	Around firefighting area	500-700	Long chain PFSAs & PFCAs , precursors
4	49	G3, G4, G5, G6	The influential factor of G1 (downstream) is smaller	400-700	Precursors rich
5	45	G1, G3, G4, G5, GC6	The influential factor of G1 (downstream) is larger	200-500	PFSAs & PFCAs rich

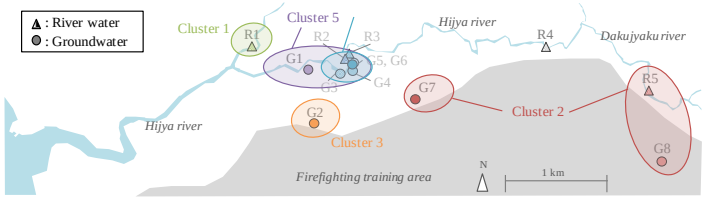

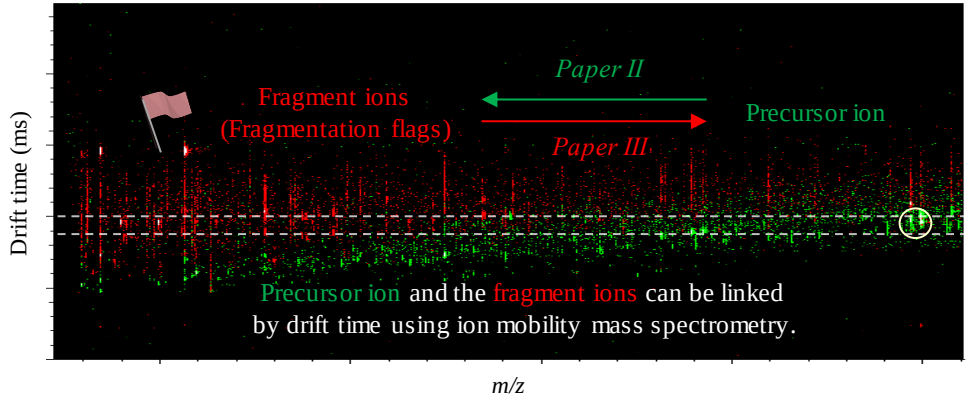

Fig. 7.1 Summary of this study

7.2 Future Perspective

The recommendations and future perspectives were shown in **Fig. 7.2**. This study examined suspect and non-target screening of PFASs in firefighting impacted waters by ion mobility mass spectrometry. The followings are remaining issues for future research based on this study. In chapter 4, additional field surveys to understand the detailed PFASs contamination, suspect screening with high identification level, and prediction of the behavior of PFAS transformation products require next. In chapter 5, improving the resolution of ion mobility mass spectrometry for separating the similar PFASs, and application of the method for other environmental matrices (e.g. soils and biota) are desirable. In chapter 6, the development of the database of PFAS fragment ions, application of the method for environmental matrices, and simplified estimation of PFAS structures using ion mobility mass spectrometry require next.

In the future perspective of this study, I proposed three research works as follows;

Research 1: Prediction of the transformation pathways of PFASs with a machine learning system

Research 2: Development of semi-quantification of PFASs with LC-QTOF and CIC

Research 3: Development of PFAS structures estimation method by ion mobility mass spectrometry.

In research 1, understanding PFASs transformation pathways in DWTPs and the prediction of the characteristics of effluent from influent with a machine learning system are desirable. In research 2, semi quantification of PFASs by LC-QTOF with a combination of LC fractionator and CIC to understand the detailed concentration of organic fluorine will require next. In research 3, the development of prediction methods of PFAS structures against their CCS database by ion mobility mass spectrometry are desirable.

Finally, in this study, I examined suspect and non-target screening of PFASs in firefighting foam impacted waters by ion mobility mass spectrometry to understand the characteristics of PFASs contamination in the environments. I hope these findings will contribute to global environmental studies and conservations.

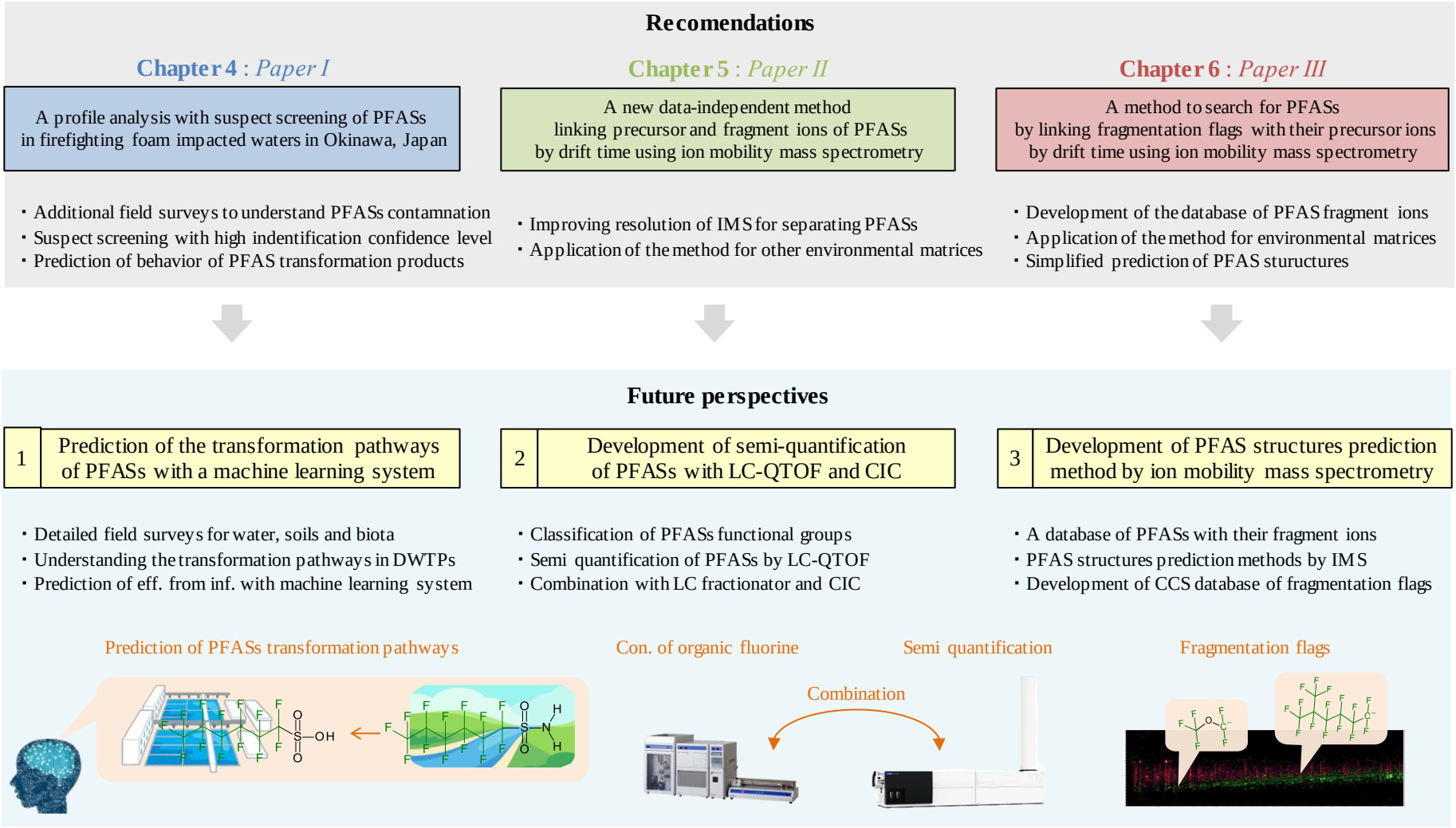

Fig. 7.2 Recomendations and future perspectives

Reference

Ahmed, E., Kabir, K. M., Wang, H., Xiao, D., Fletcher, J., Donald, W. A. 2019. Rapid separation of isomeric perfluoroalkyl substances by high-resolution differential ion mobility mass spectrometry. Analytica chimica acta 1058, 127-135.

Anderson, R. H., Long, G. C., Porter, R. C., Anderson, J. K. 2016. Occurrence of select perfluoroalkyl substances at US Air Force aqueous film-forming foam release sites other than fire-training areas: Field-validation of critical fate and transport properties. Chemosphere 150, 678-685.

Ahrens, L., Norström, K., Viktor, T., Cousins, A. P., Josefsson, S. 2015. Stockholm Arlanda Airport as a source of per-and polyfluoroalkyl substances to water, sediment and fish. Chemosphere 129, 33-38.

Arsenault, G., McAlees, A., McCrindle, R., Riddell, N., 2007. Analysis of perfluoroalkyl anion fragmentation pathways for perfluoroalkyl carboxylates and sulfonates during liquid chromatography/tandem mass spectrometry: evidence for fluorine migration prior to secondary and tertiary fragmentation. Rapid Comm. in Mass Spectrom. 21 (23), 3803-3814.

Baduel, C., Mueller, J. F., Rotander, A., Corfield, J., Gomez-Ramos, M. J., 2017. Discovery of novel per- and polyfluoroalkyl substances (PFASs) at a fire fighting training ground and preliminary investigation of their fate and mobility. Chemosphere 185, 1030-1038.

Barzen-Hanson, K. A., Roberts, S. C., Choyke, S., Oetjen, K., McAlees, A., Riddell, N., McCrindle, R., Ferguson, P. L., Higgins, C. P., Field, J. A., 2017. Discovery of 40 Classes of Per-and Polyfluoroalkyl Substances in Historical Aqueous Film-Forming Foams (AFFFs) and AFFF-Impacted Groundwater. Environ. Sci. Technol. 51 (4), 2047-2057.

Bielawski, J., Szulc, Z. M., Hannun, Y. A., Bielawska, A. 2006. Simultaneous quantitative analysis of bioactive sphingolipids by high-performance liquid chromatography-tandem mass spectrometry. Methods 39(2), 82-91.

Björnsdotter, M. K., Yeung, L. W., Kärrman, A., Jogsten, I. E., 2019. Ultra-Short-Chain Perfluoroalkyl Acids Including Trifluoromethane Sulfonic Acid in Water Connected to Known and Suspected Point Sources in Sweden. Environ. Sci. Technol. 53(19), 11093-11101.

Boone, J. S., Vigo, C., Boone, T., Byrne, C., Ferrario, J., Benson, R., Donohue, J., Simmons, E. J., Kolpin, W. D., Furlong, T. E., Glassmeyer, S. T., 2019. Per-and polyfluoroalkyl substances in source and treated drinking waters of the United States. Sci. of the Total Environ. 653, 359-369.

Borsdorf, H., Eiceman, G. A. 2006. Ion mobility spectrometry: principles and applications. App. Spectrosc. Rev. 41(4), 323-375.

Bräunig, J., Baduel, C., Barnes, C. M., Mueller, J. F., 2019. Leaching and bioavailability of selected perfluoroalkyl acids (PFAAs) from soil contaminated by firefighting activities. Sci. of the Total Environ. 646, 471-479.

Creaser, C. S., Griffiths, J. R., Bramwell, C. J., Noreen, S., Hill, C. A., Thomas, C. P. 2004. Ion mobility spectrometry: a review. Part 1. Structural analysis by mobility measurement. Analyst 129(11), 984-

994.

D'Agostino, L. A., Mabury, S. A. 2013. Identification of novel fluorinated surfactants in aqueous film forming foams and commercial surfactant concentrates. Environ. Sci. Technol. 48(1), 121-129.

Dauchy, X., Boiteux, V., Colin, A., Hémard, J., Bach, C., Rosin, C., Munoz, J. F., 2019. Deep seepage of per-and polyfluoroalkyl substances through the soil of a firefighter training site and subsequent groundwater contamination. Chemosphere 214, 729-737.

Dimzon, I. K., Trier, X., Frömel, T., Helmus, R., Knepper, T. P., de Voogt, P. 2016. High resolution mass spectrometry of polyfluorinated polyether-based formulation. J. American Society for Mass Spec. 27, 309.

Dubocq, F., Wang, T., Yeung, L. W. Y., Sjöberg, V., Kärrman, A. 2019. Characterization of the chemical contents of fluorinated and fluorine-free firefighting foams using a novel workflow combining non-target screening and total fluorine analysis. Environ. Sci. Technol. In press

Eberle, D., Ball, R., Boving, T. B. 2017. Impact of ISCO treatment on PFAA co-contaminants at a former fire training area. Environ. Sci. Technol. 51(9), 5127-5136.

Filipovic, M., Woldegiorgis, A., Norström, K., Bibi, M., Lindberg, M., Österås, A. H. 2015. Historical usage of aqueous film forming foam: A case study of the widespread distribution of perfluoroalkyl acids from a military airport to groundwater, lakes, soils and fish. Chemosphere 129, 39-45.

Fujii, Y., Harada, K. H., Koizumi, A., 2013. Occurrence of perfluorinated carboxylic acids (PFCAs) in personal care products and compounding agents. Chemosphere 93 (3), 538-544.

Garcia, R. A., Chiaia-Hernández, A. C., Lara-Martín, P. A., Loos, M., Hollender, J., Oetjen, K., Huggins, C. P., Field, J. A. 2019. Suspect Screening of Hydrocarbon Surfactants in AFFFs and AFFF-Contaminated Groundwater by High Resolution Mass Spectrometry. Environ. Sci. Technol. 53(14), 8068-8077

Gebbink, W. A., van Asseldonk, L., van Leeuwen, S. P., 2017. Presence of emerging per-and polyfluoroalkyl substances (PFASs) in river and drinking water near a fluorochemical production plant in the Netherlands. Environ. Sci. Technol. 51 (19), 11057-11065.

Gyllenhammar, I., Benskin, J. P., Sandblom, O., Berger, U., Ahrens, L., Lignell, S., Wiberg, K., Glynn, A., 2019. Perfluoroalkyl Acids (PFAAs) in Children's Serum and Contribution from PFAA-Contaminated Drinking Water. Environ. Sci. Technol. 53(19), 11447-11457.

Harding-Marjanovic, K. C., Houtz, E. F., Yi, S., Field, J. A., Sedlak, D. L., Alvarez-Cohen, L., 2015. Aerobic biotransformation of fluorotelomer thioether amido sulfonate (Lodyne) in AFFF-amended microcosms. Environ. Sci. Technol. 49 (13), 7666-7674.

Hollender, J., Schymanski, E. L., Singer, H. P., Ferguson, P. L., 2017. Nontarget screening with high resolution mass spectrometry in the environment: ready to go?. Environ. Sci. Technol. 51 (20), 11505-11512.

Hopkins, Z. R., Sun, M., DeWitt, J. C., Knappe, D. R. 2018. Recently detected drinking water contaminants: GenX and other per-and polyfluoroalkyl ether acids. Journal-American Water Works Association 110(7), 13-28.

Houtz, E. F., Higgins, C. P., Field, J. A., Sedlak, D. L., 2013. Persistence of perfluoroalkyl acid precursors in AFFF-impacted groundwater and soil. Environ. Sci. Technol. 47(15), 8187-8195.

Houtz, E. F., Sedlak, D. L. 2012. Oxidative conversion as a means of detecting precursors to perfluoroalkyl acids in urban runoff. Environ. Sci. Technol. 46(17), 9342-9349.

Høisæter, Å., Pfaff, A., Breedveld, G. D., 2019. Leaching and transport of PFAS from aqueous film-forming foam (AFFF) in the unsaturated soil at a firefighting training facility under cold climatic conditions. J. contaminant hydrology 222, 112-122.

Hu, X. C., Andrews, D. Q., Lindstrom, A. B., Bruton, T. A., Schaider, L. A., Grandjean, P., Lohmann, P., Carignan, C. C., Blum, A., Balan, A. S., Higgins, C. P., Sunderland, M. E., 2016. Detection of poly- and perfluoroalkyl substances (PFASs) in US drinking water linked to industrial sites, military fire training areas, and wastewater treatment plants. Environ. Sci. Technol. Letters 3(10), 344-350.

IARC Monographs on the Evaluation of Carcinogenic Risk to Humans. List of Classifications. Volumes 1-123 https://monographs.iarc.fr/wp-content/uploads/2018/07/Table4.pdf

Joudan, S., Liu, R., Jessica, C., Mabury, S. A. 2019. Unique analytical considerations for laboratory studies identifying metabolic products of per-and polyfluoroalkyl substances (PFASs). TrAC Trends in Anal. Chem. In press

Kar, S., Sepúlveda, M. S., Roy, K., Leszczynski, J., 2017. Endocrine-disrupting activity of per-and polyfluoroalkyl substances: Exploring combined approaches of ligand and structure based modeling. Chemosphere 184, 514-523.

KEMI (Swedish Chemicals Agency). Occurrence and use of highly fluorinated substances and alternatives. 2015; https://www.kemi.se/en/global/rapporter/2015/report-7-15-occurrence-and-use-of-highly-fluorinated-substances-and-alternatives.pdf

Koch, A., Aro, R., Wang, T., Yeung, L. W. 2019. Towards a comprehensive analytical workflow for the chemical characterisation of organofluorine in consumer products and environmental samples. TrAC Trends in Anal. Chem. 115423

Koch, A., Kärrman, A., Yeung, L. W., Jonsson, M., Ahrens, L., Wang, T., 2019. Point source characterization of per-and polyfluoroalkyl substances (PFASs) and extractable organofluorine (EOF) in freshwater and aquatic invertebrates. Environ. Sci.: Processes & Impacts 21(11), 1887-1898.

Kong, A. T., Leprevost, F. V., Avtonomov, D. M., Mellacheruvu, D., Nesvizhskii, A. I. 2017. MSFragger: ultrafast and comprehensive peptide identification in mass spectrometry–based proteomics. Nature methods 14(5), 513.

Kotthoff, M., Müller, J., Jürling, H., Schlummer, M., Fiedler, D., 2015. Perfluoroalkyl and polyfluoroalkyl substances in consumer products. Environ. Sci. and Pollut. Res. 22 (19), 14546-14559.

Lang, J. R., Allred, B. M., Peaslee, G. F., Field, J. A., Barlaz, M. A., 2016. Release of per-and polyfluoroalkyl substances (PFASs) from carpet and clothing in model anaerobic landfill reactors. Environ. Sci. Technol. 50 (10), 5024-5032.

Lanucara, F., Holman, S. W., Gray, C. J., Eyers, C. E. 2014. The power of ion mobility-mass spectrometry for structural characterization and the study of conformational dynamics. Nature chem. 6(4), 281.

Lee, E. S., Han, S., Oh, J. E., 2016. Association between perfluorinated compound concentrations in cord serum and birth weight using multiple regression models. Reproductive Toxicol. 59, 53-59.

Li, R., Munoz, G., Liu, Y., Sauvé, S., Ghoshal, S., Liu, J. 2019. Transformation of novel polyfluoroalkyl substances (PFASs) as co-contaminants during biopile remediation of petroleum hydrocarbons. J. hazardous materials 362, 140-147.

Li, Y., Oliver, D. P., Kookana, R. S. 2018. A critical analysis of published data to discern the role of soil and sediment properties in determining sorption of per and polyfluoroalkyl substances (PFASs). Sci. of the Total Environ. 628, 110-120.

Liu, C., J. Liu., 2016. Aerobic biotransformation of polyfluoroalkyl phosphate eth (PAPs) in soil. Environ. Pollut. 212, 230-237.

Liu, Y., D'Agostino, L. A., Qu, G., Jiang, G., Martin, J. W. 2019. High-Resolution Mass Spectrometry (HRMS) Methods for Nontarget Discovery and Characterization of Poly-and Per-fluoroalkyl Substances (PFASs) in Environmental and Human Samples. TrAC Trends in Anal. Chem. (In Press)

Liu, Y., Pereira, A. D. S., Martin, J. W., 2015. Discovery of C5–C17 poly-and perfluoroalkyl substances in water by in-line SPE-HPLC-Orbitrap with in-source fragmentation flagging. Anal. Chem. 87 (8), 4260-4268.

Liu, Y., Qian, M., Ma, X., Zhu, L., Martin, J. W., 2018. Nontarget Mass Spectrometry Reveals New Perfluoroalkyl Substances in Fish from the Yangtze River and Tangxun Lake, China. Environ. Sci. Technol. 52 (10), 5830-5840.

Liu, Y., Ruan, T., Lin, Y., Liu, A., Yu, M., Liu, R., Meng, M., Wang, Y., Liu, J., Jiang, G., 2017. Chlorinated polyfluoroalkyl ether sulfonic acids in marine organisms from Bohai Sea, China: Occurrence, temporal variations, and trophic transfer behavior. Environ. Sci. Technol. 51 (8), 4407-4414.

Loi, E. I., Yeung, L. W., Taniyasu, S., Lam, P. K., Kannan, K., Yamashita, N., 2011. Trophic magnification of poly-and perfluorinated compounds in a subtropical food web. Environ. Sci. Technol. 45 (13), 5506-5513.

Luo, Q., Lu, J., Zhang, H., Wang, Z., Feng, M., Chiang, S. Y. D., Woodward, D., Huang, Q. 2015. Laccase-catalyzed degradation of perfluorooctanoic acid. Environ. Sci. Technol. Letters 2(7), 198-203.

Martin, D., Munoz, G., Mejia-Avendaño, S., Duy, S. V., Yao, Y., Volchek, K., Brown, C. E., Sauvé, S. 2019. Zwitterionic, cationic, and anionic perfluoroalkyl and polyfluoroalkyl substances integrated into total oxidizable precursor assay of contaminated groundwater. Talanta 195, 533-542.

McCord, J., Newton, S., Strynar, M., 2018. Validation of quantitative measurements and semi-quantitative estimates of emerging perfluoroethercarboxylic acids (PFECAs) and hexfluoroprolyene oxide acids (HFPOAs). J. Chromatogr. A 1551, 52-58.

McCord, J., Strynar, M. 2019. Identifying Per-and Polyfluorinated Chemical Species with a Combined Targeted and Non-Targeted-Screening High-Resolution Mass Spectrometry Workflow. JoVE (Journal of Visualized Experiments), (146), e59142.

McCord, J., Strynar, M. 2019. Identification of Per-and Polyfluoroalkyl Substances in the Cape Fear River by High Resolution Mass Spectrometry and Nontargeted Screening. Environ. Sci. Technol. 53(9),

4717-4727

McDonough, C. A., Guelfo, J. L., Higgins, C. P. 2019. Measuring total PFASs in water: the tradeoff between selectivity and inclusivity. Current Opinion in Environ. Sci. & Health 7, 13-18.

Mejia-Avendaño, S., Munoz, G., Vo Duy, S., Desrosiers, M., Benoît, P., Sauvé, S., Liu, J., 2017. Novel fluoroalkylated surfactants in soils following firefighting foam deployment during the Lac-Megantic railway accident. Environ. Sci. Technol. 51(15), 8313-8323.

Mejia-Avendaño, S., Munoz, G., Vo Duy, S., Desrosiers, M., Benoît, P., Sauvé, S., Liu, J. 2017. Novel fluoroalkylated surfactants in soils following firefighting foam deployment during the Lac-Megantic railway accident. Environ. Sci. Technol. 51(15), 8313-8323.

Milley, S. A., Koch, I., Fortin, P., Archer, J., Reynolds, D., Weber, K. P. 2018. Estimating the number of airports potentially contaminated with perfluoroalkyl and polyfluoroalkyl substances from aqueous film forming foam: A Canadian example. J. environ. mgmt. 222, 122-131.

Miyake, Y., Yamashita, N., So, M. K., Rostkowski, P., Taniyasu, S., Lam, P. K., Kannan, K., 2007. Trace analysis of total fluorine in human blood using combustion ion chromatography for fluorine: a mass balance approach for the determination of known and unknown organofluorine compounds. J. Chromatogr. A 1154 (1-2), 214-221.

Moreta, C., M. T. Tena 2014. Determination of perfluorinated alkyl acids in corn, popcorn and popcorn bags before and after cooking by focused ultrasound solid–liquid extraction, liquid chromatography and quadrupole-time of flight mass spectrometry. J. Chromatogr. A 1355: 211-218.

Moschet, C., Anumol, T., Lew, B. M., Bennett, D. H., Young, T. M. 2018. Household dust as a repository of chemical accumulation: new insights from a comprehensive high-resolution mass spectrometric study. Environ. Sci. Technol. 52(5), 2878-2887.

Mullin, L., Katz, D., Riddell, N., Plumb, R., Burgess, J. A., Yeung, L. W., Jogsten, I. E. 2019. Analysis of hexafluoropropylene oxide-dimer acid (HFPO-DA) by liquid chromatography-mass spectrometry (LC-MS): Review of current approaches and environmental levels. TrAC Trends in Anal. Chem. 118, 828-839

Mumtaz, M., Bao, Y., Liu, L., Huang, J., Cagnetta, G., Yu, G. 2019. Per-and Polyfluoroalkyl Substances in Representative Fluorocarbon Surfactants Used in Chinese Film-Forming Foams: Levels, Profile Shift, and Environmental Implications. Environ. Sci. Technol. Letters. 6(5), 259-264

Munoz, G., Ray, P., Mejia-Avendaño, S., Duy, S. V., Do, D. T., Liu, J., Sauvé, S. 2018. Optimization of extraction methods for comprehensive profiling of perfluoroalkyl and polyfluoroalkyl substances in firefighting foam impacted soils. Analytica chimica acta 1034, 74-84.

Munoz, G., Desrosiers, M., Duy, S. V., Labadie, P., Budzinski, H., Liu, J., Sauvé, S. 2017. Environmental occurrence of perfluoroalkyl acids and novel fluorotelomer surfactants in the freshwater fish Catostomus commersonii and sediments following firefighting foam deployment at the Lac-Mégantic railway accident. Environ. Sci. Technol. 51(3), 1231-1240.

Newton, S., McMahen, R., Stoeckel, J. A., Chislock, M., Lindstrom, A., Strynar, M., 2017. Novel polyfluorinated compounds identified using high resolution mass spectrometry downstream of

manufacturing facilities near Decatur, Alabama. Environ. Sci. Technol. 51 (3), 1544-1552.

NORMAN Suspect List Exchange, No.25 List of PFAS from the OECD, 2019, https://www.norman-network.com/?q=suspect-list-exchange

Nørgaard, A. W., Wolkoff, P., Lauritsen, F. R. 2010. Characterization of nanofilm spray products by mass spectrometry. Chemosphere 80(11), 1377-1386.

Organization for Economic Co-operation and Development (OECD) PFASs Global Database. 2019. https://www.oecd.org/chemicalsafety/portal-perfluorinated-chemicals/

Padilla-Sánchez, J. A., Haug, L. S. 2016. A fast and sensitive method for the simultaneous analysis of a wide range of per-and polyfluoroalkyl substances in indoor dust using on-line solid phase extraction-ultrahigh performance liquid chromatography-time-of-flight-mass spectrometry. J. Chromatogr. A 1445, 36-45.

Pan, Y., Wang, J., Yeung, L. W., Wei, S., Dai, J. 2019. Analysis of emerging per-and polyfluoroalkyl substances: progress and current issues. TrAC Trends in Anal. Chem. In press

Pan, Y., Zhang, H., Cui, Q., Sheng, N., Yeung, L. W., Sun, Y., Guo, Y., Dai, J., 2018. Worldwide Distribution of Novel Perfluoroether Carboxylic and Sulfonic Acids in Surface Water. Environ. Sci. Technol. 52 (14), 7621-7629.

Picó, Y., Farré, M., Barceló, D. 2015. Quantitative profiling of perfluoroalkyl substances by ultrahigh-performance liquid chromatography and hybrid quadrupole time-of-flight mass spectrometry. Anal. and bioanal. chem. 407(15), 4247.

Place, B. J., Field, J. A., 2012. Identification of novel fluorochemicals in aqueous film-forming foams used by the US military. Environ. Sci. Technol. 46(13), 7120-7127.

Portolés, T., Rosales, L. E., Sancho, J. V., Santos, F. J., Moyano, E. 2015. Gas chromatography–tandem mass spectrometry with atmospheric pressure chemical ionization for fluorotelomer alcohols and perfluorinated sulfonamides determination. J. Chromatogr. A 1413, 107-116.

Rewerts, J. N., Morré, J. T., Massey Simonich, S. L., Field, J. A. 2018. In-Vial Extraction Large Volume Gas Chromatography Mass Spectrometry for Analysis of Volatile PFASs on Papers and Textiles. Environ. Sci. Technol. 52(18), 10609-10616.

Rich, C. D., Blaine, A. C., Hundal, L., Higgins, C. P. 2015. Bioaccumulation of perfluoroalkyl acids by earthworms (Eisenia fetida) exposed to contaminated soils. Environ. Sci. Technol. 49(2), 881-888.

Riedel, T. P., Lang, J. R., Strynar, M. J., Lindstrom, A. B., Offenberg, J. H. 2019. Gas-Phase Detection of Fluorotelomer Alcohols and Other Oxygenated Per-and Polyfluoroalkyl Substances by Chemical Ionization Mass Spectrometry. Environ. Sci. Technol. Letters 6(5), 289-293.

Rodriguez-Freire, L., Abad-Fernández, N., Sierra-Alvarez, R., Hoppe-Jones, C., Peng, H., Giesy, J. P., Snyder, S., Keswani, M. 2016. Sonochemical degradation of perfluorinated chemicals in aqueous film-forming foams. J. hazardous materials 317, 275-283.

Rotander, A., Kärrman, A., Toms, L. M. L., Kay, M., Mueller, J. F., Gómez Ramos, M. J., 2015. Novel fluorinated surfactants tentatively identified in firefighters using liquid chromatography quadrupole time-of-flight tandem mass spectrometry and a case-control approach. Environ. Sci. Technol. 49 (4),

2434-2442.

Ruan, T., Lin, Y., Wang, T., Jiang, G., Wang, N. 2015. Methodology for studying biotransformation of polyfluoroalkyl precursors in the environment. TrAC Trends in Anal. Chem. 67, 167-178.

Ruan, T., Lin, Y., Wang, T., Liu, R., Jiang, G., 2015. Identification of novel polyfluorinated ether sulfonates as PFOS alternatives in municipal sewage sludge in China. Environ. Sci. Technol. 49 (11), 6519-6527.

Ruiz-Delgado, A., Plaza-Bolaños, P., Oller, I., Malato, S., Agüera, A. 2020. Advanced evaluation of landfill leachate treatments by low and high-resolution mass spectrometry focusing on microcontaminant removal. J. hazardous materials 384, 121372.

Qu, Y., Jiang, X., Cagnetta, G., Liu, L., Bao, Y., Li, W., Wang, Q., Liang, C., Huang, J., Yang, H., Yu, G. 2019. Poly-and perfluoroalkyl substances in a drinking water treatment plant in the Yangtze River Delta of China: Temporal trend, removal and human health risk. Sci. of the Total Environ. 696, 133949.

Sammut, G., Sinagra, E., Sapiano, M., Helmus, R., de Voogt, P. 2019. Perfluoroalkyl substances in the Maltese environment–(II) sediments, soils and groundwater. Sci. of the Total Environ. 682, 180-189.

Schaefer, C. E., Choyke, S., Ferguson, P. L., Andaya, C., Burant, A., Maizel, A., Strathmann, T. J., Higgins, C. P. 2018. Electrochemical transformations of perfluoroalkyl acid (PFAA) precursors and PFAAs in groundwater impacted with aqueous film forming foams. Environ. Sci. Technol. 52(18), 10689-10697.

Schymanski, E. L., Jeon, J., Gulde, R., Fenner, K., Ruff, M., Singer, H. P., Hollender, J. 2014. Identifying small molecules via high resolution mass spectrometry: communicating confidence. Environ. Sci. Technol. 48 (4), 2097-2098.

Sedlak, M. D., Benskin, J. P., Wong, A., Grace, R., Greig, D. J., 2017. Per-and polyfluoroalkyl substances (PFASs) in San Francisco Bay wildlife: Temporal trends, exposure pathways, and notable presence of precursor compounds. Chemosphere 185, 1217-1226.

Sha, B., Schymanski, E. L., Ruttkies, C., Cousins, I. T., Wang, Z. (2019). Exploring open cheminformatics approaches for categorizing per-and polyfluoroalkyl substances (PFASs). Environ. Sci.: Processes & Impacts 21(11), 1835-1851.

Shaw, D. M., Munoz, G., Bottos, E. M., Duy, S. V., Sauvé, S., Liu, J., Van Hamme, J. D., 2019. Degradation and defluorination of 6:2 fluorotelomer sulfonamidoalkyl betaine and 6:2 fluorotelomer sulfonate by Gordonia sp. strain NB4-1Y under sulfur-limiting conditions. Sci. of the Total Environ. 647, 690-698.

Sheng, N., Pan, Y., Guo, Y., Sun, Y., Dai, J., 2018. Hepatotoxic Effects of Hexafluoropropylene Oxide Trimer Acid (HFPO-TA), A Novel Perfluorooctanoic Acid (PFOA) Alternative, on Mice. Environ. Sci. Technol. 52 (14), 8005-8015.

Shi, G., Guo, H., Sheng, N., Cui, Q., Pan, Y., Wang, J., Guo, Y., Dai, J., 2018. Two-generational reproductive toxicity assessment of 6: 2 chlorinated polyfluorinated ether sulfonate (F-53B, a novel alternative to perfluorooctane sulfonate) in zebrafish. Environ. pollut. 184, 514-523.

Steiner, W. E., Clowers, B. H., Fuhrer, K., Gonin, M., Matz, L. M., Siems, W. F., Schultz, A. J., Hill Jr, H. H., 2001. Electrospray ionization with ambient pressure ion mobility spectrometry and mass analysis by orthogonal time-of-flight mass spectrometry. Rapid Comm. Mass Spectrom. 15 (23), 2221-2226.

Steiner, W. E., Clowers, B. H., Haigh, P. E., Hill, H. H., 2003. Secondary ionization of chemical warfare agent simulants: atmospheric pressure ion mobility time-of-flight mass spectrometry. Anal. Chem. 75 (22), 6068-6076.

Stockholm Convention. PFOS, its salts and PFOSF overview. http://chm.pops.int/Implementation/IndustrialPOPs/PFOS/Overview/tabid/5221/Default.aspx

Stockholm Convention. POPRC Recommendations for listing Chemicals. http://chm.pops.int/TheConvention/ThePOPs/ChemicalsProposedforListing/tabid/2510/Default.aspx

Sun, M., Arevalo, E., Strynar, M., Lindstrom, A., Richardson, M., Kearns, B., Adam, P., Smith, C., Knappe, D. R., 2016. Legacy and emerging perfluoroalkyl substances are important drinking water contaminants in the Cape Fear River Watershed of North Carolina. Environ. Sci. Technol. Letters 3 (12), 415-419.

Trier, X., Granby, K., Christensen, J. H. 2011. Tools to discover anionic and nonionic polyfluorinated alkyl surfactants by liquid chromatography electrospray ionisation mass spectrometry. J. Chromatogr. A 1218(40), 7094-7104.

Wang, Y., Yu, N., Zhu, X., Guo, H., Jiang, J., Wang, X., Shi, W., Wu, J.; Yu, H., Wei, S., 2018. Suspect and Nontarget Screening of Per-and Polyfluoroalkyl Substances in Wastewater from a Fluorochemical Manufacturing Park. Environ. Sci. Technol. 52 (19), 11007-11016.

Wang, Z., DeWitt, J. C., Higgins, C. P., Cousins, I. T., 2017. A never-ending story of per-and polyfluoroalkyl substances (PFASs)?. Environ. Sci. Technol. 51 (5), 2508-2518.

Weber, A. K., Barber, L. B., LeBlanc, D. R., Sunderland, E. M., Vecitis, C. D. 2017. Geochemical and hydrologic factors controlling subsurface transport of poly-and perfluoroalkyl substances, Cape Cod, Massachusetts. Environ. Sci. Technol. 51(8), 4269-4279.

Wu, C.; Siems, W. F., Klasmeier, J., Hill, H. H., 2000. Separation of isomeric peptides using electrospray ionization/high-resolution ion mobility spectrometry. Anal. Chem. 72 (2), 391-395.

Xiao, F., Golovko, S. A., Golovko, M. Y., 2017. Identification of novel non-ionic, cationic, zwitterionic, and anionic polyfluoroalkyl substances using UPLC–TOF–MSE high-resolution parent ion search. Analytica chimica acta 988, 41-49.

Xiao, P., Mori, T., Kondo, R. 2011. Biotransformation of the organochlorine pesticide trans-chlordane by wood-rot fungi. New biotech. 29(1), 107-115.

Ye, F., Zushi, Y., Masunaga, S., 2015. Survey of perfluoroalkyl acids (PFAAs) and their precursors present in Japanese consumer products. Chemosphere 127, 262-268.

Yu, N., Guo, H., Yang, J., Jin, L., Wang, X., Shi, W., Zhang, X., Yu, H., Wei, S., 2018. Non-target and suspect screening of per-and polyfluoroalkyl substances in airborne particulate matter in China. Environ. Sci. Technol. 52 (15), 8205-8214.

Yu, N., Guo, H., Yang, J., Jin, L., Wang, X., Shi, W., Zhang, X., Yu, H., Wei, S., 2018. Non-target and suspect screening of per-and polyfluoroalkyl substances in airborne particulate matter in China. Environ. Sci. Technol. 52 (15), 8205-8214.

Yukioka, S., Tanaka, S., Suzuki, Y., Fujii, S., Echigo, S. 2020. A new method to search for per-and polyfluoroalkyl substances (PFASs) by linking fragmentation flags with their molecular ions by drift time using ion mobility spectrometry. Chemosphere 239, 124644.

Zabaleta, I., Negreira, N., Bizkarguenaga, E., Prieto, A., Covaci, A., Zuloaga, O., 2017. Screening and identification of per-and polyfluoroalkyl substances in microwave popcorn bags. Food chem. 230, 497-506.